



Université de Montréal

**Biopacemaker acceleration without increased  
synchronization by chronic exposure to phorbol myristate  
acetate**

par

Yashar Alami Alamdari

Département de physiologie moléculaire et intégrative

Faculté de médecine

Thèse présentée à la Faculté des études supérieures et postdoctorales  
en vue de l'obtention du grade de Maîtrises en science (M.Sc.)  
en physiologie moléculaire et intégrative

Décembre 2015

© Yashar Alami Alamdari, 2015

## Résumé

L'activité électrique du coeur est initiée par la génération spontanée de potentiels d'action venant des cellules pacemaker du noeud sinusal (SN). Toute dysfonction au niveau de cette région entraîne une instabilité électrique du coeur. La majorité des patients souffrant d'un noeud sinusal déficient nécessitent l'implantation chirurgicale d'un pacemaker électronique; cependant, les limitations de cette approche incitent à la recherche d'une alternative thérapeutique. La base moléculaire des courants ioniques jouant un rôle crucial dans l'activité du noeud sinusal sont de plus en plus connues. Une composante importante de l'activité des cellules pacemakers semble être le canal HCN, responsable du courant pacemaker  $I_f$ . Le facteur T-box 3 (Tbx3), un facteur de transcription conservé durant le processus de l'évolution, est nécessaire au développement du système de conduction cardiaque. De précédentes études ont démontré que dans différentes lignées cellulaires le Phorbol 12-myristate 13-acetate (PMA) active l'expression du gène codant Tbx3 via des réactions en cascade partant de la protéine kinase C (PKC).

L'objectif principal de cette étude est de tester si le PMA peut augmenter la fréquence et la synchronisation de l'activité spontanée du pacemaker biologique en culture. Plus précisément, nous avons étudié les effets de l'exposition chronique au PMA sur l'expression du facteur de transcription Tbx3, sur HCN4 et l'activité spontanée chez des monocouches de culture de myocytes ventriculaires de rats néonataux (MVRN). Nos résultats démontrent que le PMA augmente significativement le facteur transcription de Tbx3 et l'expression ARNm de HCN4, favorisant ainsi l'augmentation du rythme et de la stabilité de l'activité autonome. De plus, une diminution significative de la vitesse de conduction a été relevée et est attribuée à la diminution du couplage intercellulaire. La diminution de la vitesse de conduction pourrait expliquer l'effet négatif du PMA sur la synchronisation de l'activité autonome du pacemaker biologique. Ces résultats ont été confirmés par un modèle mathématique multicellulaire suggérant que des fréquences et résistances intercellulaires plus élevée pourraient induire une activité plus stable et moins synchrone. Cette étude amène de nouvelles connaissances très importantes destinées à la production d'un pacemaker biologique efficient et robuste.

**Mots-clés :** pacemaker biologique, activité autonome, synchronisation, stabilité spatiotemporelle

## Summary

The normal heartbeat is initiated by the spontaneous generation of action potentials in pacemaker cells of the sinoatrial node (SAN) region. Dysfunction of this region leads to electrical instability of the heart. The majority of the patients with sinus node dysfunction require surgical implantation of electronic pacemaker devices; however, limitations of this therapeutic approach lead to a need to search for alternatives. To date, the molecular basis of the ionic currents which play pivotal role in SAN action potential has been discovered. It is thought that an important component of the pacemaker cells are HCN channels, responsible for the funny current ( $I_f$ ) in the SAN. Meanwhile, T-box factor 3 known as an evolutionary conserved transcription factors is necessary for development of the conduction system. In previous studies, it has been shown that Phorbol 12-myristate 13-acetate (PMA) activates Tbx3 gene expression in a PKC-dependent manner in several cell lines.

The main objective of this study is to test if PMA can increase the frequency and synchronization of spontaneous activity of cultured biopacemakers. More precisely, we studied the effects of chronic exposure to PMA on the expression of the Tbx3 transcription factor and HCN4 in neonatal rat ventricular myocytes monolayers and how spontaneous activity was altered. Our results show that PMA significantly increases the Tbx3 transcription factor and HCN4 mRNA expression favoring an increased in the rate and spatial-temporal stability of the spontaneous activity. In addition, a significant decrease in conduction velocity was found that is attributed to decrease electrical intercellular coupling of the cells. The decrease in the conduction velocity could explain the negative effect PMA has on synchronization of spontaneous activity of the biopacemaker. These findings are confirmed by a multicellular mathematical model implying that faster frequency and higher intercellular resistance of the pacemaker cells may lead to a more stable and less synchronous activity. This study provides important new knowledge to produce efficient and robust biological pacemakers.

**Keywords:** biopacemaker, spontaneous activity, synchronization, spatial-temporal stability.

# Table of contents

Résumé.....	i
Summary.....	iii
Table of contents.....	iv
List of Figures.....	vi
List of abbreviations.....	vii
Acknowledgments.....	x
1 Introduction.....	1
1.1 Heart physiology.....	3
1.1.1 Cardiomyocyte.....	3
1.1.2 Pacemaker cells.....	3
1.1.3 Fibroblasts.....	4
1.1.4 Spontaneous activity.....	5
1.2 Sino-atrial node (SAN).....	5
1.2.1 Primary pacemaker cells.....	5
1.2.2 Secondary pacemakers (AVN and Purkinje fibers).....	7
1.2.3 Rhythm.....	7
1.2.4 Clocks.....	9
1.2.5 Pathology of the rhythm.....	20
1.3 Pacemakers.....	21
1.3.1 Electronic pacemakers.....	21
1.3.2 Biopacemakers.....	22
1.4 Phorbol 12-myristate 13-acetate (PMA).....	28
1.4.1 PMA link with Tbx3.....	28
1.4.2 Structural and physiological features.....	28
1.4.3 Pathophysiological effects.....	29

1.5	HCN blockers.....	30
1.6	Project hypothesis .....	30
2	ARTICLE.....	31
	Abstract.....	33
	Introduction.....	33
	Methods.....	36
	Results.....	41
	Discussion and conclusion.....	45
	References.....	48
	Figure captions.....	55
	Table and figures.....	58
3	DISCUSSION AND CONCLUSION .....	71
3.1	PMA increases the rate of spontaneous activity through Tbx3 re-expression.....	71
3.2	PMA modulates the spatial-temporal activity in multicellular patches .....	72
3.3	The increase in frequency of spontaneous activity does not yield greater synchronization.....	74
3.4	CONCLUSION.....	74
4	BIBLOGRAPHY .....	75

## List of Figures

<b>Figure 1: Schematic of sarcomeric structure .....</b>	<b>4</b>
<b>Figure 2: Electrical system of the heart .....</b>	<b>6</b>
<b>Figure 3: Schematic model of the embrionic heart presenting the various gene expression zones .....</b>	<b>15</b>
<b>Figure 4: SAN action potential traces underling the Ca<sup>2+</sup> transactions .....</b>	<b>16</b>
<b>Figure 5: Schematic model of the calcium clock of the heart .....</b>	<b>17</b>
<b>Figure 6: Different electrical features and various distributions of ion channels and gap junctions between central and peripheral cells of the SAN .....</b>	<b>19</b>
<b>Figure 7: Different gene therapy-based strategies .....</b>	<b>23</b>

## List of abbreviations

AC: adenylyl cyclase  
Ach: acetylcholine  
ACP: artificial pacing  
AKAP: A-kinase anchor  
AP-1: activator protein-1  
APD: AP duration  
AVN: atrioventricular node  
bpm: beats per minute  
CaM: Calmodulin  
cAMP: cyclic adenosine monophosphate  
CCT: cardiac cell therapy  
CFs: cardiac fibroblasts  
CLL: chronic lymphocytic leukemia  
CMs: cardiomyocytes  
cPKC: classical PKC  
CRT: cardiac resynchronization therapy  
cTnT: Cardiac Troponin-T  
DAG: 1, 2-diacylglycerol  
DD: diastolic depolarization Discoidin domain receptor 2 (DDR2)  
DHP: dihydropyridines  
EPCs: endothelial progenitor cells  
GPCR: G-protein-coupled receptor  
Gs: G proteins  
HCN: Hyperpolarization-activated cyclic nucleotide-gated channels  
hESCs: human embryonic stem cells  
HIV-1: human immunodeficiency virus-1  
hMSCs: human mesenchymal stem cells  
HSCs: hematopoietic stem cells

ICD: implantable cardioverter-defibrillators  
LCP: local  $\text{Ca}^{2+}$  period  
LCRs: local  $\text{Ca}^{2+}$  releases  
LTCC: L-type  $\text{Ca}^{2+}$  Channel  
MDP: maximum diastolic potential  
NCX:  $\text{Na}^+/\text{Ca}^{2+}$  exchanger  
NE: norepinephrine  
NF $\kappa$ B: nuclear factor-kappa-B  
nPKC: novel PKC  
NRVMs: neonatal rat ventricular myocytes  
ODC: ornithine decarboxylase  
PIP2: phosphatidylinositol 4,5-bisphosphate  
PKA: protein kinase A  
PMA: phorbol 12-myristate 13-acetate  
PPM: permanent pacemakers  
PS: phosphatidylserine  
RyRs: ryanodine receptors  
SACPs: specialized sinoatrial conduction pathways  
SAN: sinoatrial node  
SERCA: ATPase pumps of the sarcoplasmic reticulum  
SR: Sarcoplasmic Reticulum  
SSS: sick sinus syndrome  
TPA: 12-O-Tetradecanoyl-phorbol-13-acetate  
TTX: tetrodotoxin

*I would like to dedicate my thesis to my parents*

## **Acknowledgments**

It would not have been possible to write this thesis without the help and support of the kind people around me to only some of whom it is possible to give particular mention here.

First and foremost, I would like to thank my supervisor Dr. Philippe Comtois for his guidance and persistent help without which this project would not have been possible.

I wish to express appreciation to my colleagues for discussion and communications, among them James Elber Duverger and Alireza Aghighi who spent extra time helping me in writing the thesis, Alexandre Blanchette, Feng Xiong and Jonathan Béland. I devote my special gratitude to James for his attention, patient and unfailing supports during my master program.

It is my privilege to thank my wife, Laleh Abbassi, for supporting me all the way.

I would certainly be remiss to not mention and sincerely thanks my parents for their love, encouragement and profound contribution in providing financial assistance for me to help with my studies. Their sacrifices have brought me to where I am today.

I am grateful to the authors for allowing us to use figures from their publications.

Above all, I thank God for his many blessings.

# 1 Introduction

Normal function of the heart is extremely dependent on the flawless activity of the sinoatrial node (SAN). Abnormal propagation from the sinoatrial node leads to serious arrhythmias called sick sinus syndrome (SSS). Nowadays, the prevalence of SSS is increasing. In spite of prominent developments of electrical pacemakers, there are a lot of shortcomings. The need to create alternative therapies and the biological pacemaker is among them.

Different concepts will be presented in the introduction (Chapter 1). Starting with section 1.1, an overview of the heart physiology is introduced with a focus on the different cell types including the pacemaker cell. Primary pacemaker cells are located in the sinoatrial node (SAN, section 1.2) which is the structure responsible for initiating the normal heart beat.

In brief, pacemaker cells differs from cardiomyocytes (CMs) having reduced maximum diastolic potential (MDP), slower action potential (AP) upstroke velocity, high intercellular resistance which leads to slow conduction velocity and spontaneous diastolic depolarization (DD) (Clocks, section 1.2.4). An important components of the pacemaker cells are HCN channels (Clocks, section 1.2.4) which conduct the funny current ( $I_f$ ). Mutations or knockout of these proteins in human or mice linked to SSS (Pathology of the rhythm, section 1.2.5). Expression of HCNs is linked to T-box factor 3 (Tbx3) which is one of the evolutionary conserved transcription factors necessary for development of many tissues. Moreover, connexin 40 and 43 expressions were down regulated in ectopic Tbx3 activated embryonic atrial myocytes (Clocks, section 1.2.4).

Probably, it happens because of the current-to-load mismatch between HCN over-expressing cells and the surrounding tissue.

The most important therapeutic approach to date for patients with bradycardia and unstable heart rate remains the electronic pacemaker (section 1.3.1). An alternative being developed, termed the biopacemaker, is based on generating pacemaking activity of cells through different approaches (presented in section 1.3.2).

Gene therapy is a key approach to modulate expression of proteins. Chemical conditioning can also be an interesting alternative to modulate transcription factors. Phorbol 12-myristate 13-acetate (PMA, section 1.4) is an extracellular PKC activator which can activate the protein-1 (AP-1) family of transcription factors. In the previous studies, it has been shown that PMA activates Tbx3 gene expression in a PKC-dependent manner via the AP-1 transcription factors in several cell lines but its effect on spontaneous activity in cardiomyocytes remains unknown.

A widely used cardiac model is rat ventricular myocytes (NRVMs) which have been shown to be useful a model system for analyzing states of cellular hypertrophy and contractile protein gene expression. More interesting is that there is a transient regenerative phase in neonatal murine heart related to cardiomyocyte DNA-synthesis activity which declines during the first 1–2 weeks of life in rodents making this model a close relative to cardiomyocyte induced from pluripotent cells. (Biopacemakers, section 1.3.2).

We hypothesized that chronic conditioning of neonatal cardiomyocytes with PMA could upregulate the Tbx3 and HCN channels expression and facilitates the development of the cardiomyocytes to the pacemaker cells (Project hypothesis, section 1.6).

To test this hypothesis, we isolated ventricular cardiomyocytes from 1- to 3-day-old Sprague-Dawley rats. Cells were cultured in the pre-coated glass bottom dishes. Cultured dishes were exposed with PMA after 24h and the experiments were done 24h and 48 h after the start of conditioning with PMA (Article, section 2). The results of chronic exposure of the NRVMs with PMA showed an increase in expression of Tbx3 and HCN4 channels which was concordant with increasing the spatial-temporal stability of the spontaneous activity. In addition, the conduction velocity of the impulse propagation decreased providing an evidence of electrical uncoupling of the cells that led to decreased synchronization of the spontaneous activity. To confirm our experimental results, we implemented a mathematical model which mimics the PMA effect in increasing of cell spontaneous rate of activity and decreasing the electrical coupling in the experimental monolayers. The results of the computational model confirmed spatial-temporal stability and lower synchronous activity of our monolayers (Article, section 2).

In the last part of the thesis, the implication of our results on the biopacemaker approach is further discussed (Discussion and conclusion, section 3).

## **1.1 Heart physiology**

### **1.1.1 Cardiomyocyte**

The human heart is built of different cell types including: cardiomyocytes, fibroblasts/myofibroblasts, vascular and immune cells, vascular smooth muscle cells and vascular endothelial cells (1). A cardiac myocyte is enclosed by a sarcolemma as cell membrane that contains a nucleus (2). Myocytes are composed of numerous mitochondria, and they supply the needed ATP for the contraction of muscles. In addition, cardiac muscles contain the machinery to perform the intact contraction including contractile proteins actin (thin filaments) and myosin (thick filaments) accompanied by troponin and tropomyosin as regulatory proteins (Fig. 1). Cardiac muscle has a striated shape, however the pattern is a little bit different with skeletal muscle (2). Cardiac myocytes composed of approximately 75% of normal heart tissue volume, but they occupy only 30–40% of the total cell population in the heart. The rest of the heart tissue comprises non-myocytes, including fibroblasts, as a predominant population and other cell types like vascular or endothelial smooth muscle cells (3). Cardiac Troponin-T (cTnT) could be used to identify the myocardial cells, as it is specifically expressed in the myocardium (4, 5). By differentiation of the cardiac chambers, the automaticity of the mature myocytes entirely disappears and they display a fast conduction velocity (6, 7).

### **1.1.2 Pacemaker cells**

In addition to the contractile myocytes, there are other types of the excitable cells in the heart with specific electrophysiological characteristics privileged them to generate and propagate electrical pulses. The pacemaker cells and their related conduction system are composed of two main nodes called sinoatrial (SAN) and atrioventricular (AVN) nodes in addition to the specified conduction system. The features of the pacemaker cells and their electrical pathways will be discussed comprehensively in the following chapters.

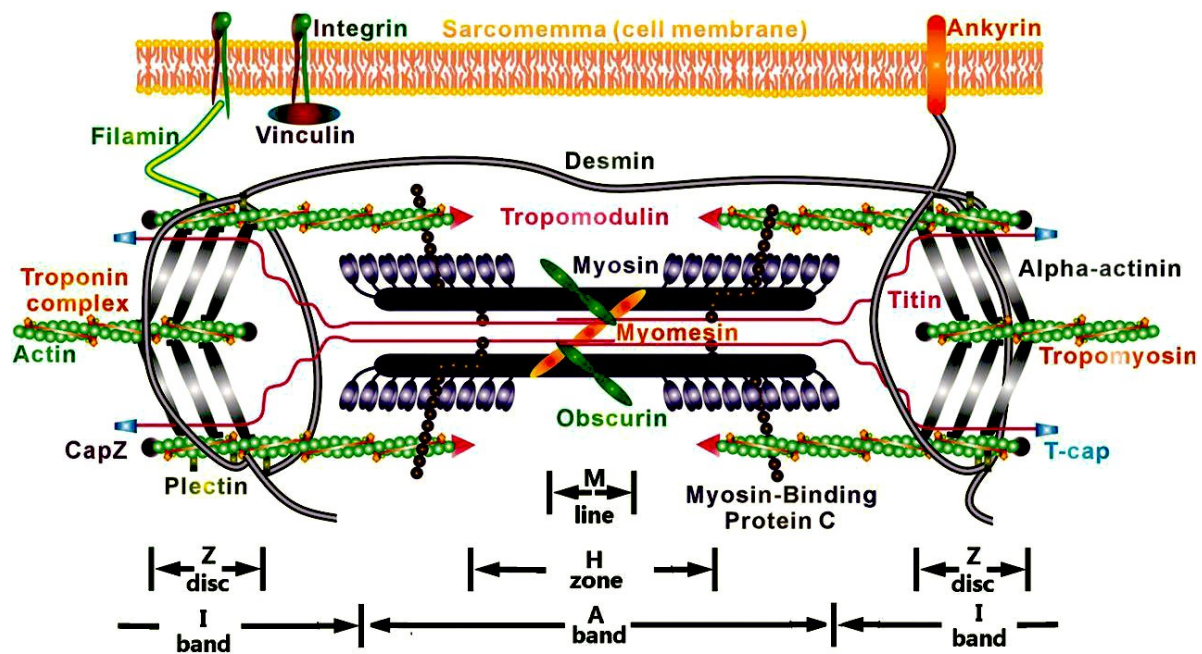


**Figure 1: Schematic of sarcomeric structure.** Actin and myosin filaments as contractile components and sarcomeric titin as a structural component are shown in the diagrammatic model. (Reproduced with permission from Liu H. *et al.* 2013 (8))

### 1.1.3 Fibroblasts

Fibroblasts are defined as flat and spindle shaped cells with numerous protrusions arising from the cell membrane. One of the outstanding morphological features of the fibroblasts is the lack of a basement membrane, and it distinguishes these kinds of cells from the other cell types of the heart. Generally, fibroblasts play a critical role in chemical, mechanical, and electrical signaling in the heart, and any pathological change of these signaling pathways can lead to cardiac dysfunction (9). Normal development and aging increase the fibroblast contents (10, 11). In fact, 5–6% of the volume of the normal adult myocardium is composed of connective tissue which is in parallel with increasing the fibroblast contents during the life time, however the fraction of the connective tissue in sinoatrial node (SAN) is more than 50% in the adult human heart (12, 13). Although cardiac fibroblasts are basically unexcitable cells, they are able to affect the electrophysiological communication of myocytes as effective components (14). In spite of non-excitable properties,

these type of cells play an important role in electromechanical functions of the heart in addition to compose of the anatomical and biochemical integrity of the heart tissue. Discoidin domain receptor 2 (DDR2) is specific marker of the cardiac fibroblasts which is not expressed on other types of the cardiac cells (15).

### **1.1.4 Spontaneous activity**

Cardiomyocytes development during embryonic period affects their electrical properties notably (16). Automaticity is a dominant aspect of cardiomyocytes in very early prenatal period. However it is going to disappear by transforming the cells into the ventricular myocytes. In the late embryonic period, sinoatrial node takes the responsibility of controlling the automaticity coincident with the complete differentiation of the cardiomyocytes to the working ventricular cells (17). Recent studies based on patch clamp techniques demonstrated increase in amplitude of several cardiac currents including the fast  $\text{Na}^+$  channel (18) current and the L-type  $\text{Ca}^{2+}$  channel (19) current during the rat embryonic developing phase which is related to increase in their channel expression level. In addition, there are some reports corresponding with increasing the outward currents from the middle to late embryonic period. Maybe these increments are to be responsible for the interruption of automaticity of working ventricular myocytes. Some studies (20, 21) have reported an increment of the inwardly rectifying background  $\text{K}^+$  current ( $I_{\text{K1}}$ ) in fetal working ventricular myocytes. Thereby, it could be proposed a hypothesis suggesting that the hyperpolarization effect of  $I_{\text{K1}}$  augmentation leads to the cessation of the spontaneous activity in fetal ventricular myocytes, nonetheless it would be beneficial to reduce or abolish some pacemaker inward currents.

## **1.2 Sino-atrial node (SAN)**

### **1.2.1 Primary pacemaker cells**

In the mammalian heart, SAN is laid at the junction of the superior vena cava and right atrium. The size of the SAN in the adult human heart is 12–20 mm long and 2–6 mm wide which is detectable by its ellipsoidal shape and intramural position. The head of the node is located around 1 mm under the epicardium isolated by a layer of lipid and connective tissue (22). The head part of the SAN extends inferiorly for 10–20 mm stretching beneath the sulcus

terminalis till the crista terminalis and has multiple extensions into the bordering atrial myocardium, which composes the specialized sinoatrial conduction pathways (SACPs) (23) (Fig. 2). The sinoatrial node is the main commander of the human heart rhythmicity by producing and propagating the electrical impulses that plays a critical role in regularity of the heart beats (22).

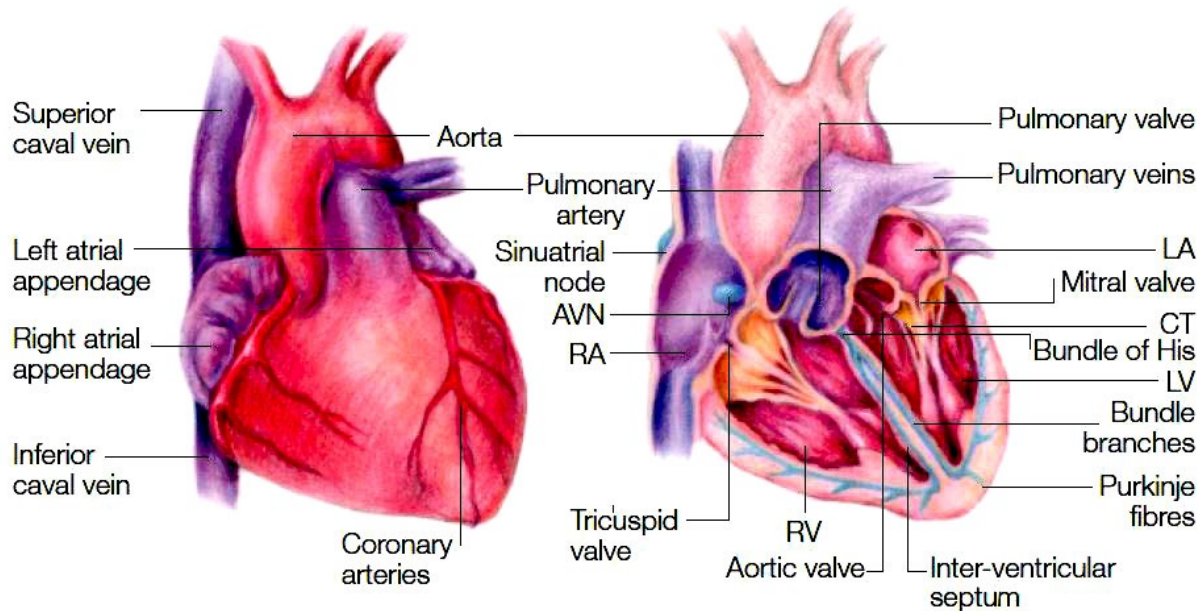


**Figure 2: Electrical system of the heart.** In normal heart electrical pulses originate from SAN and propagate through the AVN to the His bundles and Purkinje fibers. (Reproduced with permission from Harvey *et al.* 2002 (24))

It is well known that the structure of the human and canine SAN is a complex multi-compartment (25). The SAN of mammals heart, is composed of clusters of developed cardiomyocytes, which are engulfed within the matrix of connective tissue including the mixture of fibroblasts and some kinds of connective proteins like collagen and elastin. Such a fibrotic structure insulates the pacemaker cells from the hyperpolarizing effect of the bordering atrial cells in addition to mechanical protection (23).

## **1.2.2 Secondary pacemakers (AVN and Purkinje fibers)**

In the intact heart, electrical impulse originates from the SAN and propagates to the surrounding atrial myocardium and reaches the atrioventricular node (AVN) after then electrical wave passes through the Purkinje bundles to depolarize the ventricles and initiate the contraction of the heart thus perform the pumping function (26).

Anatomical position of the AVN is at the junction of the atrial and ventricular septum which is dubbed as the triangle of Koch (27) and it is bounded by tendon of Todaro, the coronary sinus ostium and the tricuspid valve. There are two different pathways which lead into the AVN the first one is transitional zone, fast pathway, and the second one is inferior nodal extension defined as slow pathways (28).

As a matter of fact, there are two electrical pathways (29). The fast route of propagation passes through the atrial septum and transitional zone, indicating the normal route. On the other hand, there is another way to conduct the propagation wave from the SAN through the AVN using the terminal crest and inferior nodal extension (30). There is also a penetrating bundle, at the position distal to the AVN, engulfed in the central fibrous body and extrudes on the ventricular spectrum crest where the His bundle begins. The AVN plays critical roles in the heart. First of all, it serves as a conduction delay barrier which is essential to perform the atrial contraction before the ventricular one. Secondly, long refractory period of the AVN helps to block the high frequency activity in atrial arrhythmias to minimize the ventricular tachycardia. Furthermore, AVN has also a potential ability to emerge as a first initiation site when the normal activity of the SAN disappears to prevent the heart arrest (31).

## **1.2.3 Rhythm**

In the intact physiological condition, the SAN which located in the right atrium initiates the rhythmic pacing discharge. Indeed, the SAN is a part of the intrinsic conduction system included in the heart. Cardiac activation starts with the SAN or pacemaker and propagates to the surrounding cells resulting in depolarization and contraction of the atrial tissue and extends in order of rate to the internodal pathway, the AVN (where the impulse is delayed), AV bundle, the left and right branches of the bundle of His and lastly the Purkinje

fibers, consequently leads to ventricular depolarization and contraction. Autonomous rhythmicity is one of the pivotal characteristic of the intrinsic conduction system, thereby in the absence of extrinsic neural or hormonal stimulation, the SAN enables to impulse with the pacing rate about 100 beats per minute (bpm). Nonetheless, the heart rate and cardiac output must be changed in response to the needs for oxygen and nutrients supply under varying conditions. In order to make an immediate response to be concordant with body's request, it is vital to provide an interacting system to control the heart rate and contractility. The SAN has two regulating systems: the sympathetic and parasympathetic systems. The sympathetic nervous system releases norepinephrine (NE) while the parasympathetic nervous system releases acetylcholine (ACh). Adrenergic  $\beta_1$  receptors are expressed in the SAN, AVN, besides in atrial and ventricular cardiomyocytes. The activation of  $\beta_1$  receptors, mediating NE, increases intracellular calcium concentrations and calcium release by the sarcoplasmic reticulum (SR) which leads to increase in contractility as a consequence and increase AVN conduction velocity. Thus, sympathetic nervous system stimulation is responsible for: "1) Positive chronotropic effect (increase in heart rate); 2) Positive inotropic effect (increase of contractility); and 3) Positive dromotropic effect (enhancement of conduction)" (32).

The parasympathetic nervous system has limited modulatory effect on the heart in contrast to sympathetic activity. Acetylcholine, as a main neurotransmitter of the parasympathetic system, produces effects that are in opposite to the sympathetic activation which includes: negative chronotropic and dromotropic effect. However, there are a lot of controversies about the probable negative inotropic effects of parasympathetic stimulation, recent in vivo studies in the atrium may suggest otherwise (32).

The catecholaminergic control of the heart rate and contractility is mediated by the G-protein-cAMP-PKA signaling pathway (32). In fact, activation of  $\beta_1$ -adrenoceptor as a G-protein-coupled receptor (GPCR) is the source of the sympathetic stimulation-induced effects in the heart. NE binding to  $\beta_1$  receptors activates stimulatory G proteins ( $G_s$ ) and consequently activates adenylyl cyclase (AC) which mediates dephosphorylation of ATP into cyclic adenosine monophosphate (cAMP). After then, cAMP accomplishes numerous functions and it plays an important role in regulating ion channels, transcription factors, or enzymes. Regarding to the cardiovascular system, protein kinase A (PKA) is the most important enzyme

activated by cAMP. In consequence, PKA phosphorylates proteins, such as contractile machinery including troponin C, I, and sarcoplasmic proteins and L-type  $\text{Ca}^{2+}$  channels (LTCC). In addition, cAMP binds directly to hyperpolarization-activated cyclic nucleotide-gated (HCN) channels, thereby increasing the heart rate (33).

G-protein-coupled receptor, muscarinic (M2) receptors in the heart, plays also a pivotal role in the parasympathetic system in the heart resulting from activation by ACh as a parasympathetic neurotransmitter. ACh binding to M2 receptors causes a conformational change within the  $G_i$  subunit of the receptor facilitating inhibitory activity of the G protein, consequently the disassociated  $\alpha_i$  subunit can bind to and inhibits AC. M2 receptors decrease cAMP formation due to negatively coupling to AC. As a result, M2 receptors inhibit PKA activity and have an opposite effect on ion channels,  $\text{Ca}^{2+}$  handling proteins, and contractile machinery, in contrast to sympathetic stimulation (32).

#### **1.2.4 Clocks**

Briefly, spontaneous excitation of “pacemaker” cells in the sinoatrial node initiates the normal cardiac electrical activity. The activation wave then travels to the adjacent atrial myocytes through intercellular gap junctions, and finally causes atrial excitation. After then, the excitation wave passes via the atrioventricular node and the Purkinje fibers to the ventricles and leads to ventricular myocyte depolarization. The self-activating characteristic of the SAN is attributed to the precise contribution between sarcolemma and sarcoplasmic membranes ion channels regulation termed as membrane and calcium clocks, respectively. Inward or outward direction of ion currents is related to the electrochemical gradient of the corresponding ions. Normally, there is a linear relationship between current amplitude (I), membrane potential (V) and the conductivity (G) of the responsible ion channels. This relation is defined in equation form as “ $I=VG$  ( $R$  as resistance is the reverse of conductivity:  $I=V/R$  [Ohm’s law])” (26), indicating that membrane potential changes affect the current amplitude. Nonetheless, there are types of membrane channels that show non-ohmically behavior called voltage-dependent channels. One such current that is important for the resting potential is the rectifying currents ( $I_{K1}$ ). The rectifying channels carry dynamic currents which vary nonlinearly at different membrane potentials. It is the interplay between inward and outward

currents that leads to the spontaneous formation of an action potential (26). It is believed that the cooperation of both the membrane and calcium clocks in SAN is responsible for the pacemaker cell activity with characteristics including:

1- “Reduced maximum diastolic potential (MDP)” (34).

2- “A slow action potential (AP) upstroke velocity” (34) which is regulated by the L-type  $\text{Ca}^{2+}$  current,  $I_{\text{CaL}}$ , in central sino-atrial nodal cells (35).

3-High intercellular resistance (34). Indeed, the lack of fast-propagating connexins including Cx40 (Gja5) and Cx43 (Gja1), besides distribution of slow-propagating connexins such as Cx30.2 (Gjd3) and Cx45 (Gjc1) (36, 37) leads to the electrical uncoupling resulting in slow conduction velocity in SAN.

4- “Spontaneous diastolic depolarization (DD)” (34). The animal studies, in particular on rabbit heart demonstrated that there is a precise control system to depolarize the membrane potential over the activation threshold.

Cellular processes are thus central to the spontaneous activity and interplay between membrane and intracellular calcium regulation would play a role. The differences between the membrane and calcium clocks are described below.

#### **1.2.4.1 Membrane clock**

According to the contribution of the variety of ionic currents in spontaneous pacemaking, and due to their time-dependent behavior and localization in the cell membrane, it has been dubbed “the membrane clock”(35). The hyperpolarization-activated cation current, or “funny” current ( $I_f$ ) is the dominant ionic current in the membrane clock (34).

The membrane clock theory of pacemaking states that precise cooperation of time- and voltage-dependent membrane ion channels enhances diastolic depolarization from MDP to threshold potential which opens L-type voltage-dependent  $\text{Ca}^{2+}$  channels to create the upstroke phase of the action potential. Consequently, activation of outward repolarizing potassium channels including transient outward ( $I_{\text{to}}$ ), fast delayed rectifier ( $I_{\text{Kr}}$ ), and slow delayed rectifier ( $I_{\text{Ks}}$ )  $\text{K}^+$  currents initiate repolarization phase by reducing the membrane potential to the maximum diastolic potential after then the next cycle starts again (35).

#### 1.2.4.1.1 HCN channels

Genes isoforms HCN1 through HCN4 are responsible to encode the voltage-gated ion channels (38, 39) although HCN2 and HCN4 are found in neonatal hearts. Different subunits possess various characteristics which proper them to do their biophysical duties such as phosphorylation by tyrosine kinases, voltage dependency and regulation by low molecular weight factors like phosphatidylinositol 4,5-bisphosphate (PIP2) and cAMP (40). Regulation of  $I_f$  by cAMP is one the most important features of the HCN channels with increment of the membrane resting potential thus increasing the current activation (41). Hence, rate of activation of the HCN4 channels is augmented with cAMP (42). Moreover, higher level of phosphorylation can increase the sensitivity of the cells to the  $\beta$ -adrenergic stimulation in which maximal conductance of the pacemaker cells increases in a voltage independent manner (41). Funny current is defined as a mixed inward  $\text{Na}^+$  and  $\text{K}^+$  current which is activated slowly at membrane potential range of -50 to -65 mV (43, 44). All of the channels in cardiac cells are activated by membrane depolarization except  $I_f$  known as funny current (35).

#### 1.2.4.1.2 CaT channels

Transient type  $\text{Ca}^{2+}$  (CaT) channels, including Cav3.1 through Cav3.3, have been encoded by three different genes, CACNA1G through CACNA1I (45). The first hypothesis regarding the role of  $I_{\text{CaT}}$  in automaticity was described by Bean who proposed that fast  $\text{Ca}^{2+}$  channels have more important effect on generating spontaneous activity, due to their activation kinetics at negative potentials, while the  $\text{Na}^+$  channels show inactivated behavior in less negative potentials (46). In addition, the previous studies on rabbit heart proved that  $I_{\text{CaT}}$  block with 40  $\mu\text{M}$   $\text{Ni}^{2+}$  has a negative chronotropic effect on pacemaker cells as a result of decreasing the slope of the late phase of DD. These types of channels show activity in more negative activation potentials in comparison with L-type  $\text{Ca}^{2+}$  channels (47).

#### 1.2.4.1.3 CaL channels

L-type  $\text{Ca}^{2+}$  (CaL) channels are other types of the calcium conductors defined as L-type  $\text{Ca}^{2+}$  channels. They include of the variety of subunits such as  $\alpha 1$ -,  $\beta$ - and  $\alpha 2$ - $\delta$  (48). Their selectivity to the  $\text{Ca}^{2+}$  ions is dependent on  $\alpha 1$ -subunit of the channel pore. Such capability is due to the high affinity of the pore for  $\text{Ca}^{2+}$  ions (49). Different isoforms of the  $\alpha 1$ -subunit are

encoded by different genes resulting in various types of the channels such as  $\text{Ca}_v1.2$  (CACNA1C) and  $\text{Ca}_v1.3$  (CACNA1D) which are presented in the human SAN. It is shown that  $\text{Ca}_v1.2$  mRNA is expressed in atrial and nodal cells, whereas  $\text{Ca}_v1.3$  is distributed much more in the SAN comparing in atrial myocytes (50, 51).

$\text{Ca}_v1.2$  channels basically have some specific characteristics including requirement of higher membrane voltage for activation, long-lasting activity performance. In addition, lower concentrations of L-type calcium channel blockers including phenylalkylamines, dihydropyridines (DHP) and benzothiazepines would be able to block the channels (52-54). L-type  $\text{Ca}^{2+}$  channels are targeted by hormones in spite of their voltage dependent characteristic (55). According to the Reuters studies (56), there is a correlation between increasing in  $I_{\text{CaL}}$  and the positive effect of NE on cardiac muscle contraction. Recent investigations demonstrated that such inotropic effect occurs due to the up-regulation of intracellular cAMP levels as a consequence of  $\beta$ -adrenergic receptor stimulation resulting in activation of cAMP-dependent protein kinase (PKA). In agreement with these studies, the experiments on guinea pig cardiomyocytes substantiated increment of action potential duration (57) and  $I_{\text{CaL}}$  (58) due to the catalytic subunit of PKA.

#### *1.2.4.1.4 NaK pump*

Sarcolemmal NaK pump plays a critical role in regulation of the automaticity by carrying three  $\text{Na}^+$  ions outward and transporting two  $\text{K}^+$  ions inward the cells. The activity of the ATPase pump decreases the rate of the spontaneous activity by producing a net outward and hyperpolarizing current ( $I_{\text{NaK}}$  or  $I_p$ ) (59). NaK pump is highly sensitive to the intracellular  $\text{Na}^+$  concentration; thereby there is a close relationship between the activity of the pump and  $I_p$ -derived  $\text{Na}^+$  ions in SAN (60). Therefore,  $I_{\text{NaK}}$  has a pivotal role in maintaining the maximum diastolic potential (61).

#### *1.2.4.1.5 $\text{K}^+$ channels*

##### *1.2.4.1.5.1 Transient outward potassium channels*

There are two different subtypes of transient outward current in the heart one of them passes  $\text{K}^+$  ions ( $I_{\text{to1}}$ ) and other one conducts  $\text{Cl}^-$  ions ( $I_{\text{to2}}$ ) (62). Distribution of three subunits

of the potassium transient channels has been recognized in human (50) and murine (51) SAN including  $K_v4.2$ ,  $K_v1.4$  and, in particular,  $K_v4.3$ . Fast activation and inactivation after depolarization kinetics is recognized as a specific feature of  $K^+$  transient outward channels, therefore they play a critical role in early phase of repolarization of ventricular cells in most of mammals, except for guinea pig (63) and pig (64). There is a big difference in action potential kinetics and duration between epicardium and endocardium tissue which is attributed to the various density in distribution of  $K^+$  transient outward channels (65).

#### 1.2.4.1.5.2 Delayed rectifying channels

These types of channels divided to two different components, rapid ( $I_{Kr}$ ) and slow ( $I_{Ks}$ ) components. They trend to pass the current inwardly rather than outward direction, duded as inward rectification. In rapid rectifying channels, very rapid inactivation of the channel occurs upon activation of the channel after membrane depolarization. Hence the effect of such a little amplitude of  $I_{Kr}$  on plateau phase of action potential would be very low. However, they play a significant role in late repolarization phase due to their recovery from inactivation which results in a huge amplitude of outward current. This outward current will be vanished gradually after slow deactivation of the channels (66).

Another component of the rectifying channels which caused a lot of debates during the last decades was termed as slow component,  $I_{Ks}$ . The gene of the channel, called minK (KCNE1) was expressed on *Xenopus* oocytes in 1988 (67). The KCNQ1 subunit is the main component of delayed rectifying channels carrying the slow rectifying current in the heart. Thereby, they put their effect on the repolarization phase of cardiac action potential (68, 69). Due to the voltage gated characteristic of the channels, they activate gradually by augmenting membrane potential and result in increasing  $K^+$  current, then their slow inactivation kinetics leads to decrease the current progressively (70). Bounding an additional protein called A-kinase anchor (AKAP), to the cytosolic surface of the  $K_vLQT$  subunits would be able the channels to be regulated by PKA (71). Thereby, slow rectifying current would be increased following sympathetic stimulation (72) as a consequence of stimulating their AKAP domain with PKA which is upregulated by  $\beta$ -adrenergic receptor activation (71). As a result of slow activation behavior, amplitude of  $I_{Ks}$  augments during the plateau phase of the action potential,

however it falls gradually when the membrane potential reach to 0 mV because of inactivation of the channel (73).

#### 1.2.4.1.5.3 Inwardly rectifying K<sup>+</sup> channels

There are only two subfamilies of the inwardly rectifying K<sup>+</sup> channels expressed in heart cells (74). Kir2 channels including Kir2.1 and Kir2.2 which are responsible to I<sub>K1</sub> (75, 76) and Kir3 channels consist of Kir3.1 and Kir3.4 conducting I<sub>KACH</sub>. I<sub>K1</sub> is remarkable in ventricular cardiomyocytes and I<sub>KACH</sub>, a receptor-activated Kir current, has been shown in atrial and SAN cells. In fact vagal nerve and AV node govern the heart rate by mediating the receptor activated channels (74).

#### 1.2.4.1.6 Sustained inward current

Sustained inward current (I<sub>st</sub>) has been found in rabbit SAN in 1995 (77). There is little information about the molecular structure of the channels. It is known as an inward current conducted by some types of channels which possess pharmacological features of voltage-gated Ca<sup>2+</sup> channels such as reactivity to nifedipine and resistance to tetrodotoxin (TTX), whereas is permeable to Na<sup>+</sup> ions. These channels are open in membrane potentials around -60 mV during depolarization phase of action potential (77). Activation of I<sub>st</sub> around diastolic potential range proposes the role of sustained inward current in membrane depolarization (78).

#### 1.2.4.1.7 Tbx3

Tbx3 is defined as one of the critical transcription factors of T-box family which plays a transcriptional repressor role during embryonic period (79, 80). It is established that homozygous mutations of Tbx3 in murine embryos would be lethal (81). Meanwhile, mammary gland abnormalities and limb deformations are reported due to the Tbx3-heterozygous mutations. Moreover, haplo-insufficiency of Tbx3 causes the ulnar-mammary syndrome in human (82, 83).

It needs to be mentioned tumorigenic effect of Tbx3 as well as its developmental role. There are obvious evidences regarding its expression in some types of malignancies such as melanoma, breast and bladder cancers, melanoma (84, 85). The origin of pacemaker activity is SAN and AVN in intact adult heart. One of the specific characteristics of these regions is slow

conduction velocity. The mechanism by which the SAN and AVN differentiate during embryonic period and perform their confined spontaneous activity has been the source of significant interest. Recently, progressive developments have been reported regarding the detection of new cellular mediators including transcription factors correlating with the differentiation regime of sinoatrial cells. Tbx3 is one of those pivotal structures which facilitate the SAN formation (6, 86-88). According to the Mommersteeg *et al.* investigations (88) the SAN stems from the inside region of the fetal heart. Tbx3 and HCN4 expression is one of the specific characteristic of the SAN region. This region is characterized by expression of the T-box transcription factor Tbx3 and the HCN4 ion channel gene. In addition Cx43 which is lead to faster propagation in ventricular cells has not been expressed in embryonic SAN (Fig. 3).

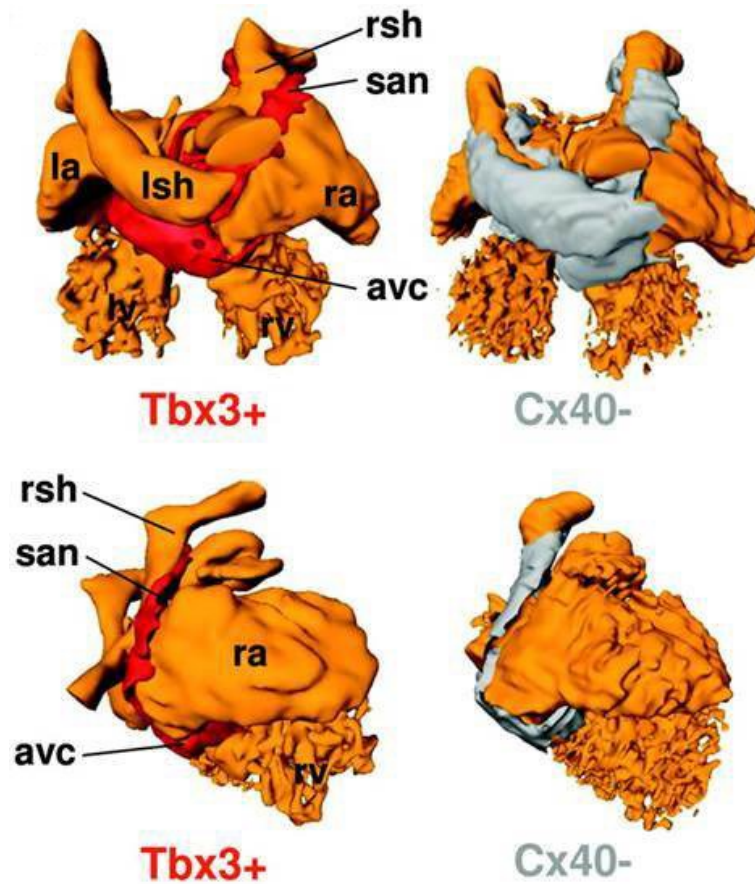


**Figure 3: Schematic model of the embrionic heart presenting the various gene expression zones.** Three-dimensional computational models of E14.5 wild-type embryos which present the heart lumen (red color) from two different prospective including dorsal view (top panels)

and right side view (bottom panels). Myocardium structure defined as *Cx40*-negative myocardium (gray areas) and *Tbx3*-positive myocardium (red areas) which is enclosed in the *Cx40*-negative myocardium. avc, atrioventricular canal; la/ra, left/right atrium; lsh/rsh, left/right sinus horn; san, sinoatrial node. (Reproduced with permission from Mommersteeg M.T. et al. 2007 (88))

### 1.2.4.2 Calcium clock

According to the calcium clock theory, SAN cells possess an intracellular mechanism to modulate the  $\text{Ca}^{2+}$  release from sarcoplasmic reticulum (SR) which is termed local  $\text{Ca}^{2+}$  releases (LCRs). In fact, there is a close interplay between LCR and membrane electrical polarization. The period between the previous peak of membrane  $\text{Ca}^{2+}$  release and the initiation of sarcoplasmic  $\text{Ca}^{2+}$  release is named the local  $\text{Ca}^{2+}$  period (LCP) (Fig. 4) (35).

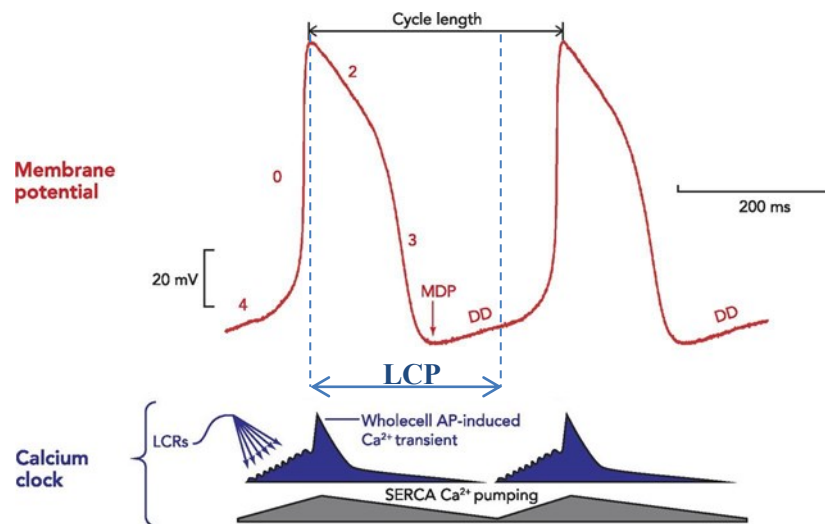


**Figure 4: SAN action potential traces underlying the  $\text{Ca}^{2+}$  transactions.** Normal action potential traces of SAN spontaneous activity labeled with different phases of the AP is shown in top red panel. Different components of the “ $\text{Ca}^{2+}$  clock” are presented at the bottom. It should be noticed concurrency of phase 4 of AP indicating diastolic depolarization with LCR outflow from the sarcoplasmic reticulum. Calcium emanating from SR increase suddenly as a result of  $\text{Ca}^{2+}$ -induced  $\text{Ca}^{2+}$  release called whole cell  $\text{Ca}^{2+}$  transient. (Adapted from Monfredi O. et al. 2013 (35))

SR ryanodine receptors (RyRs) play an important role in creating local calcium sparks in sinoatrial cells (89, 90). Neural stimulation or  $\text{Ca}^{2+}$  overload has no effect on LCR. Generally, local  $\text{Ca}^{2+}$  release starts during the diastolic depolarization concomitant with dissipation of global action potential-induced  $\text{Ca}^{2+}$  transient. It is believed to lead to activation

threshold of SR ryanodine receptors. Consequently, the signals called  $\text{Ca}^{2+}$ -induced- $\text{Ca}^{2+}$ -release goes up gradually which in turn leads to overall  $\text{Ca}^{2+}$  release of the SR, activating the  $\text{Na}^+$ - $\text{Ca}^{2+}$  exchanger, depolarizing the cell membrane and leading to activation of the action potential. Then, a new cycle begins with activation of ATPase pumps of the sarcoplasmic reticulum (SERCA) with replenishing the  $\text{Ca}^{2+}$  stores (Fig. 5) (35). Briefly, the reason of nomenclature of the SR as “ $\text{Ca}^{2+}$  clock” is the periodic regime of LCR (91).

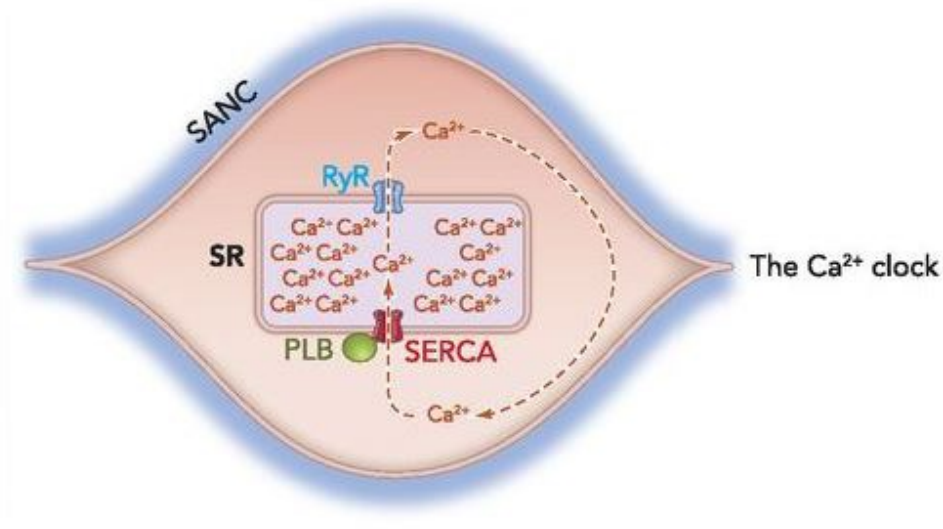


**Figure 5: Schematic model of the calcium clock of the heart.** RyRs and SERCA pump are the main components of the  $\text{Ca}^{2+}$  clock which are responsible to the release and restoring of the  $\text{Ca}^{2+}$  ions, respectively. (Reproduced with permission from Monfredi O. et al. 2013 (35))

#### 1.2.4.2.1 SERCA

Morphologically, the SERCA protein as a transmembrane protein is composed of 3 different components. Its molecular weight is 110 kD. The calcium binding kinetics of the protein is related to the transmembrane part including 2 sites to bind  $\text{Ca}^{2+}$  ions (92). Another domain of the protein is cytoplasmic head. The head domain is divided to 3 separate units including actuator, phosphorylation and nucleotide domains. Each of them plays an important role in function of the pump. The actuator domain acts as a  $\text{Ca}^{2+}$  binding site. While, junction of nucleotide and the phosphorylation domains facilitates ATP hydrolysis (93). SERCA is the most important pump in mammals facilitates refilling of the  $\text{Ca}^{2+}$  capacity of the SR (94). Indeed, it mediates around 92% of mouse and 70% of human cardiac  $\text{Ca}^{2+}$  removal, hence plays a remarkable role in heart contraction activity (94, 95).

#### 1.2.4.2.2 *RyR*

Ryanodine receptors (RyRs) are composed of four subtypes (96). They mediate the join of t-tubules and junctional SR in both cardiac and skeletal myocytes (97, 98). Mammalian tissues are composed of three subfamilies of ryanodine receptors. Skeletal muscles express ubiquitously RyR1 and heart cells are composed of RyR2 and RyR3 isoforms, however RyR3 quantity in the heart is negligible and its function is not critical in cardiac cells function (99). RyRs are essential in cardiac automaticity, so that prenatal knockout of RyR2 could be fatal in mice embryos (100). Cardiac-specific RyR knockout mice in which RyR expression decreased around 50% show cardiomyopathy symptoms in addition to severe arrhythmias and bradycardia (101). RyR2 channels regulation is mediated by several parameters including Calmodulin (CaM),  $\text{Ca}^{2+}$  ions, phosphorylation, thiol oxidation and nitrosylation (102).

#### 1.2.4.2.3 *NCX*

$\text{Na}^+/\text{Ca}^{2+}$  exchanger (NCX) is one of critical membrane components of the cardiac cells that regulates intracellular  $\text{Na}^+$  and  $\text{Ca}^{2+}$  concentrations. Indeed, NCX acts as a transporter passing 3  $\text{Na}^+$  ions for outflowing 1  $\text{Ca}^{2+}$  ion through the cell membrane (103). It is demonstrated even NCX contribution with the L-type  $\text{Ca}^{2+}$  current in regulating the subsarcolemmal  $\text{Ca}^{2+}$  concentration in up-regulated levels (104). Previous studies show the existence of a fuzzy space between the junctional SR and cytoplasmic layer. It could be a proper explanation for occurrence of calcium sparks in limited zones called “diadic clefts” (105).  $\text{Ca}^{2+}$ -induced  $\text{Ca}^{2+}$ -release prominently is confined to the diadic clefts. It is concordant with the ubiquitous distribution of NCX in the T-tubular membranes (106).

#### 1.2.4.3 **Multicellular spontaneous activity**

One of the important issues correspondent with proper function of the SAN is coordination of the dominant pacemaker cells with the surrounding tissue which is termed the source-sink relationship. Nonetheless, how the depolarizing “source” current generated by the SAN propagates and activates the surrounding atrial tissue (current “sink”) remains to be resolved. It has been corroborated that the SAN is not functionally and anatomically continuous with the surrounding myocardium, but rather areas of functional or anatomical conduction block exist, providing discrete pathways at which SAN electrical pulses pass

through to activate the atrial myocardium (107). Previous studies in rabbit, canine, and human SAN have demonstrated the presence of such functional block and discrete exit pathways (108-110). Such source-sink mismatch facilitates electrical insulation of the SAN from the surrounding atrial myocardium. Histological studies over the years have failed to confirm proof of insulating fibrotic sheath surrounding the SAN in the human heart (111, 112) which could increase the probability of the existence of a functional barrier rather than anatomical mismatch. However a recent study showed that the SAN border is composed of fibrosis, fat, and/or discontinuous fibers between SAN and atria (113). It remains that various ion channel and gap junction expression in SAN would be extremely critical in performance of pacemaker cells (114). Therefore, three-dimensional architecture of SAN provides a complex structure comprised of central and peripheral or “paranodal” components composed of variety of ion channels and gap junctions. It is shown that there is a significant difference between electrical characteristics and conduction properties of central and peripheral cells (Fig. 6) (31).

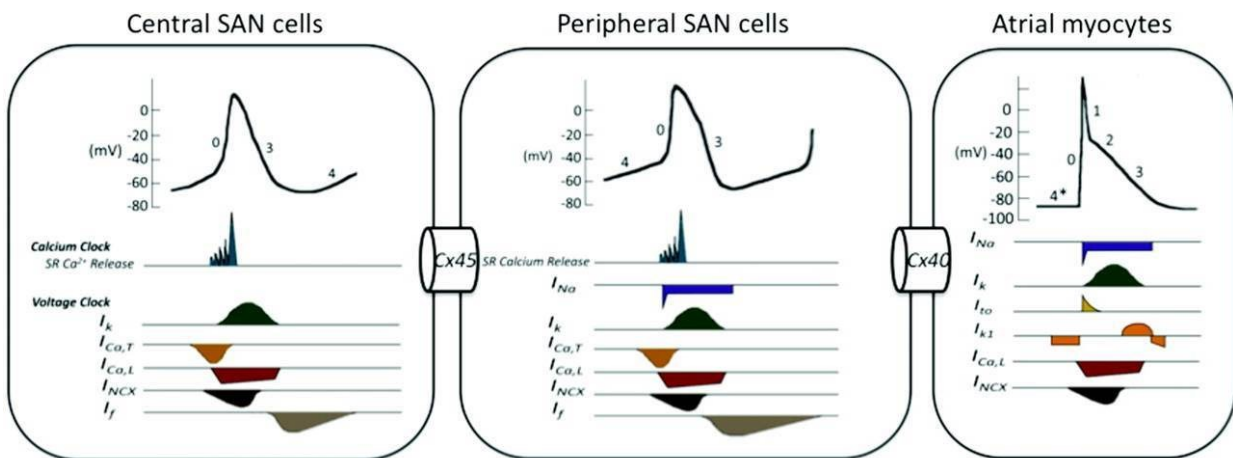


**Figure 6: Different electrical features and various distributions of ion channels and gap junctions between central and peripheral cells of the SAN.** Lack of the fast activating Na<sup>+</sup> channels in the central cells of the sinoatrial node disposes them to have a slow upstroke velocity than peripheral cells, in addition distribution of slow propagating connexin proteins like Cx45 decrease the conduction velocity of the wave propagation in the SAN. (Reproduced with permission from Park D.S. *et al.* 2011 (115))

Regarding the experimental and computational studies, heterogeneity of the pacemaker cells gives an eminent capability to the SAN to perform the normal pacemaking activity and

impulse conduction. To date, two different hypotheses have been proposed to explain the electrical machinery of the SAN. Boyett and colleagues proposed the “gradient model” indicating that AP properties show a gradual transition from the central to peripheral SAN (116), whereas some of the other researchers proposed “mosaic model” suggesting that there are only a few different types of nodal cells which are interspersed with each other and with atrial cells (117). Apart from the cell heterogeneity model, it is well known that central SAN APs show slower rate of upstroke velocity, longer AP duration (APD), and lower potential level of negative maximum diastolic in comparison with peripheral SAN and atrial APs (118). These AP changes are contributed to the differential expression of several ion channels between these areas, as cited above (114).

#### *1.2.4.3.1 Gap junctions*

Conduction of impulse among heart muscles and consequently their coordinated contractions is highly dependent on the heart cells electrical association (119).

Gap junctions are responsible for electrical communication among heart cells. These types of junctions are made up of a network of membrane proteins complexes named as connexons (120). The counterpart complexes from adjacent cells form head-to-head connections with each other, and therefore create gaps with 2-3 nm of diameter between every two neighbor cells. There are six protein subunits in each connexon that surround a central aqueous pore which is 1.5-2 nm in diameter. This pore is wide enough to allow ions, second messengers, and any molecule smaller than ~1 kDa to pass through and reach the cytosol of the neighboring cell (119). It has been shown that Cx43 (the principal connexin of the working myocardium) is not expressed at the center of the SAN while there is expression of Cx45 and Cx30.2, however at the periphery of the SAN, Cx43 as well Cx45 is found (121). It has been shown that in co-cultured cardiac fibroblasts (CFs) and cardiomyocytes (CMs) obtained from neonatal rat ventricles, both Cx43 and Cx45 are expressed (122).

### **1.2.5 Pathology of the rhythm**

One of the congenital or acquired diseases of the SAN is sinus node dysfunction which is also called sick sinus syndrome (SSS). The clinical symptoms of SAN dysfunction include

bradycardia, pause, and arrest of sinus as well as tachy-brady syndrome. In addition, patients with permanent pacemaker implantation usually suffer from SAN dysfunction (123). It has been shown that sinoatrial node remodeling leading to heart failure and fibrillation of atrium is a potential factor involved in the formation of SAN dysfunction in some patients (124-126). Although SAN dysfunction is usually developed in older adults, it can occur at any age, as well. In fact, old age in addition to a couple of cardiovascular diseases is considered as risk factors for the formation of SA node dysfunction. Indeed, it has been shown that there is a positive correlation between the prevalence of cardiovascular disorders due to aging and the prevalence of clinical symptoms of sick sinus syndrome (127).

## **1.3 Pacemakers**

Before the middle of 20th century, the mortality rate of patients with complete heart block was dramatically high (128). Although typical therapeutic approaches have shown encouraging results, numerous limitations remain to be solved (129).

### **1.3.1 Electronic pacemakers**

It is well understood that the heart pacemaker cells are trigger the normal heartbeat, maintain the blood circulation, and adjust the rhythm of heart muscles contractions (130). Any disease that disables or damages pacemaker cells could result in circulatory collapse which must be compensated by the implantation of artificial electronic pacemaker (131). To date, a huge number of patients in the world are candidate for the treatment with artificial cardiac pacemaker devices annually, thereby artificial pacing (ACP) is considered as a safe and proper treatment strategy. Even though, patients treated by permanent pacemakers (PPM) and implantable cardioverter-defibrillators (ICD), associated or not with cardiac resynchronization therapy (CRT), show encouraging prognosis, cardiomyopathy has been reported in some cases due to the artificial anti-physiological ventricular activation induced by the ACP (132). In spite of prominent achievements in electronic pacemaker approaches, there are important drawbacks which need to be solved such as insufficient autonomic reactions, necessity for changing the battery due to its limited life, infections that might arise from the presence of pocket/lead, likely fractures of lead, electromagnetic interference, pacing-induced remodeling,

and troubles in dealing with pediatric patients (133). These complications highlight the interference of alternative methods compatible with the normal and physiological condition.

### 1.3.2 Biopacemakers

Recent studies on biological pacemakers have provided promising results to prevail the shortcomings of the electronic pacemakers. The SAN as a natural biopacemaker is an appropriate template to fabricate the biological pacemakers, since all types of the essential channels and transporters to produce the electrical impulse in mammals' heart are included in the SA node myocyte membrane. Although direct applicability of gene/cell therapy to arrhythmia prevention and treatment is questionable yet, there are encouraging developments in gene and cell transfer techniques promising the feasibility to generate pacemaker cells and related conduction system to trigger and propagate the electrical impulses through the heart (129). The main approach in designing the biological pacemakers is efficiency in generating the heart beats and an optimal safety for the patients, even if the native SAN is not a perfect pacemaker necessarily. The final aim is to produce functional pacemaker cells by generating a net inward current during diastole. One of the methods is gene overexpression for specific proteins, however there are some other alternatives like overexpression of transcription factors to reprogram cardiac myocytes towards induced SAN cells (134) (Fig. 7).

As mentioned above, the ratio of the net inward and outward currents determine the rate of diastolic depolarization. Indeed, any increase in outward currents due to the inward rectifier current  $I_{K1}$  decreases the rate of the spontaneous activity. Therefore, in atrial cells, a constant inwardly pacemaker current will induce the spontaneous activity in a faster rate comparing to the ventricular cells, considering the lower  $I_{K1}$  environment of the atrium versus ventricle. This is applicable in both single cells and multicellular preparations. In multicellular patterns, rate of pacemaker activity in pacemaker cells is affected by the electrical (hyperpolarizing) load generated by surrounding non-pacemaker syncytium (134). Ideal biological pacemaker possesses some characteristic including: 1) stability in generating spontaneous rhythm for whole life of the patients; 2) independency to the external management such as battery or electrode replacement; 3) effective competition in direct comparison with electronic pacemakers; 4) tolerance against inflammation/infection; 5) non-

neoplastic; 6) capability to make rapid changes in heart rate in response to the physiological changes of the body condition; 7) generate electrical pulses propagating through an optimal pathway of activation to maximize efficiency of contraction and cardiac output; 8) possessing no arrhythmic potential; 9) performing a permanent effect rather than temporary palliation (129).

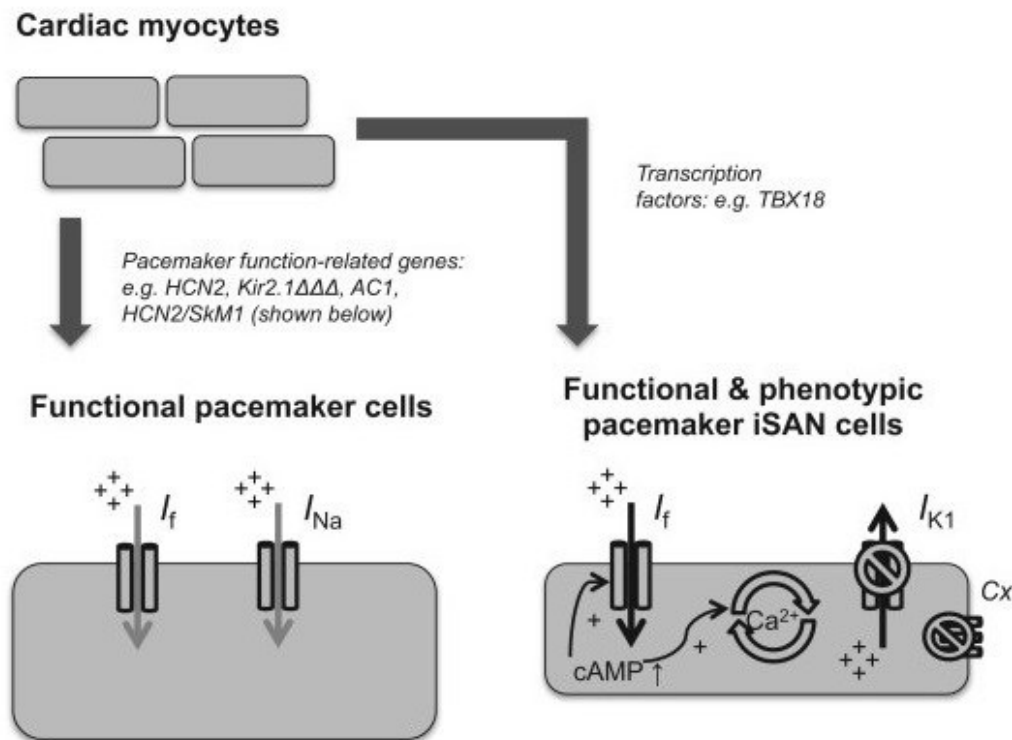


**Figure 7: Different gene therapy-based strategies.** There are two different gene-therapy approaches including pacemaker function-related genes overexpression (left) and transcription factors overexpression (right). (Reproduced with permission from Boink G.J. et al. 2015 (134))

### 1.3.2.1 Gene therapy

Gene therapy is applied to remove a genetic problem or to promote the therapeutic process in target cells. To this point, related genes included in biological vectors (e.g. plasmid DNA or sRNA) are transferred to cells, tissues or organs (135). Gene therapy is applicable through different methods such as inducing the overexpression of a certain molecule,

manipulating the transporting paths of the host cells by means of decoy molecules, deactivating processes by the use of dominant negative molecules or small RNAs. It is also performed through the fixation of genes which have been affected by mutations/deletions or even by introduction of the genetically modified donor cells (136). One of the considerable differences between gene therapy and pharmaceutical treatment is that the gene therapy is able to exclusively change the disease mechanisms while pharmaceutical methods directly aim the symptoms and need long-term treatment. However, it should be taken into consideration that applying gene therapy with the goal of simulation of growth signaling pathways may increase the risk of overgrowth and tumorigenesis (137). One of the other aspects of gene therapy usage is in the field of biopacemaker generation. Some benefits of using gene transfer to generate biomedical pacemakers are high consistency of the generated pacemakers with sympathetic and parasympathetic stimuli, capacity of forming multiple initiation sites within the heart tissue, and permanent effect during the whole life-time. Related preliminary studies were mostly done in the area of inducing a single gene created according to the individual SAN ion channels (134).

The genes expressing HCN channels were transferred to pigs and dogs by means of adenovirus and the result was the generation of a biopacemaker which was sensitive to  $\beta$ -adrenergic modulation. However, significant variations of heart beating rate was diagnosed in biopacemaker rhythms which is considered as a disadvantage of this approach (138, 139). Adenoviral vectors possess strong capability in being transferred to cardiomyocytes, however these vectors can induce only transient gene expression, hence there is doubt about their efficacy as a potential therapeutic tool (140). Apart from adenoviral vectors, lentiviral vectors obtained from the human immunodeficiency virus-1 (HIV-1) are also potent to be introduced to cardiomyocytes (141, 142). However, a significant advantage of lentiviral comparing to adenoviral vectors is that lentiviral vectors are able to be merged with target cell genome. This exclusivity of lentiviral vectors allows them to insert long-term gene expression which makes them to be considered as a suitable candidate in treatment of chronic cases such as SAN dysfunction (143).

Generation of biological pacemaker function is possible through three approaches including increase of neurohormonal activity on heart rate (143, 144), decrease of the current of repolarization (145), and elevation of diastole inward current (146).

### **1.3.2.2 Cell therapy**

Because of the lack of clear-cut successes with viral vectors for gene therapy in particular feeling of dismay associated to the transmission of viral based illnesses, other strategies of creating biological pacemakers have been revised (147).

To this point, either of human embryonic stem cells (hESCs) (which need to be differentiated into a pacemaker cell line through cell culture) (148), or adult human mesenchymal stem cells (hMSCs) could be used (149, 150). The main limitation of using hMSCs in the cell cultures is the need to prescribe the immunosuppressive medications in the animals and this is also a general problem with hESCs. Other issues which should be considered are the risk of evolving neoplastic cells or generation of the other cardiac cell types like ventricular myocytes rather than intact pacemaker cells (147). In contrary to hESCs, multipotent hMSCs do not have the essential subunits of ion channel and therefore are not able to produce cardiac action potential, however, the presence of gap junctions which are built up of Cx43 and Cx40 allow hMSCs to develop pathways for the flow of electric current among neighbor cells (151).

The adult heart has been known as a postmitotic organ for years (152, 153). In fact, it was believed that heart endothelial, smooth muscle, and fibroblast cells could undergo mitosis whereas myocardium cells are fully differentiated and thus do not have the capacity of proliferation any more (152-154). However, it has been revealed that the adult heart include a population of stem and progenitor cells which are capable of proliferating to new cardiomyocytes (155-159).

Cardiac cell therapy (CCT) is a newly introduced technique. ESCs can differentiate into cardiomyocytes. However, using human ESCs is complicated due to a couple of issues. First of all, since human ESCs must be derived from conception products, ethical permission is required. Secondly, immune system should be repressed as ESCs have allogenic effect. Thirdly, following the graft of ESC-derived cardiomyocytes into the host myocardium, there is

a high risk of grafted ESCs death due to ischemia. Fourthly, it has been shown that human ESCs are able to develop to teratomas. Taken together all the above difficulties, the necessity of applying undifferentiated cells, instead of ESCs, for CCT is evident. Considering that adult stem cells can be used as autologous counterparts and show plasticity nature, these cells could be interesting candidates. However, it is not yet confirmed and there are controversies concerning this idea (160-162).

The most challenging issue in the therapeutic approach is to identify the ideal cells. Some of the key points which have to be taken into account are: 1) accessibility and capacitance of the source of cells 2) the period of time needed between yielding and differentiation of cells; and 3) consistency and efficiency of cells in the host organ (163).

In order to reconstitute the damaged myocardium following infarcts in experimental animals, several types of cells have been used including embryonic stem cells, fetal myocytes, skeletal myoblasts, endothelial progenitor cells (EPCs), and mesenchymal or hematopoietic stem cells derived from bone marrow (164).

Although embryonic stem cells are identified as the most favorable and appropriate source for cardiac cell therapy approaches, their disposition to generate teratomas is one of the important limitations for their use. Meanwhile, there are a lot of ethical controversies to use of human source embryonic cells in the field of clinical medicine. Furthermore, the necessity of using immunosuppressive medications in the patients treated by this technic is one the major drawbacks (165). To date, it is supposed that hematopoietic stem cells (HSCs) are the best option in terms of versatility which has been provided new insight into the subject of cardiac cell therapy. Hence, adult HSCs may possess the intrinsic potency to develop the new cell lines as well as embryonic stem cells.

In spite of all endeavors, achieving the ideal approach to cellular therapy for myocardial injury is still a matter of debate (163).

### **1.3.2.3 Re-expression of Tbx3**

In embryonic, post-natal, and adult heart Tbx3 is expressed in any member of the conduction system except from the Purkinje fibres (166). What Tbx3 does in the embryonic heart is that it inhibits the differentiation of sinus node and atrioventricular bundle into

myocardium and therefore allows these cells to become pacemaker (87, 167). One of the other roles of Tbx3 is that, in its high dosage, it promotes the functional development and post-natal homeostasis of the heart conduction system (168). However in vivo culture, it has been shown that abnormal function of Tbx3 in embryonic atrial myocytes causes Gja5 and Gja1 inhibition, HCN4 stimulation, and the development of pacemaker in abnormal places within atrial myocardium (87). Tbx3 is able to repress the gene expression of working myocardium, stimulate DD, change the basic mechanism of spontaneous function, and reduce the conduction velocity. In addition, Tbx3 inhibits the conduction of  $I_{Na}$  and  $I_{K1}$  among neighboring cells. Altogether, it can be concluded that Tbx3 has the capacity to change working myocardial phenotype to a pacemaker phenotype and thus scientists can benefit from this property of Tbx3 in developing biological pacemaker. The heart rate in HCN channel gene transferred cases is lower than the optimal rate. This suboptimal function may be due to the mismatch between the HCN over-expressed cells and the normal surrounding cells. The best solution to bypass this mismatch could be the expression of Tbx3 and HCN or other pacemaker genes, at the same time (34).

#### **1.3.2.4 Monolayer of neonatal cardiomyocytes as a biopacemaker model**

Mammalian cardiomyocytes mostly terminate their differentiation after birth. Fully differentiated cardiomyocytes are not able to proliferate any more although they can keep their hypertrophic growth during the whole life-time. Cardiomyocytes undergo synchronized changes during differentiation. These changes include a decrease in the expression level of cell division and embryonic markers in CMs (169), an increase in the expression of CM differentiation genes; and development of sarcomeres which are involved in the formation of the myoskeletal system in CMs. Other compartments involved in establishment of mechanical and electrical communication between adjacent CMs are intercalated discs, which consist of gap junctions, adherents junctions and desmosomes (170, 171). After birth, heart tissue becomes stiffer through an increase in the level and cross-linking of the extracellular matrix (ECM) proteins (172-174). During the first 1-2 weeks of murine postnatal life, heart undergoes a temporary regenerative phase, before the reduction in the DNA-synthesis of cardiomyocytes (175, 176) and this regenerative period disappears during the first week after birth (177). In addition, appearance of binuclear cardiomyocyte happens in mice and rats

during early postnatal life (169, 176). Accordingly, neonatal rat ventricular myocytes (NRVMs) are ideal models for in vivo studies of heart cellular electrophysiology. It has been shown that following a confluent monolayer culture of NRVMs, these cells undergo spontaneous beating for up to 40 days (178, 179). Interestingly, monolayer culture of NRVMs show a more efficient electrophysiological property comparing to isolated single cells which could be due to the physical communication among neighboring cells and wave front distribution (180).

## **1.4 Phorbol 12-myristate 13-acetate (PMA)**

As mentioned above, there is a clear link between Tbx3 and expression of key players of the membrane clock and some studies suggested that PMA could interact with Tbx3 as we will discussed below.

### **1.4.1 PMA link with Tbx3**

There are clear evidences regarding the significant level of Tbx3 expression with PMA in human PNT1A and MRC-5 cell lines. The results confirmed that PMA significantly increases Tbx3 expression as a consequence of upregulating some of the AP-1 subfamilies proposing the role of PMA signaling pathway in Tbx3 modulation which is correspondent with increment of Tbx3 in both of the tested cell lines (181).

### **1.4.2 Structural and physiological features**

Molecular construction of phorbol esters are built of the tetracyclic diterpene carbon pivot termed as tigliane which is the alcohol part of the phorbol esters. Tiglane is composed of 4 components including A, B, C, and D subunits. These compounds are responsible for hydroxylation of the basic structure at bonding positions to acid moieties (182). PMA is known as an activator of the certain types of protein kinase C (PKC) such as the Ca<sup>2+</sup>-dependent or classical PKC (cPKC) ( $\alpha$ ,  $\beta$ I,  $\beta$ II and  $\gamma$ ) isoforms as a Ca<sup>2+</sup>-dependent subtypes and the novel PKC (nPKC) isozymes ( $\delta$ ,  $\epsilon$ ,  $\eta$ ,  $\theta$  and  $\mu$ ) which have no Ca<sup>2+</sup>-binding domain. The novel isozymes are regulated by phosphatidylserine (PS), 1, 2-diacylglycerol (DAG) and unsaturated fatty acids instead of Ca<sup>2+</sup> ions (183). Indeed, PMA mimics DAG role to activate

two of the three protein kinase C isozymes via the tandem cysteine-rich repeat of their C1 domains (184, 185). It is well identified that, PMA increases target-gene expression of a transcription factor family called the activator protein-1 (AP-1) (186, 187). AP-1 transcription factors (Fos, Fra-1, Fra-2, FosB, c-Jun, JunB and JunD) mediate some cell signaling procedures like differentiation, proliferation, cellular malignancy and apoptosis (188, 189). PMA can activate AP-1 factors by mediating the PKC dependent transcriptional activation. According to the Kieser *et al.* studies (190) performed on NIH3T3 cells, the JunB promoter targeted by the PKC- $\theta$  isoform can directly target the *JunB* promoter. There is another report which presents PKC- $\epsilon$  upregulatory effect on JunB via the mitogen-activated protein kinase signaling pathway (191). Hence, PMA regulating mechanism of AP-1 is strongly dependent on the different PKC isoforms (181).

PMA governs also some other transcription factors like ETS and GATA family through the MAP kinase pathway (192, 193).

Recently, it has been demonstrated that PMA differentiates Mesenchymal stem cells (MSCs) to the cardiogenic cells through the PKC pathway. The sudden death ratio in infarcted rats which were grafted by these treated cells decreased significantly (194).

### **1.4.3 Pathophysiological effects**

There are several reports regarding the detrimental effects of phorbol esters. It was shown that 12-O-Tetradecanoyl-phorbol-13-acetate (TPA) has tumorigenic properties due to the alteration of the biochemical pathways correspondent to the proliferation of the cells following the augmentation of PKC and ornithine decarboxylase (ODC) activity, increment of DNA synthesis, prostaglandin synthesis, and by oxidative stress generation (195).

According to the investigations on blood cells, PMA is defined as a mitogen of B type cells which leads to chronic lymphocytic leukemia (CLL) (196,197) in which PMA differentiates B cells independent of a T cells (197). Murine skin cells treatment with TPA has shown to cause a series of biochemical alterations such as sustained epidermal hyperplasia, formation of dark basal keratinocytes, formation of free radical oxygen in epidermis, augmentation of epidermal cyclooxygenase and ODC activity and lipoxygenase activities (198). Collagen production increased in intestinal fibrosis model mice treated with PMA due

to the activation of nuclear factor-kappa-B (NF $\kappa$ B) through the PKC mediating manner (199). PMA conditioning of A549 cell lines showed a significant increase in producing inflammatory factors like Interleukin 6 IL-6 (200).

Furthermore, there are various reports related to the toxicity symptoms in the animals consuming the plants enriched of ester components. In addition, ester components has been used against different species of mollusks (182).

## **1.5 HCN blockers**

The crucial role of the funny current in generating the diastolic depolarization phase of the action potential in SAN makes HCN channels interesting pharmacological targets. It is supposed that the HCN blockers are able to reduce the heart tissue damages as a result of oxygen insufficiency. There is several types of HCN blockers termed as specific “heart rate lowering” drugs used in experimental and therapeutic treatments (201). Ivabradine has been considered as a unique drug with least side effects and highest selectivity to the channels (43). Ivabradine blocks the open channels, since its binding sites are exposed in opening phase of the channel (202). In addition, the use-dependent manner of the drug predisposes it as an excellent candidate in therapeutic approaches (203).

## **1.6 Project hypothesis**

Our hypothesis is that PMA can favor re-expression of Tbx3 inducing an increase in HCN expression thus augmenting the membrane clock in cultured neonatal cardiomyocytes. The increased membrane clock activity would lead to increased and stabilized rate of spontaneous activity with greater synchronization in multicellular monolayers.

## 2 ARTICLE

The paper is the result of interdisciplinary work and will be submitted to PNAS. Here is the role of each co-author.

Yashar Alami Alamdari performed the experiments and did the data acquisition and part of the statistical analysis.

James Elber Duverger is a PhD candidate in Biomedical Engineering. He helped in analyzing the optical mapping data, developing the analysis algorithms and writing the code.

Alireza Aghighi is a PhD candidate in Biomedical Engineering. He participated in designing the simulation software.

Alexandre Blanchette is a research assistant in Montreal Heart Institute. He helped in performing qPCR experiments.

Jonathan Béland is a PhD candidate in the Department of Cellular and Integrative Physiology. He participated in designing the cell culture method and did preliminary experiments with PMA.

Estelle Petit-Jean was a summer student at the Montreal Heart Institute. She participated in designing the cell culture method and did preliminary experiments with PMA.

Jonathan Ledoux is an associate professor in the Department of Medicine. He helped with the qPCR experiments and writing the paper.

Philippe Comtois is an associate professor in the Department of Cellular and Integrative Physiology. He designed the project, analyzed, interpreted the data, and helped write the modeling code and the paper.

**Biopacemaker acceleration without increased synchronization by chronic exposure to  
phorbol myristate acetate**

Yashar Alami Alamdari<sup>1,2,\*</sup>, James Elber Duverger<sup>1,3,\*</sup>, Alireza Aghighi<sup>1,3</sup>, Alexandre Blanchette<sup>1</sup>, Jonathan Béland<sup>1,2</sup>, Estelle Petit-Jean<sup>1</sup>, Jonathan Ledoux<sup>1,2</sup>, Philippe Comtois<sup>1,2,3,#</sup>

<sup>1</sup> Research Centre , Montreal Heart Institute , Montreal, H1T 1C8, Canada

<sup>2</sup> Department of Molecular and Integrative Physiology, Université de Montréal, Montreal, H3T 1J4, Canada

<sup>3</sup> Institute of Biomedical Engineering, Université de Montréal, Montreal, H3T 1J4, Canada

\* These authors contributed equally.

**# Corresponding author:**

Philippe Comtois, PhD  
Montreal Heart Institute – Research Centre  
5000 Belanger E.,  
Montreal, Qc  
Canada, H1T 1C8

There is no potential conflict of interest to disclose.

This work was supported by the Montreal Heart Institute Foundation and the Natural Sciences and Engineering Research Council of Canada (NSERC).

## **Abstract**

The study of collective behaviour of interconnected elements is important to the general theory of reaction-diffusion systems and is applicable to different areas of science from physics to physiology. The cardiac tissue is such a biological system with interconnected cells responsible for spontaneous and propagating electrical activity crucial to the normal heart function. Spontaneous electrical activity, designated the “membrane” or “voltage” clock, is the result of a delicate balance between inward and outward currents resulting from the activity of several voltage-dependent ion channels. Primary cultures of isolated neonatal ventricular cardiomyocytes revealed the existence of both pacemaker (PM) cells and resting excitable cells. The transcription factor T-box3 is central to the developing sinus node and atrioventricular unit, allowing these cells to develop a pacemaker phenotype. Re-expression of Tbx3 has been shown to be induced by Phorbol 12-myristate 13-acetate (PMA) in breast cancer cells. Here, we show that chronic exposure to PMA can modulate the multicellular spontaneous activity of neonatal cardiomyocytes through expression of T-box3 leading to higher expression of HCN4 and decreased conduction velocity. The increased activity of the voltage clock yields faster rate and more stable spatial-temporal spontaneous activity but decreased synchronization of activation in our experiments. Simulations confirm the synergistic role of increase cellular spontaneous activity rate and decreased intercellular coupling of sample mean rate of activity. Although decreasing the intercellular coupling helps spontaneous activation it has a deleterious effect on synchronization. This knowledge could be important in the process of creating optimized and robust biological pacemakers, an alternative to electronic pacemakers in the treatment of bradycardia.

## **Introduction**

The study of collective behaviour of interconnected elements is important to the general theory of reaction-diffusion systems and is applicable to different areas of science from physics to physiology (1-4). Diverse behaviours can be observed in networks of connected elements including a variety of synchronous regimes, pattern formation, spiral wave propagation, and spatial-temporal chaos. The cardiac tissue is such a biological system with

interconnected cells responsible for spontaneous and propagating electrical activity crucial to the normal heart function. Spontaneous activity can be physiologically necessary (sinoatrial node as the primary pacemaker site, atrioventricular node, and Purkinje fibers) (5) or detrimental (ectopic activity leading to arrhythmia genesis) (6). Spontaneous electrical activity, designated the “membrane” or “voltage” clock, is the result of a delicate balance between inward and outward currents resulting from the activity of several voltage-dependent ion channels (5). An increase in membrane potential (slow diastolic depolarization) above threshold initiates an action potential through the sequential opening and closing of membrane ionic channels, generating membrane currents that trigger contraction of the cell (7). HCN forming the funny current ( $I_f$ ), L-type  $Ca^{2+}$  channels, T-type  $Ca^{2+}$  channels, and delayed rectifier  $K^+$  channels are among the ion channels expressed at the cardiomyocyte plasma membrane that contribute most to the membrane clock (8).  $I_f$  is believed to be a key player in pacemaker driving capabilities (9). In the intracellular space,  $Ca^{2+}$  cycling contributes to activation through  $Ca^{2+}$  release and reuptake from the sarcoplasmic reticulum and membrane flux via the  $Na^+/Ca^{2+}$  exchanger, and has been designated the “calcium” clock (10).

An example of physiologically-relevant system is the monolayer cultures of neonatal rat ventricular myocytes (NRVMs) that is often used as experimental models to study multicellular cardiac electrophysiology (11-14). These monolayers usually exhibit electrical spontaneous activity (15-17), defined as the ability to generate action potentials without external (electrical, mechanical, or chemical) stimulations. Primary cultures of isolated NRVMs revealed the existence of pacemaker (PM) cells and resting excitable cells (18). Thus, it is highly probable that monolayers of NRVMs are heterogeneous networks of these two cell types. The spontaneous beating rate in these cultures is reportedly modulated by plating density (19). Understanding the impact of density and spatial distribution of PM cells on automaticity of the global cardiac network is highly relevant to several clinical situations, such as the reliability of heart activation by the sinoatrial node (SAN) and the initiation of arrhythmias by cells susceptible to delayed afterdepolarizations. When the heart is being activated, the SAN PM cells act as initial depolarising current sources and the surrounding myocardial cells as related sinks. Considering the electrotonic depression of the SAN by electrical connection with the myocardium, the number of PM cells must be large enough to

initiate this activation (20, 21). We recently showed that a clear non-linear dependency of spontaneous multicellular activity (occurrence and amplitude of spontaneous period) on the spatial pattern of pacemaker cells exists (20).

As a matter of fact, the spontaneous rate and minimum diastolic potential of the SAN dramatically increase when it is isolated from atrial tissue (22). This knowledge is used in the process of creating biological pacemakers, an alternative to electronic pacemakers in the treatment of bradycardia (23). Indeed, to create a sustained PM function in canine ventricle, xenografted cell-containing fluid injected in the left ventricular myocardium must contain at least 700,000 adult human mesenchymal stem cells, and consist of ~40% PM cells (24). This is a clear example of where the number of PM cells is important, and must be locally high enough to activate the surrounding tissue.

Monolayer cultures of NRVMs may provide a useful biological tool to investigate the role of PM-cell-cluster patterns on automaticity and therefore gain better understanding of clinical issues, including creation of biopacemakers (25). However, the seeding process is random and the final spatial distribution of the 2 cell types is unknown. Experimental assessment of density and spatial distribution of PM cells within a monolayer remains an unsolved problem. Mathematical modelling may help gain insight into the complex source-sink mechanism behind the effects of PM cell clusters on the spontaneous behaviour of the 2D network. Rather than concentrating on PM cell aggregate spatial characteristics, simulation studies on monolayers of excitable cells have predominantly focussed on ion channel properties (26, 27), effects of coexistence of non-excitable cells (17, 28, 29), intercellular electrical connectivity (30-33), or sink (cells clamped at steady state potential) and break (regions with no conductivity) densities (34).

T-box factor 3 (Tbx3) is a transcription factor required for development of many tissues. Tbx3 is specifically expressed in components of the cardiac conduction system at different development stages (35). In the embryonic heart, Tbx3 suppresses differentiation into excitable contractile cardiomyocytes in the developing sinus node and atrioventricular unit, allowing these cells to develop the pacemaker phenotype (36, 37). Moreover, ectopic activation of Tbx3 in embryonic atrial myocytes *in vivo* resulted in induction of HCN4, and

the formation of ectopic pacemaker sites within the atrial myocardium (37). Tbx3 can also reprogram differentiated adult cardiomyocytes to a phenotype with pacemaker properties (38).

Re-expression of Tbx3 induced by Phorbol 12-myristate 13-acetate (PMA) has been shown to occur in breast cancer cells (39). On the other end, PMA applied to cardiomyocytes is known to induce the expression of immediate early genes (40) and secondary response genes such as atrial natriuretic factor (41),  $\beta$ -myosin heavy chain (42, 43), and  $\alpha$ -skeletal actin (44). PMA exposure also increases the overall cell protein expression (45) yet decreases the expression level and function of the sarcoplasmic reticulum  $\text{Ca}^{2+}$ -ATPase in NRVMs (46-48). PMA exposure for 48–72 h increased the membrane current through the  $\text{Na}^{+}/\text{Ca}^{2+}$  exchanger but downregulated the transient outward and delayed rectifier  $\text{K}^{+}$  currents (49).

Here, we show that chronic exposure to PMA can modulate the multicellular spontaneous activity of neonatal cardiomyocytes through expression of Tbx3 leading to higher expression of HCN4 and decreased conduction velocity. The increased activity of the voltage clock yields faster rate and more stable spatial-temporal spontaneous activity. Simulations confirm the synergistic role of increase cellular spontaneous rate and decreased intercellular coupling of sample mean rate of activity. Although decreasing the intercellular coupling helps spontaneous activation it has a deleterious effect on synchronization.

## Methods

### Cell isolation and culture

The use and care of the animals in these experiments were approved by Montreal Heart Institute Animal Research Ethics Committee and were concordant with the Canadian Council on Animal Care guidelines. 1- to 3-day-old Sprague-Dawley rats were decapitated. Isolation was done following the protocol of the neonatal cardiomyocyte isolation kit (Worthington, Lakewood, NJ, USA). In brief, beating hearts were extracted immediately and immersed in ice-cold  $\text{Ca}^{2+}$ - and  $\text{Mg}^{2+}$ -free Hank's balanced salt solution. Ventricular muscle was excised and tissue was minced on ice into 1–3mm pieces. The mixture was exposed to enzymatic digestion (50  $\mu\text{g}/\text{mL}$  trypsin and 136  $\mu\text{g}/\text{mL}$  collagenase) to release cardiomyocytes. Isolated cells were counted at a density of  $3 \times 10^6$  cells  $\text{mL}^{-1}$ . After isolation, cells were plated at a

density of  $9 \times 10^5$  cells per 20 mm diameter well glass-bottom culture dishes (D29-20-0-N, In vitro Scientific, Sunnyvale, CA) pre-coated with 0.2% porcine-derived gelatin (G1890, Sigma-Aldrich, Oakville, Ontario, Canada) and 0.00125% fibronectin solution (F1141, Sigma-Aldrich). Cells were cultured in an incubator (37°C, 5% CO<sub>2</sub>) in phenol-free Dulbecco's modified Eagle's medium (DMEM, 319-050-CL, Wisent, St-Bruno, Canada) with 1% penicillin/ streptomycin (P/S, 450-201-EL, Wisent) and 10% foetal bovine serum (FBS, SH30396.03, Fisher Scientific). After 24h foetal bovine serum was removed of the culture medium and 1µM Phorbol 12-myristate 13-acetate (PMA, P8139, Sigma-Aldrich) was added for samples in PMA group. The dishes were incubated for an additional 48h. Samples for the control group (CTL) were also cultured in parallel without PMA. Herein, the specified time points (either at 24h and 48h) corresponds to the time following complete removal of FBS and start of chronic exposure to PMA in the PMA group.

## **Videomicroscopy**

Method and analysis of videomicroscopy (VM) study was done as previously described (50). Here recordings of 30 s duration after changing to DMEM without PMA were performed at two time points specifically at 24h and 48h post PMA, to determine the mean spontaneous frequency (<freq>) and temporal standard deviation of interbeat period (std(T)).

Moreover, acute effect of ivabradine (SML0281, Sigma-Aldrich) dissolved in pure dimethyl sulfoxide (DMSO, 4-X-5, ATCC, Manassas, VA) with the concentration of 3µM (51) was tested to evaluate the spontaneous frequency variations in PMA-48h group.

## **Optical mapping setup**

For the optical mapping experiments, the membrane potential dye FluoVolt (F-10488, Life Technologies, Carlsbad, CA) was used to stain cells for fluorescence imaging experiments. To prepare the solution, 5 µg of FluoVolt™ dye 1000X (Component A) was dissolved in 50 µL of 100X PowerLoad™ concentrate (Component B) which were supplied with the kit. The dissolved dye was added to 5mL DMEM. Post-cultured dishes were loaded with 200 µL/well of staining solution and incubated for 30 min. The dye was then washed out with DMEM and replaced with fresh DMEM.

Mapping experiments were performed with an in-house setup using a high-speed CCD camera system ( $80 \times 80$  pixels, RedShirtImaging, LLC, Decatur, GA). The dye received filtered excitation light from a quartz tungsten halogen lamp (Oriel Instruments, Stratford, CT). The filters used for excitation and emission were  $\lambda_{\text{excitation}} \approx 480 \pm 20$  nm (Chroma Technology, Bellows Falls, VT) and  $\lambda_{\text{emission}} \approx 535 \pm 25$  nm (Semrock, Rochester, NY), respectively. The system was set to image a field of view of  $\sim 4$  cm<sup>2</sup> and the acquisition frame rate was 500 Hz for all experiments. Optical mapping (OM) acquisitions were acquired in both spontaneous and point stimulation mode to evaluate spontaneous frequencies (SF), activation patterns, voltage threshold, and conduction velocity (CV). The recording period for each acquisition was 15 s.

## **Stimulation setup and protocol**

Point stimulation was done for evaluation of conduction velocities. The point electrode consisting of a 1 mm diameter wire (AS633, Cooner wire, Chatsworth, CA) inserted inside a syringe needle which serves as a ground. The wire tip was the anode and the syringe tip the cathode. The programmable voltage source and setup used has been previously described (52). Pacing at CL of 500, 750, 1000, 1250, and 1500 ms was done at 48h post-PMA for both CTL and PMA groups after positioning the electrode at the border of the sample with a voltage 1.5 x threshold.

## **Optical mapping data analysis**

A custom analysis software was developed in Matlab (R2008, MathWorks, Natick, MA). Each video file was first spatially (gaussian lowpass filter with size of  $7 \times 7$  pixels and standard deviation of 2.5) and temporally (110 Hz lowpass filter, 60 Hz band-stop filter, 5-sample window moving average smoothing) filtered. Then a mask was applied to only consider the pixels with action potential optical signal. The first time derivative of fluorescence ( $dF/dt$ ) was used to detect activation times (s), propagation times (ms, activation times minus by the time of 1<sup>st</sup> activation site of the beat) and spontaneous cycle lengths (ms). CV (cm/s) was estimated by Bayly's method (53).

Further analysis was performed in post-processing. The activation delay ( $\delta_{act}$  in s/cm), characterizing how neighboring sites are synchronized, was assessed by calculating the inverse of the conduction velocity in spontaneously beating monolayer. To evaluate the spatial stability of the first initiation site, shift of the first initiation site was calculated by Euclidian distance on a beat-to-beat basis for each recording. First initiation sites were defined as centroid of pixel clusters having the lowest activation times for a given beat. Furthermore, to characterize the stability of the propagation pattern, the average interbeat propagation pattern difference (ms) was also calculated from the beat-to-beat difference of the normalized activation maps (activation maps where the mean of each map was subtracted).

## **qPCR method**

For quantitative real-time PCR, total RNA from freshly isolated CMs was extracted using RNeasy Mini kits (Qiagen) from 48h post-PMA and related control samples. The purity and concentration of RNA were assessed using a Nanodrop spectrophotometer. Next, reverse transcription was performed using iScript kits (Bio-Rad) according to manufacturer's instructions. Primers (Table 1) and 1 $\mu$ g of cDNA were used for PCR amplification in a final volume of 20  $\mu$ l. qPCR was performed on a Stratagene MX3000 system using iTaq fast Syber Green with ROX (Bio-Rad) and values were normalized to the geometric mean of Glyceraldehyde 3-phosphate dehydrogenase (GAPDH) Gapdh, hypoxanthine guanine phosphoribosyl transferase (HPRT) and Beta-2 microglobulin ( $\beta$ 2M) expressions.

## **Statistical analysis**

All data reported are means $\pm$ SEM. Statistical significance was determined for all individual data points and fitting parameters using one-way ANOVA unless stated otherwise. Analyses were performed in R (version 3.1.3). A p value of less than 0.05 was considered statistically significant.

## **Mathematical model**

A discrete monolayer of cardiac cells has been implemented with a 6-neighbor connectivity unless at the boundary where the number is decreased to between 2 and 5

depending on the position at the boundary (see suppl. fig. 1). The coupling coefficient between the cells ( $\sigma_{\text{cell}}$ ) is constant and uniform throughout the 2D layout. Two different  $\sigma_{\text{cell}}$  were simulated corresponding to the control condition (CTL:  $\sigma_{\text{cell}} = 4.0$ ) and decreased coupling ( $R_{\text{increased}} : \sigma_{\text{cell}} = 2.47$ ). Assuming a cell dimension of  $30 \mu\text{m}$  (54), the control condition yields an effective CV of  $\sim 20 \text{ cm/s}$  while the decreased coupling results in a CV of  $\sim 15 \text{ cm/s}$ .

The ionic model that was implemented is based on the Luo-Rudy model and was used as in these studies (29, 33). This choice was based on simplicity of the model (limited number of variables and parameters) and that spontaneous activity can be easily induced by applying a bias current ( $I_{\text{bias}}$ ) in the voltage ordinary differential equation. Spontaneous activity first appears for  $I_{\text{bias}}$  slightly greater than 2.5 with a long period ( $T_{\text{cell}} > 2 \text{ s}$ ) up to  $I_{\text{bias}} = 4.7 \mu\text{A}/\text{cm}^2$ . The minimum period of activity is found around  $I_{\text{bias}} = 4.04 \mu\text{A}/\text{cm}^2$  with period of  $\sim 0.54 \text{ s}$  (see suppl. fig. 2 for details on the bifurcation). We assumed that our cultures are based on the co-existence of two populations of cardiomyocytes corresponding to resting but excitable cells and pacemaker cells (PMs, spontaneously beating cells) as studied previously (20). Here, two sets of  $I_{\text{bias}}$  values were used in two groups of simulation. In CTL,  $I_{\text{bias}} = 0 \mu\text{A}/\text{cm}^2$  for resting but excitable cells and  $I_{\text{bias}} = 3 \mu\text{A}/\text{cm}^2$  for pacemaker cells. To mimic very simplistically an increase in spontaneous activity through increased funny current (group labeled  $\text{Rate}_{\text{faster}}$ ), all  $I_{\text{bias}}$  values have been offset by 0.5 such that  $I_{\text{bias}} = 0.5 \mu\text{A}/\text{cm}^2$  for resting but excitable cells and  $I_{\text{bias}} = 3.5 \mu\text{A}/\text{cm}^2$  for PM cells.

The spatial distribution of the PM cells within a  $200 \times 200$  cell layout has been done using a stochastic algorithm (55, 56). In summary, the starting point was an empty lattice of dimension  $200 \times 200$  cardiomyocytes. For the first iteration, an initial PM cell was randomly seeded in one of the available sites. The status of a site containing a PM cell was referred to as a PM site. During the second and following iterations, a random number  $p$  ( $0 \leq p \leq 1$ ) was drawn from a uniform distribution and compared with a user-defined iteration-independent parameter  $p_{\text{thr}}$  ( $0 \leq p_{\text{thr}} \leq 1$ ) that decided whether the new PM cell would or would not be in contact an existing cluster (a group of one or more interconnected PM cells). Here, all samples were created using  $p_{\text{thr}} = 0.3^{1/4}$  as it is at the transition between low and high minimal density for multicellular spontaneous activity to occur and PM cell density of 30% (20).

The model was numerically integrated using a forward Euler numerical scheme with time step of 10  $\mu$ s with a simulation time of 10 s. A total of 100 simulations per group were used as a final set of *in silico* data. Four different groups were simulated: CTL, Rate<sub>faster</sub>, R<sub>increased</sub>, and combined Rate<sub>faster</sub> + R<sub>increased</sub>.

## Results

### Increased frequency and temporal stability of spontaneous activity

The temporal dynamic of spontaneous contraction was studied by videomicroscopy at 24h and 48h post-PMA (labeled PMA-24h and PMA-48h) with equivalent control (CTL-24h and CTL-48h). PMA increased the number of samples with spontaneous activity. At 24h, 89% of samples had spontaneous activity in CTL compared to 94 % with PMA (the ratio of the samples with spontaneous activity is 280/312 in CTL and 289/305 in PMA groups,  $p < 0.05$ ). This difference between the groups increased more importantly at 48h with 49 % for CTL compared to 95 % with PMA (the ratio of the samples with spontaneous activity is 131/265 in CTL and 242/253 in PMA groups  $p < 0.0001$ ). The distributions of frequencies are presented in fig. 1A which show that PMA has an increased frequency of activity compared to CTL with some samples having very rapid activity ( $> 3$  Hz). With time, PMA keeps the monolayer spontaneous activity relatively stable while a clear bimodal distribution of spontaneous activity is found in CTL with one at low frequency activity and others with high frequency. We label the high frequency ( $> 3$ Hz) activity as reentrant based on a previous study (50). In total, 43% of total samples corresponded to reentrant activity in control compared to 0.4% with PMA. After removal of the samples with reentrant activity, a mean frequency of  $1.09 \pm 0.03$  Hz compared to  $1.57 \pm 0.03$  Hz with PMA at 24h (the ratio of samples without reentry is 248/280 in CTL and 248/289 in PMA groups). The changes became more important at 48h where the frequency is now of  $0.55 \pm 0.06$  Hz in CTL compared to  $1.30 \pm 0.03$  Hz in the PMA group (the ratio of samples without reentry is 74/131 in CTL and 241/242 in PMA groups  $p < 0.0001$ ). Temporal stability of spontaneous (but not reentrant activity) was evaluated and is presented in panel B. A clear significant increased stability in the PMA group is found (red points) at both time points while the stability in the control group decreases with time

(24h: average of  $0.26 \pm 0.03$  s in CTL-24h vs.  $0.05 \pm 0.004$  s with PMA-24h,  $p < 0.0001$  ; 48h: average of  $1.99 \pm 0.27$  s in CTL-48h vs  $0.06 \pm 0.01$  s in PMA-48h,  $p < 0.0001$ ). An example of a videomicroscopy signal is shown in panel C for spontaneous activity in CTL (top), having a clear variation in the interbeat intervals, and for a sample in PMA group (bottom) with clear fast and stable contractile activity ( $\langle \text{freq} \rangle$  of 0.56 Hz in CTL vs. 1.3 Hz with PMA;  $\text{std}(T)$  of 0.75 s in CTL vs. 0.02 s with PMA).

Spontaneous activity was also studied by optical mapping at 48h post-PMA. Evaluation of the rate of activity resulted in an average decrease in period of activity with PMA compared to control (fig. 2A; pre-stim  $3.1 \pm 0.5$  s in CTL-48h vs.  $2.6 \pm 0.1$  s in PMA-48h,  $p < 0.05$ ; post-stim  $3.3 \pm 0.4$  s in CTL-48h vs.  $2.4 \pm 0.2$  s in PMA-48h,  $p < 0.05$ ), a characteristic that correlates with the videomicroscopy data. A note that the protocol of electrical stimulation used to measure conduction properties (see method section) did not significantly affect the spontaneous rate (pre-stimulation vs. post-stimulation bars in panel A). Examples of spontaneous activity are presented in panel B for a CTL sample (top, blue line) and PMA sample (bottom, red line). Similarly to the videomicroscopy data, the activity in CTL-48h is slower with greater interbeat interval than in the PMA-48h sample.

## **Re-expression of Tbx3 and HCN4 stabilizes the spontaneous activity of the monolayer**

Evaluation of expression of Tbx3 and HCN4 at the mRNA level was done by qPCR and is shown in figs. 3 A and B. A trend for increased in Tbx3 mRNA is found with PMA at 48h compared to CTL ( $p=0.07$ ). However, there is a significant increase of  $\sim 75\%$  in HCN4 mRNA expression at PMA-48h ( $p<0.02$ ). To test for the role of HCNs in the spontaneous activity with PMA, the effect on the frequency of activity under pharmacological block by Ivabradine was tested. Addition of Ivabradine resulted in a significant and clear decreased of spontaneous rate from  $1.2 \pm 0.2$  Hz to  $0.68 \pm 0.05$  Hz in paired samples ( $p<0.05$ , paired t-test). The mean frequency with Ivabradine is close to the mean in CTL of  $0.55 \pm 0.06$  Hz as presented in the previous section.

## **Conduction velocity is decreased with chronic exposure to PMA**

Conduction properties were evaluated using local bipolar stimulation at 48h. Treatment with PMA resulted in 1.44 fold increase of voltage threshold for initiation of propagating waves with a CL of 1000 ms (fig. 4A;  $3.9 \pm 0.2$  V vs.  $5.6 \pm 0.3$  V,  $p < 0.01$ ). The median of spatial CV obtained for different CL (between 500 ms to 1500 ms) was always lower in the PMA group than in CTL (group effect,  $p < 0.01$ , two-way repeated measurement ANOVA) independently of the CL (see fig. 4B). Examples of cumulative spatial CV distribution are shown in fig. 4C highlighting the shift to lower CV by PMA. Activation maps used to calculate the spatial CV distribution are shown in panel D for a CTL sample and panel E for a PMA-48h samples with the monolayers paced from the bottom of the dish (blue colors) and the propagation going upward to the top.

## **Chronic treatment with PMA also stabilizes the pattern of activity**

Visual inspection of the sequence of activation maps obtained by timing of optical mapping data shows that the number of activation sites is higher in CTL compared to PMA at 48h as shown in fig. 5A (pre-stim.:  $1.8 \pm 0.3$  site in CTL-48h vs.  $1.00 \pm 0.03$  site in PMA-48h,  $p < 0.05$ ; post-stim.:  $1.8 \pm 0.2$  site in CTL-48h vs.  $1.2 \pm 0.2$  site in PMA-48h,  $p < 0.05$ ). Measuring the distance between 1<sup>st</sup> activation sites in a sample and calculating the mean ( $\langle d \rangle$ ) gives an approximation of the spatial stability of the activity. The result is presented in panel C which shows that  $\langle d \rangle$  is significantly higher in CTL ( $\langle d \rangle = 3.7 \pm 0.9$  mm in CTL-48h vs.  $0.8 \pm 0.2$  mm in PMA-48h) which highlights the greater competition between slow pacemaking sites in control. The greater changes in the position of 1<sup>st</sup> activation sites (focal sites) also results in more variation of the activation patterns measured by difference in sequential normalized activation maps ( $\langle \Delta_{t,act} \rangle = 19.0 \pm 5.2$  ms in CTL-48h vs.  $8.7 \pm 1.9$  ms in PMA-48h, panel D). Focal sites are usually located close to the boundaries of the monolayer (20, 27, 50). Chronic exposure to PMA does not seem to clearly change that behavior as the cumulative distribution of 1<sup>st</sup> activation sites are similar between the two groups (fig. 5B, blue line for CTL and red line for PMA).

Representative examples are presented in fig. 6 and fig. 7 respectively for a control and a PMA samples. The CTL example has a slow and more unstable temporal activity (see the optical voltage trace in panel A). Two activations maps corresponding to the beats labeled B and C in panel A are respectively shown in fig. 6B and 6C. A clear change in pacemaker 1<sup>st</sup> activation sites can be seen with a bottom left site around  $t=6.1$  s and the following beat initiating from the top right section at  $t = 8.3$  s. The example for the PMA group had a faster and more stable temporal dynamics (see fig. 7A). Two activation maps are shown corresponding to the beats labeled B and C in panel A. All the beats have highly similar maps as the ones shown in fig. 7B and C with a bottom 1<sup>st</sup> activation site followed by upward activation.

So far, chronic treatment by PMA increased not only the frequency but also the temporal and spatial stability of spontaneous activity. However, it remains to investigate how it affects the synchronization of the pacemaking activity. The activation delay ( $\delta_{act}$ ) measured during spontaneous activity has been calculated and is presented in fig. 5E. The result is a significant increase in activation delay in the PMA group compared to CTL ( $\delta_{act} = 0.09 \pm 0.01$  s/cm for CTL compared to  $\delta_{act} = 0.15 \pm 0.01$  s/cm for PMA,  $p < 0.05$ ). A perfectly synchronized pacemaker monolayer would have  $\delta_{act} = 0$  s/cm because all cells would activate at the same time. Here, chronic exposure to PMA, although clearly increasing the rate and stability of activity, shows a decrease in synchronization.

## **Simulations of multicellular pacemaking activity**

One question remains on the possible respective effects of increased cellular automaticity and decrease coupling between cells. Simulations of 4 groups was done: CTL, Rate<sub>faster</sub>, R<sub>higher</sub>, Rate<sub>faster</sub> + R<sub>higher</sub> (groups are detailed in the method section). The percentage of simulations having spontaneous activity is of 49% in CTL while the Rate<sub>faster</sub> group had 100%, R<sub>higher</sub> has 91% and the combined group had 100%.

Results of mean period ( $\langle T \rangle$ ) for all groups are shown in fig. 8A with means of  $1.22 \pm 0.03$  s (CTL),  $0.78 \pm 0.01$  s (Rate<sub>faster</sub>),  $1.04 \pm 0.02$  s (R<sub>higher</sub>), and  $0.67 \pm 0.01$  s (Rate<sub>faster</sub> + R<sub>higher</sub>). Apart from the period of activity, the temporal dynamics is exactly the same for all groups with a std(T) around  $\sim 0.4$  ms per group (below the 1 ms sampling interval that was

recorded during simulations) as depicted in fig. 8B. Examples of APs (the last 5 s of simulations) for all groups are shown in fig. 8C which highlights the change in rate of activity between the groups and highly stable interbeat intervals even in the CTL group.

The spatial-temporal activity of simulations shows similarities with experiments with as expected greater density of 1<sup>st</sup> activation sites near the borders (fig. 9A). However, a slight increase in the density a little further away of the borders are found for all groups other than CTL. Highly stable beating pattern are found in all groups which is shown by the limited  $\langle \Delta_{t,act} \rangle$  values of less than 1 ms (panel B). The synchronisation of spontaneous activity was evaluated in simulations as a total time needed to activate all cells for each beat (labeled  $\tau_{delay}$ , fig. 9C). Groups where the intercellular coupling was decreased to mimic a slower CV showed an increase in activation delay consistent with experiments. Examples of activation maps for a specific distribution of spontaneous cell (shown on the left of panel D) are presented on the right of panel D.

## Discussion and conclusion

This study is the first to our knowledge to look at the effect of PMA for re-expression of Tbx3 on multicellular cardiomyocyte monolayer spontaneous activity. We found that chronic exposure to PMA is increasing the frequency of spontaneous activity in NVRM monolayers (fig. 1A) which correlates with an increase in Tbx3 and HCN4 mRNA (fig. 3A and B respectively) and a decrease in conduction velocity (fig. 4B). Thus, as with breast cancer cells (39), PMA modulates Tbx3 expression in NRVMs. PMA has been proposed as a modulator of stem cell differentiation to a cardiomyocyte phenotype (57) and helped restore electromechanical function post-infarct cell therapy (58). The spread of the samples distribution of spontaneous frequency is also found to be decreased in the PMA-48h group compared to the CTL-48h. The same is found in simulations where  $I_{bias}$  was increased (to mimic an increased single spontaneous rate induced by higher funny current). Only a slight decrease in period of activity was found with only a decrease in intercellular coupling. The combination of a cellular faster rate combined with the decreased intercellular coupling yielded the narrower dispersion of the distribution of mean period of activity.

Ivabradine has been shown to reduce the slope of diastolic depolarization by specific use-dependent intracellular blockade of the funny current without affecting either  $\text{Ca}^{2+}$  currents nor the delayed  $\text{K}^+$  current (59). Block by Ivabradine significantly decreased the rate of spontaneous activity (PMA-48h group, fig. 3C) pushing towards the idea that increased funny current level through higher expression of HCN proteins would be an important factors inducing the increase in rate in our experiments and thus augmenting the voltage clock action (8).

T-box transcription factor Tbx3 has been shown to reprogram mature cardiomyocytes into pacemaker-like cells (38). An important documented change was a reduced intercellular coupling through connexin down-expression. The decrease in intercellular coupling would reduce the conduction velocity (60, 61) which is concordant with the decreased conduction velocity found in our PMA-treated samples compared to CTL (fig. 4B-E). However, decreased intercellular coupling has also been associated to higher risk of reentrant activity (62) which is not the case here with PMA where the ratio of reentry-like rapid activity was highly diminished. This aspect would indicate that factors other than coupling may be important in the initiation of reentry that is lost with the increased rate of spontaneous activity with PMA.

Monolayer cultures of NRVMs may provide a useful biological tool to investigate the role of PM-cell-cluster patterns on automaticity and therefore gain better understanding of clinical issues, including creation of biopacemakers (25). However, the seeding process is usually random, the impact of culture environment unknown, and thus the real spatial distribution of the two cell types remains to be uncovered. As such, the stochastic variability of PM cells in the monolayer could explain, at least in part, the variability in spontaneous mean rate of activation observed in CTL since both the experimental (fig. 1A) and modeling (fig. 8A) data correlate on that point. One would expect that an overall increase in HCNs proteins and funny current amplitude could not only favor the rate but also the synchronization of the activity. However, a marker of synchronization, the activation delay (fig. 5E) is increased which would indicate a lesser synchronized spontaneous activity.

Similar to previous experimental and modeling data (20, 27, 50), the new results confirmed that initiation sites of spontaneous activity are mostly located at the edge of the monolayer (fig. 5B). This finding may be explained by the source-sink mechanism (63, 64)

and the position of large PM cluster. At the edge, which has no-flux boundary conditions, PM cells are effectively connected with fewer resting excitable cardiomyocytes; as such, they are less electrotonically depressed and possess increased capacity to initiate activation. However, a theoretical monolayer composed of only identical PM cells could be synchronized and have simultaneous activation times. In this case, the mapping analysis would detect a single large cluster of 1<sup>st</sup> activation sites with centroid at the center of the monolayer. Such a behaviour would modify the sites distribution from the border to within the center region which is however not the case here in the PMA group (fig. 5B). Propagation in monolayer spontaneous regimes like we found here are by definition phase waves because of the spontaneous dynamics. It remains to see if phase waves can be found in uniform and homogeneous PM cell monolayers as it can occur in interconnected chemical oscillators (2) and in ventricular tissue exhibiting early after depolarization (65).

The increase in rate of activity correlates with an increased temporal stability (less variation in inter-beat intervals). This result is concordant with the idea of decreased slow diastolic depolarization of the cell membrane being more sensitive to noise (66). However, the intrinsic rate also correlates with spatial stability (more stable 1<sup>st</sup> activation sites and activation maps as highlighted in fig. 5). Indeed the competition of different spatial pacemaker sites are significantly decreased with PMA compared to control (fig. 5A). Those characteristics are key for a robust biopacemaker function where activity will be strong enough to damp the neighbor stochastic modulation. Simulations for the CTL group did not reproduce experimental variations in the 1<sup>st</sup> initiation sites which indicates that temporal and spatial stability are more linked to cellular temporal randomness than a spatial distribution stochastic process. For example, Ponard *et al* (27) found this type of temporal instabilities when incorporating a stochastic change in cellular properties. While increased membrane noise level has been shown to statistically augment the mean rate of activation (67), it remains to investigate how temporal noise and spatial stochastic distribution of PM cells can affect multicellular pacemaker activity. These knowledge could be important in the process of creating optimized and robust biological pacemakers, an alternative to electronic pacemakers in the treatment of bradycardia (23).

## References

1. Haken H. Advanced synergetics : instability hierarchies of self-organizing systems and devices. Berlin ; New York: Springer-Verlag; 1983. xv, 356 p. p.
2. Kuramoto Y. Chemical oscillations, waves, and turbulence. Berlin ; New York: Springer-Verlag; 1984. viii, 156 p. p.
3. Winfree AT. When time breaks down : the three-dimensional dynamics of electrochemical waves and cardiac arrhythmias. Princeton, N.J. :: Princeton University Press; 1987.
4. Tass PA. Phase resetting in medicine and biology : stochastic modelling and data analysis. Berlin ; New York: Springer Verlag; 1999. xiii, 329 p. p.
5. Mangoni ME, Nargeot J. Genesis and regulation of the heart automaticity. *Physiol Rev.* 2008;88(3):919-82.
6. Rozanski GJ, Lipsius SL. Electrophysiology of functional subsidiary pacemakers in canine right atrium. *The American journal of physiology.* 1985;249(3 Pt 2):H594-603.
7. Sirenko S, Yang D, Li Y, Lyashkov AE, Lukyanenko YO, Lakatta EG, et al. Ca(2)(+)-dependent phosphorylation of Ca(2)(+) cycling proteins generates robust rhythmic local Ca(2)(+) releases in cardiac pacemaker cells. *Science signaling.* 2013;6(260):ra6.
8. Lakatta EG, Maltsev VA, Vinogradova TM. A coupled SYSTEM of intracellular Ca<sup>2+</sup> clocks and surface membrane voltage clocks controls the timekeeping mechanism of the heart's pacemaker. *Circulation research.* 2010;106(4):659-73.
9. Kurata Y, Matsuda H, Hisatome I, Shibamoto T. Roles of hyperpolarization-activated current I<sub>f</sub> in sinoatrial node pacemaking: insights from bifurcation analysis of mathematical models. *Am J Physiol Heart Circ Physiol.* 2010;298(6):H1748-60.
10. Maltsev VA, Lakatta EG. Normal heart rhythm is initiated and regulated by an intracellular calcium clock within pacemaker cells. *Heart Lung Circ.* 2007;16(5):335-48.
11. Chlopcikova S, Psotova J, Miketova P. Neonatal rat cardiomyocytes--a model for the study of morphological, biochemical and electrophysiological characteristics of the heart. *Biomed Pap Med Fac Univ Palacky Olomouc Czech Repub.* 2001;145(2):49-55.

12. Bursac N, Papadaki M, Cohen RJ, Schoen FJ, Eisenberg SR, Carrier R, et al. Cardiac muscle tissue engineering: toward an in vitro model for electrophysiological studies. *Am J Physiol.* 1999;277(2 Pt 2):H433-44.
13. Bursac N, Parker KK, Irvanian S, Tung L. Cardiomyocyte cultures with controlled macroscopic anisotropy: a model for functional electrophysiological studies of cardiac muscle. *Circ Res.* 2002;91(12):e45-54.
14. Badie N, Scull JA, Klinger RY, Krol A, Bursac N. Conduction block in micropatterned cardiomyocyte cultures replicating the structure of ventricular cross-sections. *Cardiovasc Res.* 2012;93(2):263-71.
15. Mark GE, Strasser FF. Pacemaker activity and mitosis in cultures of newborn rat heart ventricle cells. *Exp Cell Res.* 1966;44(2):217-33.
16. Vink MJ, Suadicani SO, Vieira DM, Urban-Maldonado M, Gao Y, Fishman GI, et al. Alterations of intercellular communication in neonatal cardiac myocytes from connexin43 null mice. *Cardiovasc Res.* 2004;62(2):397-406.
17. Fahrenbach JP, Mejia-Alvarez R, Banach K. The relevance of non-excitabile cells for cardiac pacemaker function. *J Physiol.* 2007;585(Pt 2):565-78.
18. Guo W, Kamiya K, Cheng J, Toyama J. Changes in action potentials and ion currents in long-term cultured neonatal rat ventricular cells. *Am J Physiol.* 1996;271(1 Pt 1):C93-102.
19. Orita H, Fukasawa M, Hirooka S, Uchino H, Fukui K, Washio M. Modulation of cardiac myocyte beating rate and hypertrophy by cardiac fibroblasts isolated from neonatal rat ventricle. *Jpn Circ J.* 1993;57(9):912-20.
20. Duverger JE, Boudreau-Béland J, Le MD, Comtois P. Multicellular automaticity of cardiac cell monolayers: effects of density and spatial distribution of pacemaker cells. *New Journal of Physics.* 2014;16(11):113046.
21. Himel HDt, Garny A, Noble PJ, Wadgoankar R, Savarese J, Liu N, et al. Electrotonic suppression of early afterdepolarizations in the neonatal rat ventricular myocyte monolayer. *J Physiol.* 2013;591(Pt 21):5357-64.
22. Kirchhof CJ, Bonke FI, Allesie MA, Lammers WJ. The influence of the atrial myocardium on impulse formation in the rabbit sinus node. *Pflugers Arch.* 1987;410(1-2):198-203.

23. Morikawa K, Bahrudin U, Miake J, Igawa O, Kurata Y, Nakayama Y, et al. Identification, isolation and characterization of HCN4-positive pacemaking cells derived from murine embryonic stem cells during cardiac differentiation. *Pacing Clin Electrophysiol.* 2010;33(3):290-303.
24. Plotnikov AN, Shlapakova I, Szabolcs MJ, Danilo P, Jr., Lorell BH, Potapova IA, et al. Xenografted adult human mesenchymal stem cells provide a platform for sustained biological pacemaker function in canine heart. *Circulation.* 2007;116(7):706-13.
25. Morris GM, Boyett MR. Perspectives -- biological pacing, a clinical reality? *Ther Adv Cardiovasc Dis.* 2009;3(6):479-83.
26. Masumiya H, Oku Y, Okada Y. Inhomogeneous distribution of action potential characteristics in the rabbit sino-atrial node revealed by voltage imaging. *J Physiol Sci.* 2009;59(3):227-41.
27. Ponard JG, Kondratyev AA, Kucera JP. Mechanisms of intrinsic beating variability in cardiac cell cultures and model pacemaker networks. *Biophys J.* 2007;92(10):3734-52.
28. Zlochiver S, Munoz V, Vikstrom KL, Taffet SM, Berenfeld O, Jalife J. Electrotonic Myofibroblast-to-Myocyte Coupling Increases Propensity to Reentrant Arrhythmias in 2-Dimensional Cardiac Monolayers. *Biophys J.* 2008.
29. Kryukov AK, Petrov VS, Averyanova LS, Osipov GV, Chen W, Drugova O, et al. Synchronization phenomena in mixed media of passive, excitable, and oscillatory cells. *Chaos.* 2008;18(3):037129.
30. Kuklik P, Zebrowski JJ. Reentry wave formation in excitable media with stochastically generated inhomogeneities. *Chaos.* 2005;15(3):33301.
31. Bub G, Shrier A, Glass L. Spiral wave generation in heterogeneous excitable media. *Phys Rev Lett.* 2002;88(5):058101.
32. Rohr S, Kucera JP, Fast VG, Kleber AG. Paradoxical improvement of impulse conduction in cardiac tissue by partial cellular uncoupling. *Science.* 1997;275(5301):841-4.
33. Kanakov OI, Osipov GV, Chan CK, Kurths J. Cluster synchronization and spatio-temporal dynamics in networks of oscillatory and excitable Luo-Rudy cells. *Chaos.* 2007;17(1):015111.

34. Shajahan TK, Borek B, Shrier A, Glass L. Scaling properties of conduction velocity in heterogeneous excitable media. *Phys Rev E Stat Nonlin Soft Matter Phys.* 2011;84(4 Pt 2):046208.
35. Hoogaars WM, Tessari A, Moorman AF, de Boer PA, Hagoort J, Soufan AT, et al. The transcriptional repressor Tbx3 delineates the developing central conduction system of the heart. *Cardiovasc Res.* 2004;62(3):489-99.
36. Hoogaars WM, Engel A, Brons JF, Verkerk AO, de Lange FJ, Wong LY, et al. Tbx3 controls the sinoatrial node gene program and imposes pacemaker function on the atria. *Genes Dev.* 2007;21(9):1098-112.
37. Bakker ML, Boukens BJ, Mommersteeg MT, Brons JF, Wakker V, Moorman AF, et al. Transcription factor Tbx3 is required for the specification of the atrioventricular conduction system. *Circ Res.* 2008;102(11):1340-9.
38. Bakker ML, Boink GJ, Boukens BJ, Verkerk AO, van den Boogaard M, den Haan AD, et al. T-box transcription factor TBX3 reprogrammes mature cardiac myocytes into pacemaker-like cells. *Cardiovasc Res.* 2012;94(3):439-49.
39. Mowla S, Pinnock R, Leaner VD, Goding CR, Prince S. PMA-induced up-regulation of TBX3 is mediated by AP-1 and contributes to breast cancer cell migration. *Biochem J.* 2011;433(1):145-53.
40. Dunmon PM, Iwaki K, Henderson SA, Sen A, Chien KR. Phorbol esters induce immediate-early genes and activate cardiac gene transcription in neonatal rat myocardial cells. *J Mol Cell Cardiol.* 1990;22(8):901-10.
41. Shubeita HE, Martinson EA, Van Bilsen M, Chien KR, Brown JH. Transcriptional activation of the cardiac myosin light chain 2 and atrial natriuretic factor genes by protein kinase C in neonatal rat ventricular myocytes. *Proc Natl Acad Sci U S A.* 1992;89(4):1305-9.
42. Kariya K, Karns LR, Simpson PC. Expression of a constitutively activated mutant of the beta-isozyme of protein kinase C in cardiac myocytes stimulates the promoter of the beta-myosin heavy chain isogene. *J Biol Chem.* 1991;266(16):10023-6.
43. Samarel AM, Engelmann GL. Contractile activity modulates myosin heavy chain-beta expression in neonatal rat heart cells. *Am J Physiol.* 1991;261(4 Pt 2):H1067-77.

44. Komuro I, Yazaki Y. Molecular mechanism of cardiac hypertrophy and failure. *Clin Sci (Lond)*. 1994;87(2):115-6.
45. Vijayan K, Szotek EL, Martin JL, Samarel AM. Protein kinase C-alpha-induced hypertrophy of neonatal rat ventricular myocytes. *Am J Physiol Heart Circ Physiol*. 2004;287(6):H2777-89.
46. Blum JL, Samarel AM, Mestril R. Phosphorylation and binding of AUF1 to the 3'-untranslated region of cardiomyocyte SERCA2a mRNA. *Am J Physiol Heart Circ Physiol*. 2005;289(6):H2543-50.
47. Porter MJ, Heidkamp MC, Scully BT, Patel N, Martin JL, Samarel AM. Isoenzyme-selective regulation of SERCA2 gene expression by protein kinase C in neonatal rat ventricular myocytes. *Am J Physiol Cell Physiol*. 2003;285(1):C39-47.
48. Qi M, Bassani JW, Bers DM, Samarel AM. Phorbol 12-myristate 13-acetate alters SR Ca(2+)-ATPase gene expression in cultured neonatal rat heart cells. *Am J Physiol*. 1996;271(3 Pt 2):H1031-9.
49. Puglisi JL, Yuan W, Timofeyev V, Myers RE, Chiamvimonvat N, Samarel AM, et al. Phorbol ester and endothelin-1 alter functional expression of Na<sup>+</sup>/Ca<sup>2+</sup> exchange, K<sup>+</sup>, and Ca<sup>2+</sup> currents in cultured neonatal rat myocytes. *Am J Physiol Heart Circ Physiol*. 2011;300(2):H617-26.
50. Boudreau-Beland J, Duverger JE, Petitjean E, Maguy A, Ledoux J, Comtois P. Spatiotemporal stability of neonatal rat cardiomyocyte monolayers spontaneous activity is dependent on the culture substrate. *PLoS One*. 2015;10(6):e0127977.
51. Bucchi A, Baruscotti M, DiFrancesco D. Current-dependent block of rabbit sino-atrial node If channels by ivabradine. *The Journal of general physiology*. 2002;120(1):1-13.
52. Duverger JE, Beland J, Maguy A, Adegbindin MM, Comtois P. Fluorescence-based system for measurement of electrophysiological changes in stretched cultured cardiomyocytes. *Ieee Eng Med Bio*. 2011:35-8.
53. Bayly PV, KenKnight BH, Rogers JM, Hillsley RE, Ideker RE, Smith WM. Estimation of conduction velocity vector fields from epicardial mapping data. *IEEE Trans Biomed Eng*. 1998;45(5):563-71.

54. Anversa P, Olivetti G, Loud AV. Morphometric study of early postnatal development in the left and right ventricular myocardium of the rat. I. Hypertrophy, hyperplasia, and binucleation of myocytes. *Circ Res.* 1980;46(4):495-502.
55. Duverger JE, Boudreau-Beland J, Le MD, Comtois P. Multicellular automaticity of cardiac cell monolayers: effects of density and spatial distribution of pacemaker cells. *New Journal of Physics.* 2014:Accepted for publication 6 october 2014.
56. Comtois P, Nattel S. Interactions between cardiac fibrosis spatial pattern and ionic remodeling on electrical wave propagation. *Conf Proc IEEE Eng Med Biol Soc.* 2011;2011:4669-72.
57. Chang W, Lim S, Song BW, Lee CY, Park MS, Chung YA, et al. Phorbol myristate acetate differentiates human adipose-derived mesenchymal stem cells into functional cardiogenic cells. *Biochem Biophys Res Commun.* 2012;424(4):740-6.
58. Song H, Hwang HJ, Chang W, Song BW, Cha MJ, Kim IK, et al. Cardiomyocytes from phorbol myristate acetate-activated mesenchymal stem cells restore electromechanical function in infarcted rat hearts. *Proc Natl Acad Sci U S A.* 2011;108(1):296-301.
59. Bucchi A, Baruscotti M, DiFrancesco D. Current-dependent block of rabbit sino-atrial node I(f) channels by ivabradine. *J Gen Physiol.* 2002;120(1):1-13.
60. Maguy A, Le Bouter S, Comtois P, Chartier D, Villeneuve L, Wakili R, et al. Ion channel subunit expression changes in cardiac Purkinje fibers: a potential role in conduction abnormalities associated with congestive heart failure. *Circ Res.* 2009;104(9):1113-22.
61. Kleber AG, Rudy Y. Basic mechanisms of cardiac impulse propagation and associated arrhythmias. *Physiol Rev.* 2004;84(2):431-88.
62. Bub G, Shrier A, Glass L. Global organization of dynamics in oscillatory heterogeneous excitable media. *Phys Rev Lett.* 2005;94(2):028105.
63. Comtois P, Vinet A. Curvature effects on activation speed and repolarization in an ionic model of cardiac myocytes. *Phys Rev E.* 1999;60(4 Pt B):4619-28.
64. Xie Y, Sato D, Garfinkel A, Qu Z, Weiss JN. So little source, so much sink: requirements for afterdepolarizations to propagate in tissue. *Biophys J.* 2010;99(5):1408-15.

65. Zimik S, Vandersickel N, Nayak AR, Panfilov AV, Pandit R. A Comparative Study of Early Afterdepolarization-Mediated Fibrillation in Two Mathematical Models for Human Ventricular Cells. PLoS One. 2015;10(6):e0130632.
66. Clay JR, DeHaan RL. Fluctuations in interbeat interval in rhythmic heart-cell clusters. Role of membrane voltage noise. Biophys J. 1979;28(3):377-89.
67. Dvir H, Zlochiver S. Interbeat interval modulation in the sinoatrial node as a result of membrane current stochasticity-a theoretical and numerical study. Biophys J. 2015;108(5):1281-92.

## Figure captions

Fig. 1: Videomicroscopy data showing increased frequency and temporal stability of spontaneous activity by PMA. A) Distribution of spontaneous frequency for both CTL (blue line) and PMA (red line) at 24h post-PMA start (top) and 48h post-PMA start (bottom). B) Temporal variation in period of activity is evaluated by the temporal standard deviation of the period  $T$  ( $\text{std}(T)$ ) at 24h post-PMA and 48h post-PMA (with control group at the same time points). C) Examples at 48h post-PMA of composite videomicroscopy data showing peaks with slower and more varying contractile activity in control (CTL-48h, top) and faster and more stable activity with PMA (PMA-48h, bottom).

Fig. 2: Period of spontaneous activity is decreased by PMA at 48h. A) Average period of activity  $\langle T \rangle$  is higher in CTL-48h compared to PMA-48h. Similar results are observed before (pre-stim) or after the pacing protocol for conduction velocity study (post-stim). B) Examples of normalized optical AP recording in control (CTL-48h, top) with slower and irregular dynamic compared to a PMA recording (PMA-48h, bottom) with faster and regular activity.

Fig. 3: Fold-change increased by PMA in mRNA expression of A) T-box 3 and B) HCN4. Re-expression of T-box 3 results in increased HCN4 expression correlating with increased frequency of spontaneous frequency of the monolayer. C) Pharmacological block with Ivabradine ( $3 \mu\text{mol/L}$ ) yielded to a significant decrease of spontaneous frequency measured by videomicroscopy ( $p < 0.05$ , paired t-test).

Fig. 4: Decreased conduction velocity (CV) under programmed stimulations with chronic exposure to PMA. A) The threshold voltage for bipolar stimulation when pacing at a cycle length (CL) of 1000 ms is higher in the PMA group compared to the control group at 48h post-PMA. B) Mean CV values obtained at different pacing CL ranging from 500 ms to 1500 ms always showing higher CVs in control (black bars) compared to PMA group (white bars) at 48h-post PMA. C) Cumulative density distribution of local CV amplitude obtained for a control (blue line) and a PMA sample (red line) paced at CL = 750 ms showing a shift to lower CVs with PMA. D) The respective control and PMA activation maps used to estimate the local CVs are shown in panel D (CTL-48h) and panel E (PMA-48h).

Fig. 5: Spatial stability of spontaneous activity is increased by chronic exposure to PMA. A) Visual examination of optical activation maps shows that the average number of activation sites is higher in control (CTL-48h, black bars) compared to PMA groups (PMA-48h, white bars). B) Cumulative distribution of 1<sup>st</sup> initiation sites from the center of the dishes to the outside border showing that most of the sites are most often found closer to the border for either the control (CTL-48h, blue line) and PMA group (PMA-48h, red line). Inset: Positions of 1<sup>st</sup> initiation sites for the control (blue points) and PMA (red points) used to calculate the cumulative distributions. C) Average of the mean distance between 1<sup>st</sup> initiation sites per recording is significantly higher in control compared to chronic exposure to PMA. D) Significant decrease in the mean difference activation maps between beats from control (CTL-48h, black bar) versus PMA (PMA-48h, white bar). E) The local activation delay is increased by PMA (PMA-48h, white bar) compared to control (CTL-48h, black bar).

Fig. 6: An example of spontaneous activity in control. A) Optical AP recording (measured as normalized fluorescence changes in the dashed square in panel B) over a 15 s duration showing slow and unstable period of activity. B) Activation map of the beat labeled by a B in panel A with initiation site from the bottom left of the map. C) Activation map for the following beat with focal site coming from the top portion of the sample.

Fig. 7: Similar to fig. 6 but for spontaneous activity in the PMA group. A) The optical signal shows a regular and faster rate of activity than in control. All beats within the recording were consistent and starting from the same initiation site. Two maps are shown corresponding to the APs labeled (B) and (C) respectively in panel B and C.

Fig. 8: Simulation results highlighting the role of increased cellular spontaneous activity or/and increased intercellular conductance on multicellular global activity. A) Plot of average (over time) period of spontaneous activity has a slower period and sparser set of values in control (CTL, blue points). Increasing the cellular individual spontaneous activity ( $I_{bias} = 3.5$  instead of 3.0 in control) decreases the mean and range of multicellular period of activity (gray points). Decreasing intercellular electrical coupling of the monolayer only slightly decreased the period of activity and range of period of the set ( $R_{higher}$ , green points). Combination of the two changes (increasing  $I_{bias}$  and decreasing coupling) although not strongly changing the minimum period of the set has a strong effects on sparsity resulting on a

more dense set of periods. B) Temporal standard deviation of the period of activity ( $\text{std}(T)$ ) for the 4 groups of simulations highlighting the highly stable activity that remains in all groups contrary to experiments. C) Examples of activity in the region of 1<sup>st</sup> activation (continuous line) and in a region without spontaneous cells (dashed line). Groups: CTL (top left),  $\text{Rate}_{\text{faster}}$  (top right),  $\text{R}_{\text{higher}}$  (bottom left), and combined  $\text{Rate}_{\text{faster}} + \text{R}_{\text{higher}}$  (bottom right).

Fig. 9: Spatial characteristics of spontaneous activity in simulations. A) Cumulative density distribution of the 1<sup>st</sup> initiation site position. B) Average of the difference between activation maps which is very low independently of the groups. C) Overall delay for total activation of the monolayer. D) Example of spatial distribution of spontaneous cells (black) within surrounded by excitable but not spontaneous cells (white) each cells having a 6-neighbor connectivity is shown on the left. On the right, last full activation maps from a 10 s simulations for each group. The colorscale shows the time of activation from the 1<sup>st</sup> initiation time (in blue) to 45 ms later.

Supplementary fig. 1: Schematic of the 2D layout of cells with a neighborhood of 6 cells. Numbers from 1 to 5 correspond different cases at the boundaries having a decreased number of neighbors (1: 3 cells, 2: 4 cells, 3: 2 cells, 4: 5 cells, and 5: 3 cells).

Supplementary fig. 2: Bifurcation of the Luo-Rudy model as a function of the bias current  $I_{\text{bias}}$ . A) Period of activity ( $T$ ) showing apparition of spontaneous activity around 2.56 with long period of activity ( $T=2000$  ms) that is decreasing with disappearance with  $I_{\text{bias}} = 4.7$ . B) Minimum and maximum transmembrane voltage  $V$  showing highest amplitude for low  $I_{\text{bias}}$  that decreases with increasing bias current. Bistability is found for  $4.47 \leq I_{\text{bias}} \leq 4.7$ . Black dots correspond to the fixed point of the system and unstable fixed points are shown by red circles.

Supplementary fig. 3: Subset of 6 different stochastically generated spatial distribution of PM cells that are part of the complete simulated data set.

## Table and figures

**Table 1: List of primers**

<b>Gene name &amp; Symbol</b>	<b>Forward Primer Sequences (5'-3')</b>	<b>Reverse Primer Sequences (5'-3')</b>
HCN4	CCCGCCTCATTCCGGTACATT	AGGTTCACGATGCGTACCAC
Tbx3	CAGTACCTTCCGCACATACC	CCTGCCATTGCCAGTATCTC
GAPDH	GCATCTTCTTGTGCAGTGCC	GAGAAGGCAGCCCTGGTAAC
HPRT	TTGGTCAAGCAGTACAGCCC	GTCTGGCCTGTATCCAACACT
$\beta$ 2M	CCGTGATCTTTCTGGTGCTT	GTGGAAGTGGACACGTAGC

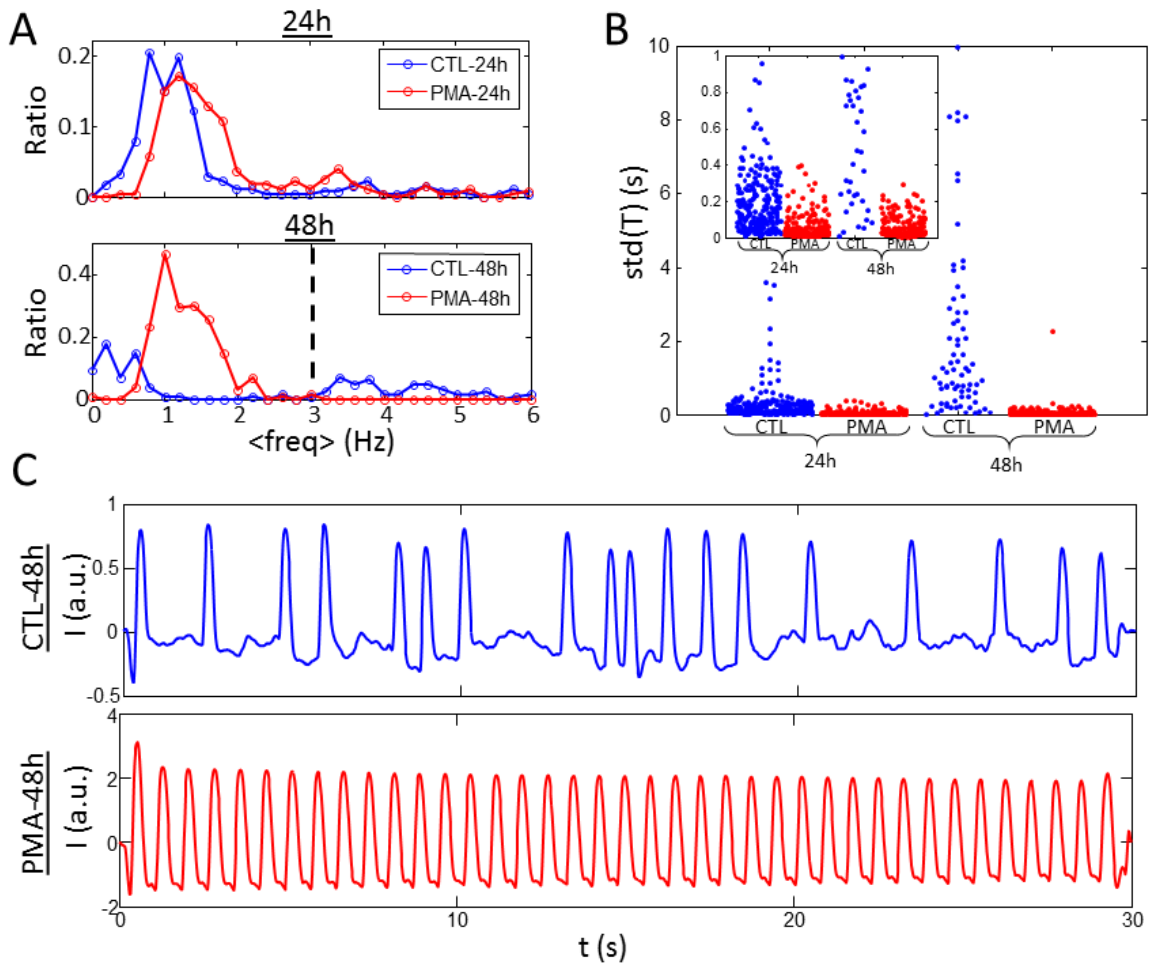


**Figure 1**

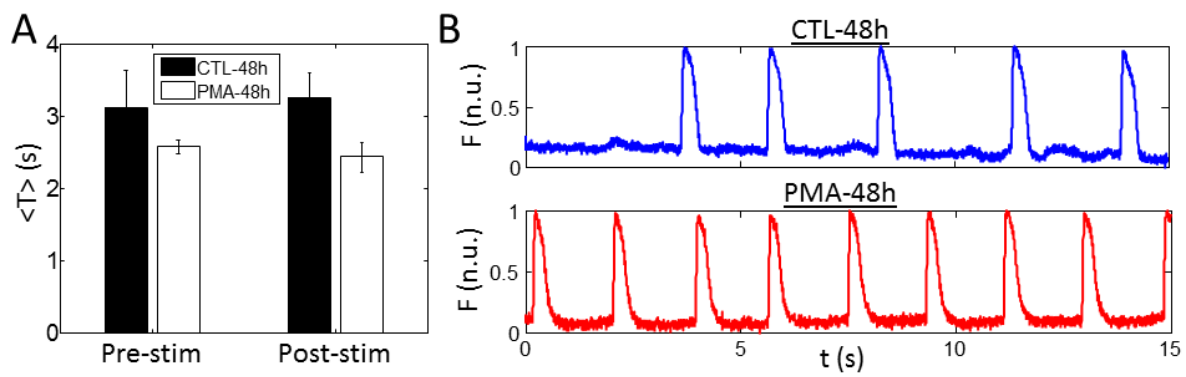


**Figure 2**

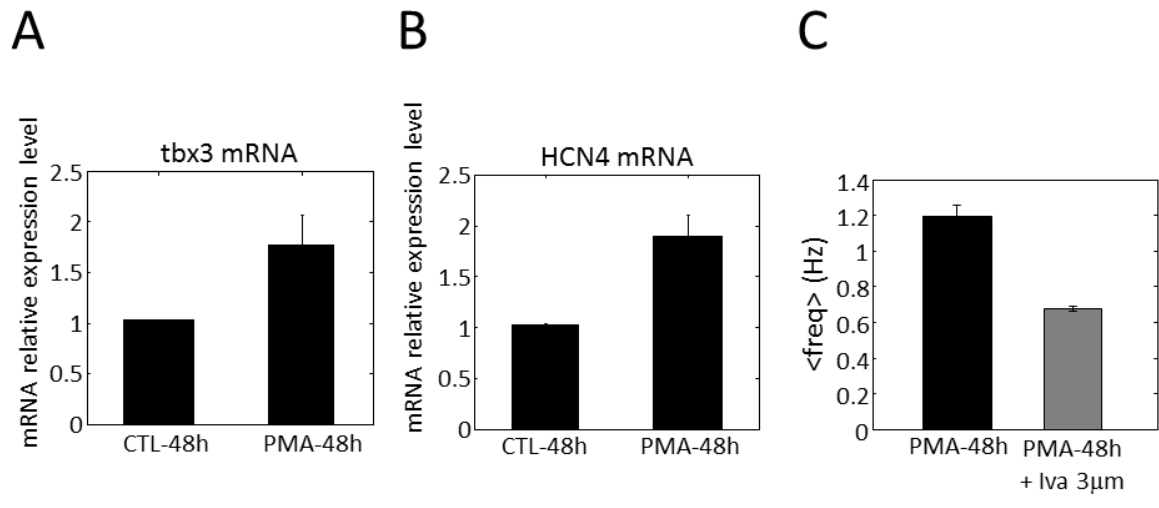


**Figure 3**

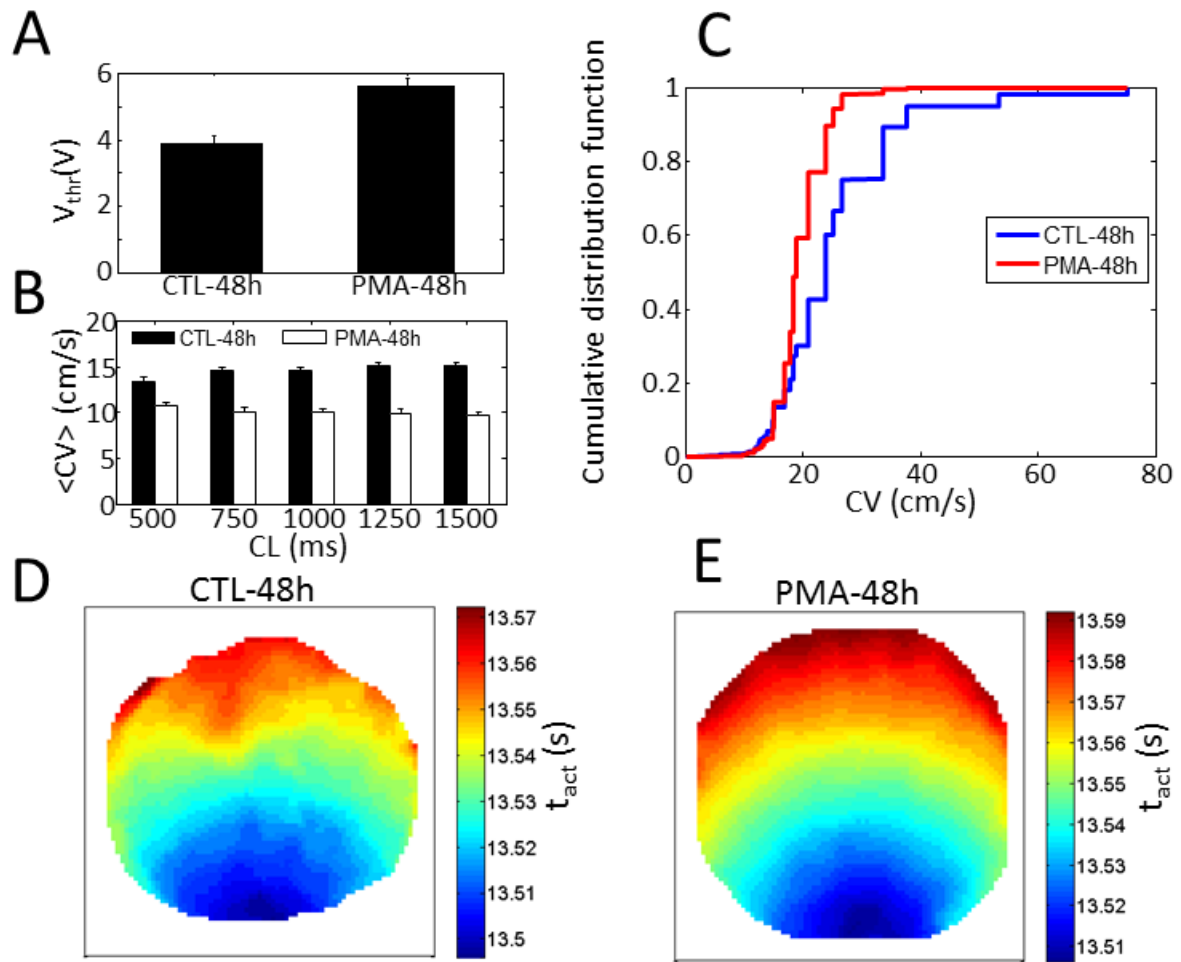


**Figure 4**

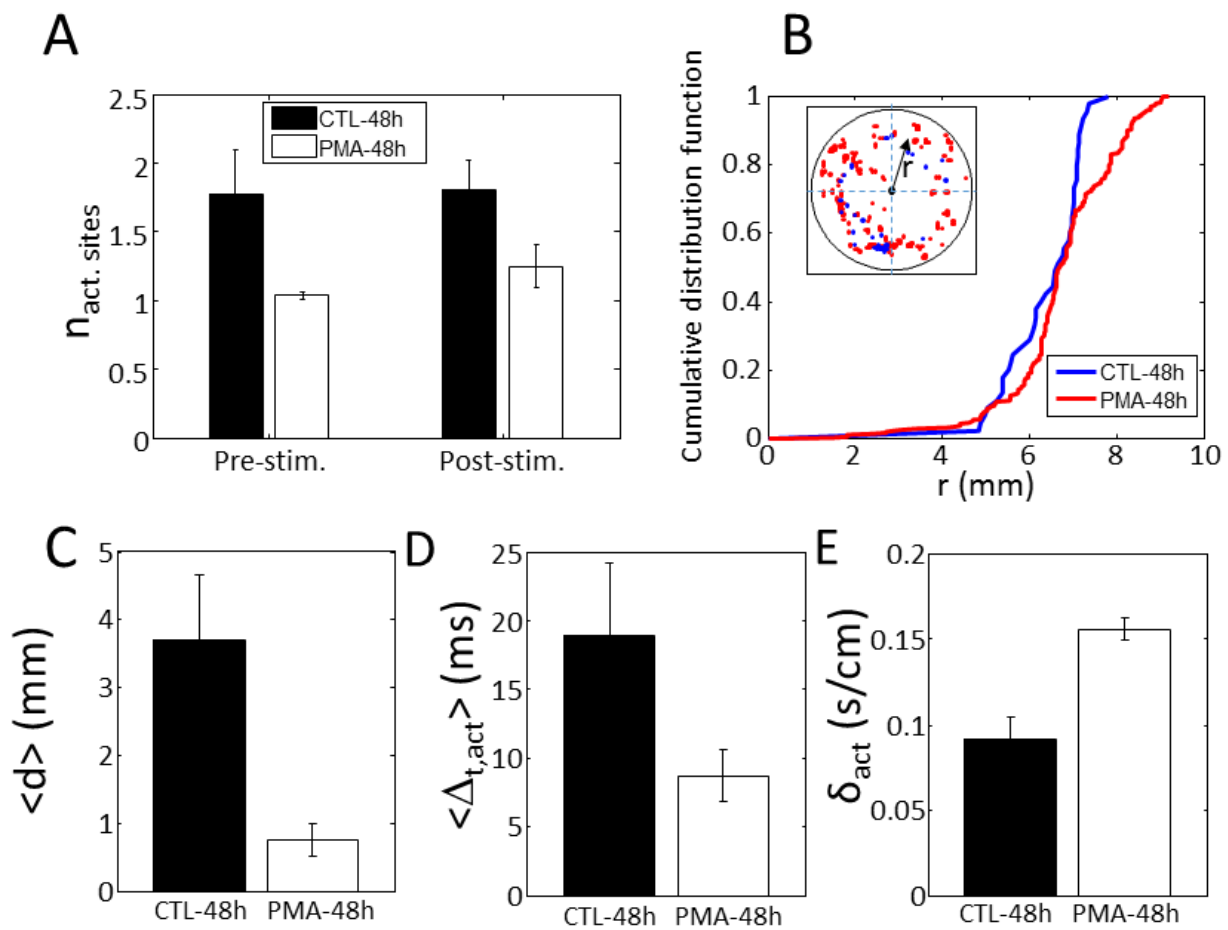


**Figure 5**

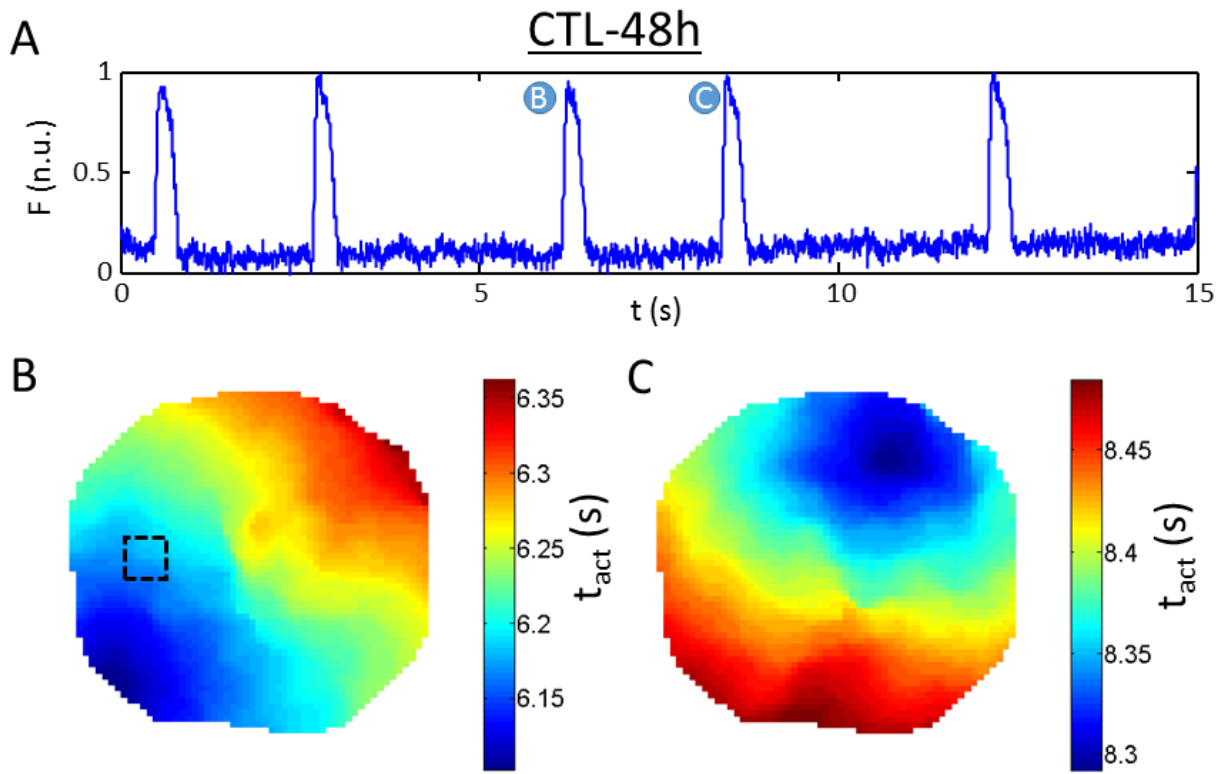


**Figure 6**

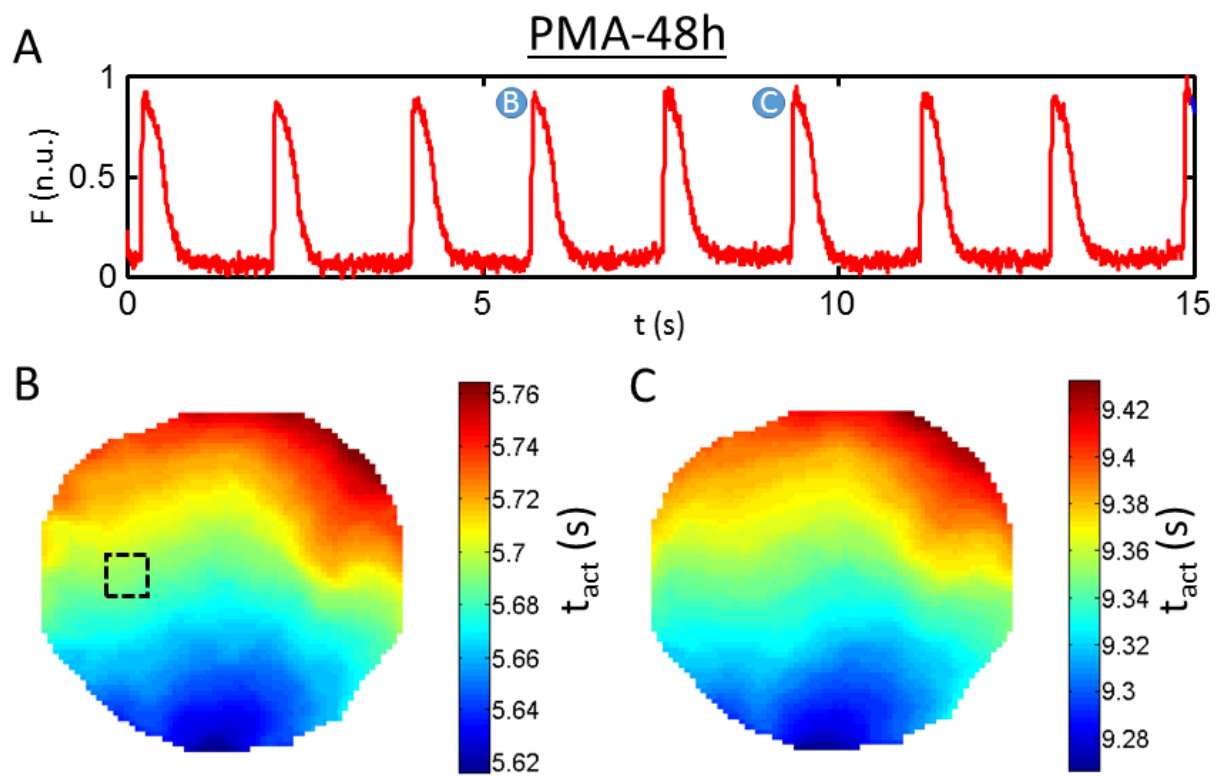


**Figure 7**

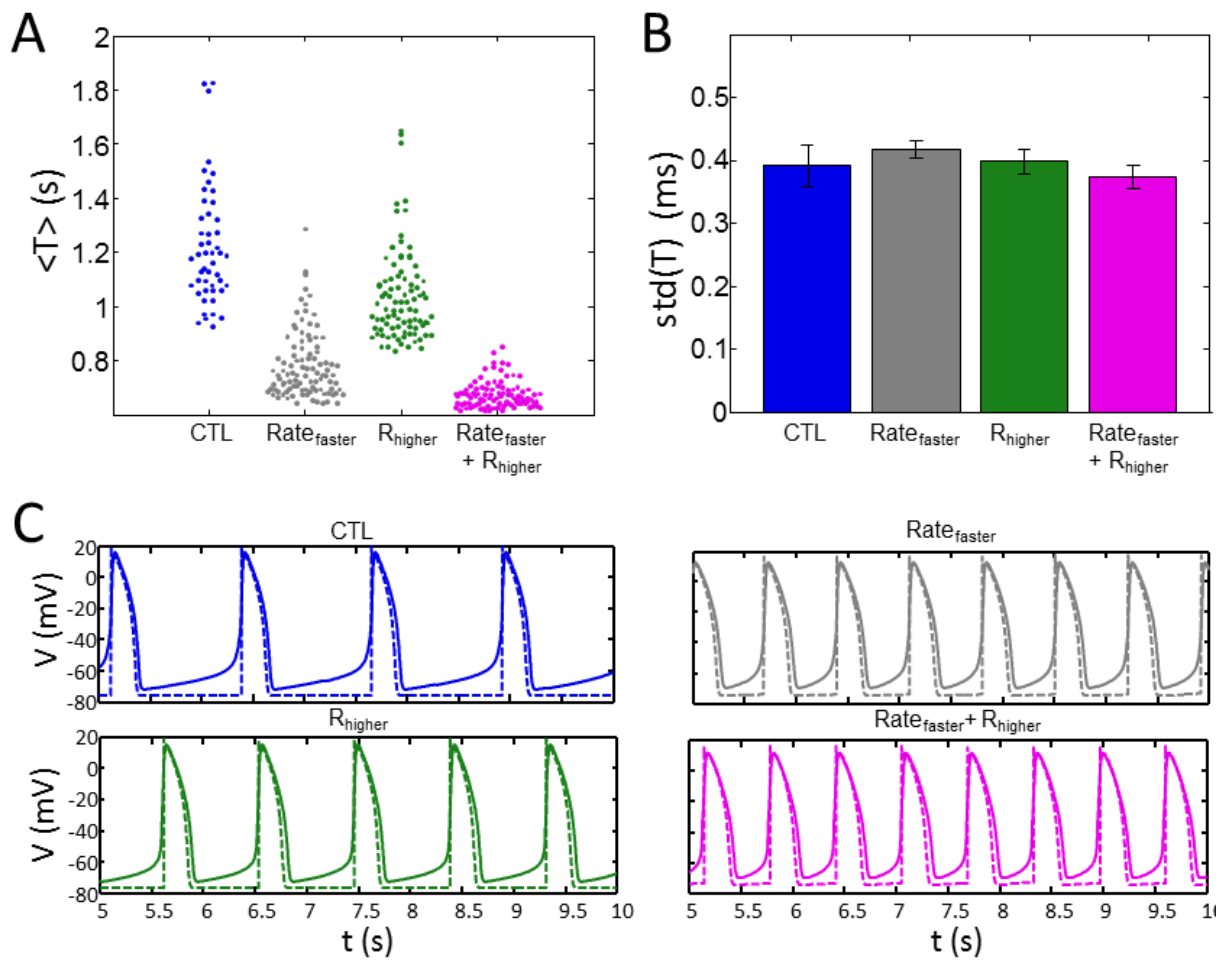


**Figure 8**

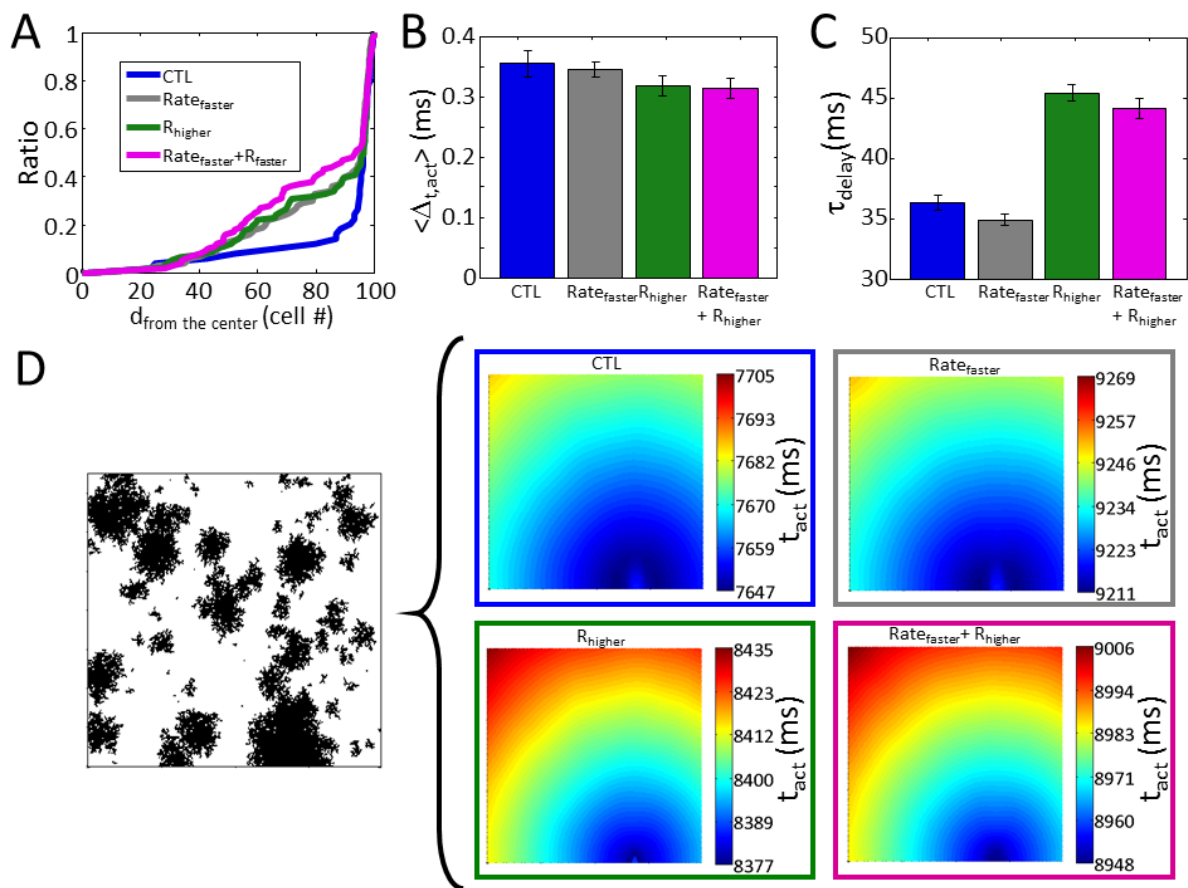
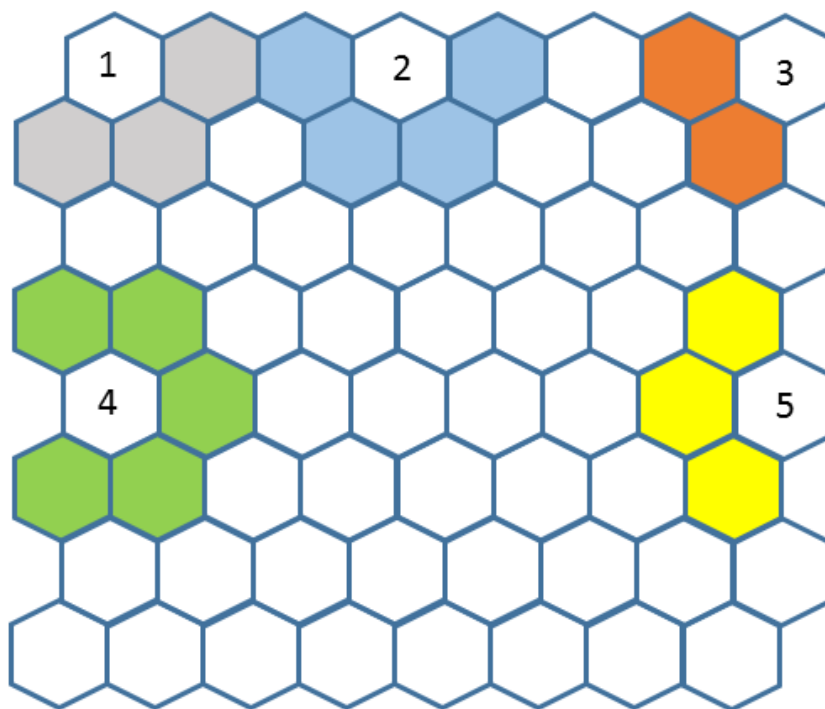
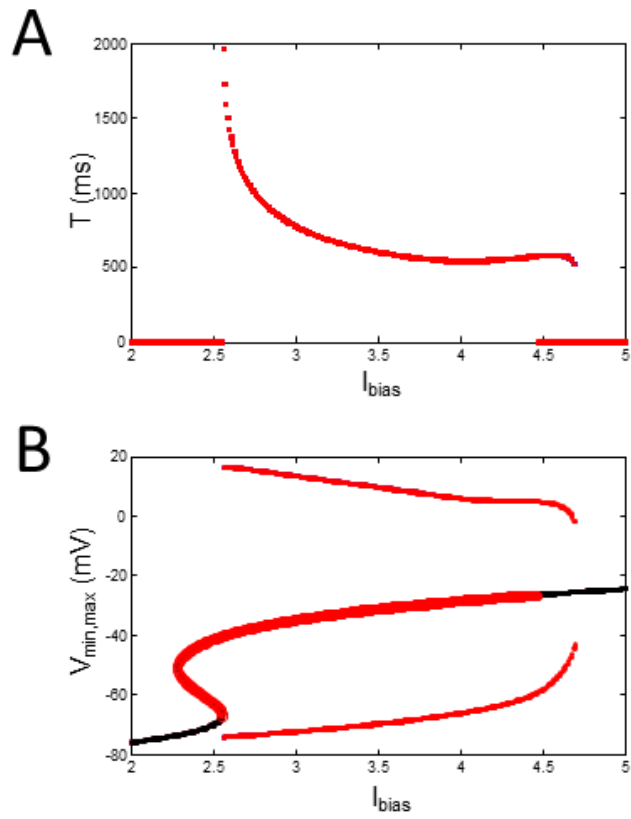


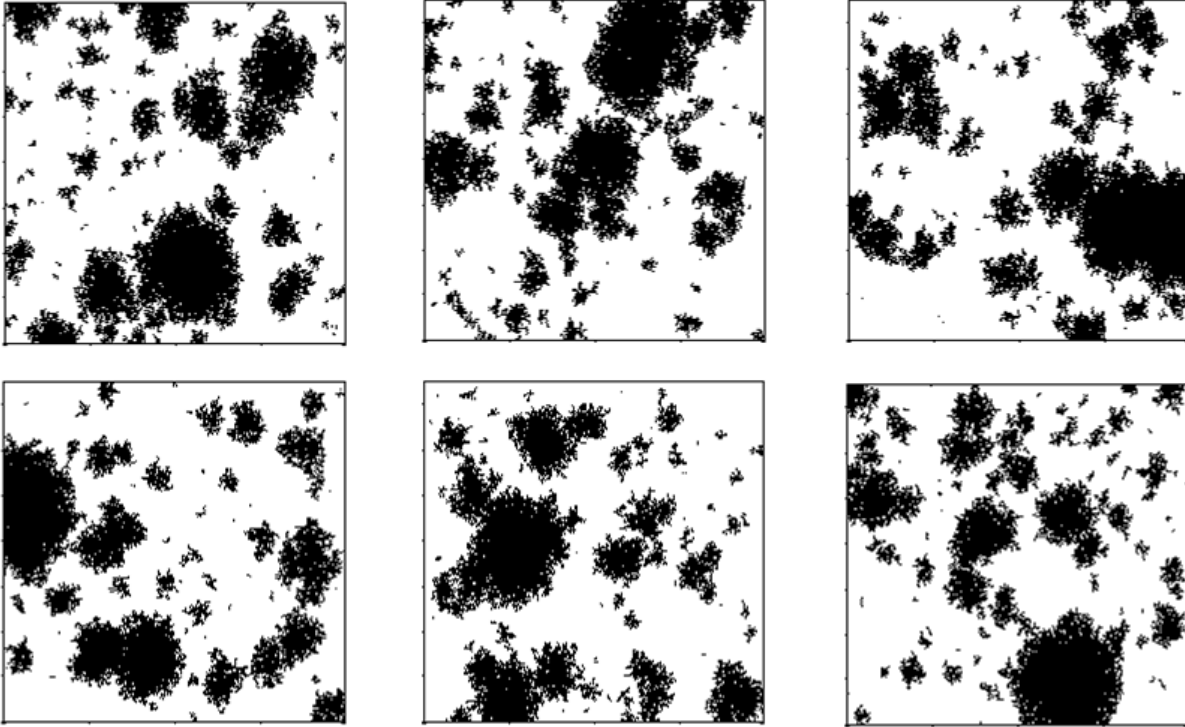
**Figure 9**



**Supplementary figure 1**



**Supplementary figure 2**



**Supplementary figure 3**

### **3 DISCUSSION AND CONCLUSION**

The present investigation illustrates the effect of PMA on NRVM monolayers which is a well-accepted model in the cardiovascular field (178, 179). This is in part possible because neonatal murine cardiac cells have a transient regenerative phase (177) which results in some differentiation capability of the cultured cells. In addition, monolayer sheets of NRVMs are more interesting than isolated single cells since cell-to-cell electrical coupling and impulse propagation can be studied (180). Initiation of the propagating wave is a pivotal and intrinsic characteristic of the pacemaker cells exciting the excitable myocardium. Characteristics of spontaneous activity and ways to control them are central to the creation of a biopacemaker patch. As such, the project focused on a pharmacological method to increase the spontaneous activity of the postnatal cardiomyocytes by favoring differentiation to a pacemaker cell phenotype.

#### **3.1 PMA increases the rate of spontaneous activity through Tbx3 re-expression**

The main objective of the study was to test if phorbol 12-myristate 13-acetate (PMA) can be used as a modulator of spontaneous activity of neonatal cardiomyocyte monolayers, since PMA has been shown to activate Tbx3 in breast cancer cells (181). Tbx3 is an essential transcription factor to suppress differentiation of the working myocardium and reprogram the cells to possess pacemaker phenotypes in the embryonic heart (167). According to previous studies, ectopic activation of Tbx3 in embryonic atrial myocytes resulted in induction of HCN4 channel expression (87) as a dominant isoform of the HCN channels in SAN cells (204-206). The funny current has been proposed to be crucial for generating the slow diastolic depolarization leading over the activation threshold of the pacemaker cells (44). Accordingly, overexpression of the HCN channels would be expected to increase the rate of spontaneous activity. We have found that chronic conditioning of the NRVMs with PMA increases spontaneous frequency of the cultured monolayers (figs. 1A and 2A in Chapter 2) as a consequence of increasing Tbx3 and HCN4 mRNA expression which is also shown in our study (fig. 3A and B, respectively). To evaluate the effect of PMA on HCN4 overexpression,

inhibition of the channels by ivabradine (3 $\mu$ M) was tested (203). Ivabradine has been shown to specifically block HCN channels. It was found that the rate of the spontaneous activity was significantly reduced by ivabradine when tested in the PMA-48h group (fig. 3C). The results are consistent with our findings where overexpression of HCN4 leading to increased funny current levels would be at least in part inducing the faster rate of activation by chronic exposure to PMA.

In order to create a model of the monolayers exposed to PMA, a simple simulation model with two main parameters leading to either a faster cellular rate of the activity or decreased coupling (higher resistance) between cells was used. Results of the mathematical model showed that the frequency of the spontaneous activity increased when increasing the bias current as to mimic the funny current augmentation in the experimental samples; however the effect of decrease in coupling of the cells has a slight effect on spontaneous activity rate. Increasing the bias current and coupling resistance simultaneously gives the minimum variability in mean period of activity similar in a way to our experimental data (fig. 8A).

### **3.2 PMA modulates the spatial-temporal activity in multicellular patches**

Temporal and spatial stability is one of the key properties of biopacemakers which is extremely important to provide the regular and constant pacing in order to drive cardiac rhythmic contractions (207). Regarding to our observations, chronic exposure of the NRVMs to PMA leads to enhanced temporal stability of the spontaneous activity in the cultured monolayers. Moreover, comparing the spontaneous activity patterns of both groups (figs. 1C and D) demonstrates a clear stability of the interbeat intervals as an indication of the regularity in PMA samples (fig. 1B). In addition, spatial stability of PM sites increased in PMA group as a consequence of fewer (fig. 5A) and closer (fig. 5C) 1<sup>st</sup> initiation sites. It is accompanied by less variability of activation maps in PMA group (fig. 5D). Temporal stability of the PMA exposed cells may be due to either a decreased sensitivity to membrane noise due to the steeper diastolic depolarization slope (208) or to their spatial stability. In fact, a lesser number of focal sites (1<sup>st</sup> initiation sites) correlates with a decreased in std(T) and thus a more stable interbeat interval.

Spatial distribution of the focal sites (1<sup>st</sup> initiation sites) tends to be at the border layer of the plated region (fig. 5B) which is concordant with previous studies (209-211). The best explanation for such finding would be the source-sink mechanism (212, 213). In essence, neighbouring the PM cells with less resting cells protect them from the electrotonic effect during the slow diastolic depolarization. Cells that are less coupled to neighbors will be less affected by diffusion current, hence resulting in MDP increases comparing to the central active cells. Nonetheless mathematical models of only PM cells hypothesize the synchronous activity of the neighbouring cells. In such simulation model a large clusters of 1<sup>st</sup> initiation sites located at the central position of the monolayers would drive the other parts which is far from our observations. Such behaviour may occur due to the heterogeneous distribution of the active and quiescent cells in our cultures and that also match the modeling results.

Although the PM cells in both experimental and mathematical models are both probably distributed randomly (fig. 9D), the variation of temporal and spatial stability is negligible among simulation groups as opposed to our experimental findings where temporal stability and changes in focal sites can be found indicating the role of another factor. Such factor could be cellular stochastic temporal noise (211) in addition to spatial random distribution of PM cells.

Meanwhile, the number of spontaneous reentry-like rapid activity substantially decreased with PMA which is favouring the cells to create cultured biopacemaker patch without arrhythmic activity. It could be explained somehow with increasing the number of the inactivated Na<sup>+</sup> channels as a consequence of decreased MDP leading to prolong effective refractory period (ERP), since shortening of ERP may give rise to relevance of functional reentry in cardiac tissue (31, 214). Another possibility may be through the spatial homogeneity of cell connectivity. According to the Gompertz cell growth mechanism (215), higher morphological homogeneity of the cultured cells could be present in the PMA group because of the PMA hypertrophic effect (216). Overexpression of the growth factors by PKC activation could favor smaller cells to grow faster leading to more homogeneous cell size population and thus filling better the 2D space, favoring neighboring cells to form gap junctions. Visual inspection of the samples seemed to show monolayers with higher density of the cells in PMA group (data not shown) which would point towards this possibility.

### **3.3 The increase in frequency of spontaneous activity does not yield greater synchronization**

A biopacemaker patch needs to be able to overcome the electrotonic propagation and depolarize the resting cells of the heart to which it is coupled. A more robust (less sensitive to surrounding less polarized cardiomyocytes) and more synchronized activation (all the PM cells activating at the same time) would theoretically favor the driving capability of the multicellular pacemaker. However, even if the pacemaking phenotype seemed to be facilitated by PMA, synchronization of the activation measured is decreased in both experimental and modeling data (corresponding to an increased activation delay in figs. 5E and 9C). In normal SAN cells, pulse propagation velocity is slower than the ventricular cells (34). Slow conduction velocity of the pacemaker cells predisposes them as a proper current source to stimulate the peripheral tissue. According to our results, CV decreased in PMA group independently of the CL (fig. 4B). Such effect correlates with decrease in coupling of the cells as a consequence of electrical uncoupling achieved through the down-regulation of fast-propagating connexin proteins (36, 217) due to the effect of Tbx3 expression (34). In addition, PMA increased the amplitude of applied voltage to stimulate the cells (fig. 4B) which may be due to the hypertrophic effect of PMA on cardiomyocytes (218) which could also induce in increase time to polarize the membrane.

### **3.4 CONCLUSION**

Limitations of electronic pacemakers could be bypassed if a regain in function of the sinus node normal automaticity or an alternative biological pacemaker was created either in situ or through a patch. The knowledge gathered by this project could be important in the process of creating optimized and robust biological pacemakers patches, an alternative to electronic pacemakers (219). Although stability was clearly increased by PMA possibly through re-expression of Tbx3 here, the added partial uncoupling correlating with the slower conduction velocity would be detrimental to synchronization within the patch. It remains to investigate if a more homogeneous population of PM cells could counteract this effect.

## 4 BIBLIOGRAPHY

1. Fujiu K, Nagai R. Contributions of cardiomyocyte-cardiac fibroblast-immune cell interactions in heart failure development. *Basic Res Cardiol*. 2013;108(4):357.
2. Pinnell J, Turner S, Howell S. Cardiac muscle physiology. *Continuing Education in Anaesthesia, Critical Care & Pain*. 2007;7(3):85-8.
3. Camelliti P, Borg TK, Kohl P. Structural and functional characterisation of cardiac fibroblasts. *Cardiovascular research*. 2005;65(1):40-51.
4. Panteghini M. Present issues in the determination of troponins and other markers of cardiac damage. *Clinical biochemistry*. 2000;33(3):161-6.
5. Moscoso I, Centeno A, Lopez E, Rodriguez-Barbosa J, Santamarina I, Filgueira P, et al., editors. Differentiation “in vitro” of primary and immortalized porcine mesenchymal stem cells into cardiomyocytes for cell transplantation. *Transplantation proceedings*; 2005: Elsevier.
6. Moorman AF, Christoffels VM. Cardiac chamber formation: development, genes, and evolution. *Physiological reviews*. 2003;83(4):1223-67.
7. Pennisi DJ, Rentschler S, Gourdie RG, Fishman GI, Mikawa T. Induction and patterning of the cardiac conduction system. *Int J Dev Biol*. 2002;46(6):765-75.
8. Liu H, Shao Y, Qin W, Runyan RB, Xu M, Ma Z, et al. Myosin filament assembly onto myofibrils in live neonatal cardiomyocytes observed by TPEF-SHG microscopy. *Cardiovascular Research*. 2013;97(2):262-70.
9. Souders CA, Bowers SLK, Baudino TA. Cardiac Fibroblast The Renaissance Cell. *Circ Res*. 2009;105(12):1164-76.
10. Adler C, Ringlage W, Böhm N. DNS-Gehalt and Zellzahl in Herz und Leber von Kindern: Vergleichende biochemische, cytophotometrische and histologische Untersuchungen. *Pathology-Research and Practice*. 1981;172(1):25-41.
11. Anversa P, Hiler B, Ricci R, Guideri G, Olivetti G. Myocyte cell loss and myocyte hypertrophy in the aging rat heart. *Journal of the American College of Cardiology*. 1986;8(6):1441-8.
12. Shiraishi I, Takamatsu T, Minamikawa T, Onouchi Z, Fujita S. Quantitative histological analysis of the human sinoatrial node during growth and aging. *Circulation*. 1992;85(6):2176-84.
13. Davies M, Pomerance A. Quantitative study of ageing changes in the human sinoatrial node and internodal tracts. *British heart journal*. 1972;34(2):150.
14. Sachse FB, Moreno AP, Abildskov J. Electrophysiological modeling of fibroblasts and their interaction with myocytes. *Annals of biomedical engineering*. 2008;36(1):41-56.
15. Goldsmith EC, Hoffman A, Morales MO, Potts JD, Price RL, McFadden A, et al. Organization of fibroblasts in the heart. *Developmental Dynamics*. 2004;230(4):787-94.
16. Tohse N, Yokoshiki H, Sperelakis N. Developmental changes in ion channels. *Cell Physiology Source Book*, 2nd ed, Academic Press Publishers, Chapt. 1998;34:518-31.
17. Kojima M, Sada H, Sperelakis N. Developmental changes in beta-adrenergic and cholinergic interactions on calcium-dependent slow action potentials in rat ventricular muscles. *British journal of pharmacology*. 1990;99(2):327.
18. Conforti L, Tohse N, Sperelakis N. Tetrodotoxin-sensitive sodium current in rat fetal ventricular myocytes-contribution to the plateau phase of action potential. *J Mol Cell Cardiol*. 1993;25(2):159-73.

19. Masuda H, Sumii K, Sperelakis N. Long openings of calcium channels in fetal rat ventricular cardiomyocytes. *Pflügers Archiv*. 1995;429(4):595-7.
20. Wahler GM. Developmental increases in the inwardly rectifying potassium current of rat ventricular myocytes. *American Journal of Physiology-Cell Physiology*. 1992;262(5):C1266-C72.
21. Xie L, Takano M, Noma A. Development of inwardly rectifying K<sup>+</sup> channel family in rat ventricular myocytes. *Am J Physiol-Heart C*. 1997;272(4):H1741-H50.
22. Keith A, Flack M. The form and nature of the muscular connections between the primary divisions of the vertebrate heart. *Journal of anatomy and physiology*. 1907;41(Pt 3):172.
23. Lev M. Aging changes in the human sinoatrial node. *Journal of gerontology*. 1954;9(1):1-9.
24. Harvey RP. Patterning the vertebrate heart. *Nature Reviews Genetics*. 2002;3(7):544-56.
25. James TN. Anatomy of the human sinus node. *The Anatomical Record*. 1961;141(2):109-39.
26. Amin AS, Tan HL, Wilde AA. Cardiac ion channels in health and disease. *Heart Rhythm*. 2010;7(1):117-26.
27. Li J, Greener ID, Inada S, Nikolski VP, Yamamoto M, Hancox JC, et al. Computer three-dimensional reconstruction of the atrioventricular node. *Circ Res*. 2008;102(8):975-85.
28. Spach MS, Lieberman M, Scott JG, Barr RC, Johnson E, Kootsey JM. Excitation sequences of the atrial septum and the AV node in isolated hearts of the dog and rabbit. *Circ Res*. 1971;29(2):156-72.
29. MOE GK, PRESTON JB, BURLINGTON H. Physiologic evidence for a dual AV transmission system. *Circ Res*. 1956;4(4):357-75.
30. Hucker WJ, Sharma V, Nikolski VP, Efimov IR. Atrioventricular conduction with and without AV nodal delay: two pathways to the bundle of His in the rabbit heart. *Am J Physiol-Heart C*. 2007;293(2):H1122-H30.
31. Bartos DC, Grandi E, Ripplinger CM. Ion channels in the heart. *Comprehensive Physiology*. 2015.
32. Gordan R, Gwathmey JK, Xie L-H. Autonomic and endocrine control of cardiovascular function. *World journal of cardiology*. 2015;7(4):204.
33. DiFrancesco D, Tortora P. Direct activation of cardiac pacemaker channels by intracellular cyclic AMP. *Nature*. 1991;351(6322):145-7.
34. Bakker ML, Boink GJ, Boukens BJ, Verkerk AO, van den Boogaard M, den Haan AD, et al. T-box transcription factor TBX3 reprogrammes mature cardiac myocytes into pacemaker-like cells. *Cardiovascular research*. 2012;94(3):439-49.
35. Monfredi O, Maltsev VA, Lakatta EG. Modern concepts concerning the origin of the heartbeat. *Physiology*. 2013;28(2):74-92.
36. Kreuzberg MM, Söhl G, Kim J-S, Verselis VK, Willecke K, Bukauskas FF. Functional properties of mouse connexin30.2 expressed in the conduction system of the heart. *Circ Res*. 2005;96(11):1169-77.
37. Schram G, Pourrier M, Melnyk P, Nattel S. Differential distribution of cardiac ion channel expression as a basis for regional specialization in electrical function. *Circ Res*. 2002;90(9):939-50.

38. Ludwig A, Zong X, Jeglitsch M, Hofmann F, Biel M. A family of hyperpolarization-activated mammalian cation channels. *Nature*. 1998;393(6685):587-91.
39. Stieber J, Hofmann F, Ludwig A. Pacemaker channels and sinus node arrhythmia. *Trends in cardiovascular medicine*. 2004;14(1):23-8.
40. Herrmann S, Hofmann F, Stieber J, Ludwig A. HCN channels in the heart: lessons from mouse mutants. *British journal of pharmacology*. 2012;166(2):501-9.
41. Das MK. *Modern Pacemakers-Present and Future*: InTech; 2011.
42. Verkerk AO, van Ginneken AC, Wilders R. Pacemaker activity of the human sinoatrial node: role of the hyperpolarization-activated current, I<sub>f</sub>. *International journal of cardiology*. 2009;132(3):318-36.
43. Baruscotti M, Bucchi A, DiFrancesco D. Physiology and pharmacology of the cardiac pacemaker (“funny”) current. *Pharmacology & therapeutics*. 2005;107(1):59-79.
44. Brown H, DiFrancesco D, Noble S. How does adrenaline accelerate the heart? 1979.
45. Perez-Reyes E. Three for T: molecular analysis of the low voltage-activated calcium channel family. *Cellular and Molecular Life Sciences CMLS*. 1999;56(7-8):660-9.
46. Bean BP. Two kinds of calcium channels in canine atrial cells. Differences in kinetics, selectivity, and pharmacology. *The Journal of general physiology*. 1985;86(1):1-30.
47. Hagiwara N, Irisawa H, Kameyama M. Contribution of two types of calcium currents to the pacemaker potentials of rabbit sino-atrial node cells. *The Journal of physiology*. 1988;395(1):233-53.
48. Benitah J-P, Alvarez JL, Gómez AM. L-type Ca<sup>2+</sup> current in ventricular cardiomyocytes. *J Mol Cell Cardiol*. 2010;48(1):26-36.
49. Yang J, Eillnor PT, Sather WA, Zhang J-F, Tsien RW. Molecular determinants of Ca<sup>2+</sup> selectivity and ion permeation in L-type Ca<sup>2+</sup> channels. *Nature*. 1993;366(6451):158-61.
50. Chandler NJ, Greener ID, Tellez JO, Inada S, Musa H, Molenaar P, et al. Molecular architecture of the human sinus node insights into the function of the cardiac pacemaker. *Circulation*. 2009;119(12):1562-75.
51. Marionneau C, Couette B, Liu J, Li H, Mangoni ME, Nargeot J, et al. Specific pattern of ionic channel gene expression associated with pacemaker activity in the mouse heart. *The Journal of physiology*. 2005;562(1):223-34.
52. Reuter H. Calcium channel modulation by neurotransmitters, enzymes and drugs. *Nature*. 1982;301(5901):569-74.
53. Reuter H. Properties of two inward membrane currents in the heart. *Annual review of physiology*. 1979;41(1):413-24.
54. Tsien R, Lipscombe D, Madison D, Bley K, Fox A. Multiple types of neuronal calcium channels and their selective modulation. *Trends in neurosciences*. 1988;11(10):431-8.
55. Hofmann F, Flockerzi V, Kahl S, Wegener JW. L-type Ca<sup>v</sup>1.2 calcium channels: from in vitro findings to in vivo function. *Physiological reviews*. 2014;94(1):303-26.
56. Reuter H. Localization of beta adrenergic receptors, and effects of noradrenaline and cyclic nucleotides on action potentials, ionic currents and tension in mammalian cardiac muscle. *The Journal of physiology*. 1974;242(2):429-51.
57. Osterrieder W, Brum G, Hescheler J, Trautwein W, Flockerzi V, Hofmann F. Injection of subunits of cyclic AMP-dependent protein kinase into cardiac myocytes modulates Ca<sup>2+</sup> current. 1982.

58. Kameyama M, Hescheler J, Hofmann F, Trautwein W. Modulation of Ca current during the phosphorylation cycle in the guinea pig heart. *Pflügers Archiv*. 1986;407(2):123-8.
59. Mangoni ME, Nargeot J. Genesis and regulation of the heart automaticity. *Physiological reviews*. 2008;88(3):919-82.
60. Sakai R, Hagiwara N, Matsuda N, Kassanuki H, Hosoda S. Sodium--potassium pump current in rabbit sino-atrial node cells. *The Journal of Physiology*. 1996;490(1):51-62.
61. Noma A, Irisawa H. Contribution of an electrogenic sodium pump to the membrane potential in rabbit sinoatrial node cells. *Pflügers Archiv*. 1975;358(4):289-301.
62. Nerbonne JM, Kass RS. Molecular physiology of cardiac repolarization. *Physiological reviews*. 2005;85(4):1205-53.
63. Sanguinetti MC, Jurkiewicz N. Two components of cardiac delayed rectifier K<sup>+</sup> current. Differential sensitivity to block by class III antiarrhythmic agents. *The Journal of general physiology*. 1990;96(1):195-215.
64. Li G-R, Du X-L, Siow YL, Karmin O, Tse H-F, Lau C-P. Calcium-activated transient outward chloride current and phase 1 repolarization of swine ventricular action potential. *Cardiovascular research*. 2003;58(1):89-98.
65. Liu D-W, Gintant GA, Antzelevitch C. Ionic bases for electrophysiological distinctions among epicardial, midmyocardial, and endocardial myocytes from the free wall of the canine left ventricle. *Circ Res*. 1993;72(3):671-87.
66. Ono K, Ito H. Role of rapidly activating delayed rectifier K<sup>+</sup> current in sinoatrial node pacemaker activity. *Am J Physiol-Heart C*. 1995;269(2):H453-H62.
67. Takumi T, Ohkubo H, Nakanishi S. Cloning of a membrane protein that induces a slow voltage-gated potassium current. *Science*. 1988;242(4881):1042-5.
68. Barhanin J, Lesage F, Guillemare E, Fink M, Lazdunski M, Romey G. KvLQT1 and IsK (minK) proteins associate to form the IKs cardiac potassium current. *Nature*. 1996;384(6604):78-80.
69. IP S. Coassembly of KvLQT1 and minK (IsK) proteins to form cardiac IKs potassium channel. *Nature*. 1996;384.
70. Jespersen T, Grunnet M, Olesen S-P. The KCNQ1 potassium channel: from gene to physiological function. *Physiology*. 2005;20(6):408-16.
71. Potet F, Scott JD, Mohammad-Panah R, Escande D, Baró I. AKAP proteins anchor cAMP-dependent protein kinase to KvLQT1/IsK channel complex. *Am J Physiol-Heart C*. 2001;280(5):H2038-H45.
72. Terrenoire C, Clancy CE, Cormier JW, Sampson KJ, Kass RS. Autonomic Control of Cardiac Action Potentials Role of Potassium Channel Kinetics in Response to Sympathetic Stimulation. *Circ Res*. 2005;96(5):e25-e34.
73. Banyasz T, Koncz R, Fulop L, Szentandrassy N, Magyar J, Nanasi PP. Profile of IKs during the action potential questions the therapeutic value of IKs blockade. *Current medicinal chemistry*. 2004;11(1):45-60.
74. Anumonwo JM, Lopatin AN. Cardiac strong inward rectifier potassium channels. *J Mol Cell Cardiol*. 2010;48(1):45-54.
75. Plaster NM, Tawil R, Tristani-Firouzi M, Canún S, Bendahhou Sd, Tsunoda A, et al. Mutations in Kir2. 1 cause the developmental and episodic electrical phenotypes of Andersen's syndrome. *Cell*. 2001;105(4):511-9.

76. Zaritsky JJ, Redell JB, Tempel BL, Schwarz TL. The consequences of disrupting cardiac inwardly rectifying K<sup>+</sup> current (IK1) as revealed by the targeted deletion of the murine Kir2. 1 and Kir2. 2 genes. *The Journal of Physiology*. 2001;533(3):697-710.
77. Guo J, Ono K, Noma A. A sustained inward current activated at the diastolic potential range in rabbit sino-atrial node cells. *The Journal of Physiology*. 1995;483(1):1-13.
78. Shinagawa Y, Satoh H, Noma A. The sustained inward current and inward rectifier K<sup>+</sup> current in pacemaker cells dissociated from rat sinoatrial node. *The Journal of Physiology*. 2000;523(3):593-605.
79. Bamshad M, Lin RC, Law DJ, Watkins WS, Krakowiak PA, Moore ME, et al. Mutations in human TBX3 alter limb, apocrine and genital development in ulnar-mammary syndrome. *Nature genetics*. 1997;16(3):311-5.
80. Carlson H, Ota S, Campbell CE, Hurlin PJ. A dominant repression domain in Tbx3 mediates transcriptional repression and cell immortalization: relevance to mutations in Tbx3 that cause ulnar-mammary syndrome. *Human molecular genetics*. 2001;10(21):2403-13.
81. Davenport TG, Jerome-Majewska LA, Papaioannou VE. Mammary gland, limb and yolk sac defects in mice lacking Tbx3, the gene mutated in human ulnar mammary syndrome. *Development*. 2003;130(10):2263-73.
82. Meneghini V, Odent S, Platonova N, Egeo A, Merlo GR. Novel TBX3 mutation data in families with Ulnar–Mammary syndrome indicate a genotype–phenotype relationship: mutations that do not disrupt the T-domain are associated with less severe limb defects. *European journal of medical genetics*. 2006;49(2):151-8.
83. Klopocki E, Neumann LM, Tönnies H, Ropers H-H, Mundlos S, Ullmann R. Ulnar-mammary syndrome with dysmorphic facies and mental retardation caused by a novel 1.28 Mb deletion encompassing the TBX3 gene. *European journal of human genetics*. 2006;14(12):1274-9.
84. Rowley M, Grothey E, Couch FJ. The role of Tbx2 and Tbx3 in mammary development and tumorigenesis. *Journal of mammary gland biology and neoplasia*. 2004;9(2):109-18.
85. Renard C-A, Labalette C, Armengol C, Cougot D, Wei Y, Cairo S, et al. Tbx3 is a downstream target of the Wnt/β-catenin pathway and a critical mediator of β-catenin survival functions in liver cancer. *Cancer research*. 2007;67(3):901-10.
86. Hoogaars W, Barnett P, Moorman A, Christoffels V. Cardiovascular development: towards biomedical applicability: T-box factors determine cardiac design. *Cellular and molecular life sciences*. 2007;64(6):646.
87. Hoogaars WM, Engel A, Brons JF, Verkerk AO, de Lange FJ, Wong LE, et al. Tbx3 controls the sinoatrial node gene program and imposes pacemaker function on the atria. *Genes & development*. 2007;21(9):1098-112.
88. Mommersteeg MT, Hoogaars WM, Prall OW, de Gier-de Vries C, Wiese C, Clout DE, et al. Molecular pathway for the localized formation of the sinoatrial node. *Circ Res*. 2007;100(3):354-62.
89. Hüser J, Blatter LA, Lipsius SL. Intracellular Ca<sup>2+</sup> release contributes to automaticity in cat atrial pacemaker cells. *The Journal of Physiology*. 2000;524(2):415-22.
90. Ju Y-K, Allen DG. The distribution of calcium in toad cardiac pacemaker cells during spontaneous firing. *Pflügers Archiv*. 2000;441(2-3):219-27.

91. Lakatta EG, Maltsev VA, Vinogradova TM. A coupled SYSTEM of intracellular Ca<sup>2+</sup> clocks and surface membrane voltage clocks controls the timekeeping mechanism of the heart's pacemaker. *Circ Res.* 2010;106(4):659-73.
92. Periasamy M, Kalyanasundaram A. SERCA pump isoforms: their role in calcium transport and disease. *Muscle & nerve.* 2007;35(4):430-42.
93. Toyoshima C, Inesi G. Structural basis of ion pumping by Ca<sup>2+</sup>-ATPase of the sarcoplasmic reticulum. *Biochemistry.* 2004;73(1):269.
94. Bers DM. Ca transport during contraction and relaxation in mammalian ventricular muscle. *Basic research in cardiology.* 1997;92(1):1-10.
95. MacLennan DH, Kranias EG. Phospholamban: a crucial regulator of cardiac contractility. *Nature reviews Molecular cell biology.* 2003;4(7):566-77.
96. Lai F, Misra M, Xu L, Smith H, Meissner G. The ryanodine receptor-Ca<sup>2+</sup> release channel complex of skeletal muscle sarcoplasmic reticulum. Evidence for a cooperatively coupled, negatively charged homotetramer. *Journal of Biological Chemistry.* 1989;264(28):16776-85.
97. Block BA, Imagawa T, Campbell KP, Franzini-Armstrong C. Structural evidence for direct interaction between the molecular components of the transverse tubule/sarcoplasmic reticulum junction in skeletal muscle. *The Journal of cell biology.* 1988;107(6):2587-600.
98. Sun X-H, Protasi F, Takahashi M, Takeshima H, Ferguson DG, Franzini-Armstrong C. Molecular architecture of membranes involved in excitation-contraction coupling of cardiac muscle. *The Journal of Cell Biology.* 1995;129(3):659-71.
99. Takeshima H, Ikemoto T, Nishi M, Nishiyama N, Shimuta M, Sugitani Y, et al. Generation and characterization of mutant mice lacking ryanodine receptor type 3. *Journal of Biological Chemistry.* 1996;271(33):19649-52.
100. Takeshima H, Komazaki S, Hirose K, Nishi M, Noda T, Iino M. Embryonic lethality and abnormal cardiac myocytes in mice lacking ryanodine receptor type 2. *The EMBO Journal.* 1998;17(12):3309-16.
101. Broun MJ, Asghari P, Wambolt RB, Bohunek L, Smits C, Philit M, et al. Cardiac ryanodine receptors control heart rate and rhythmicity in adult mice. *Cardiovascular research.* 2012;cvs260.
102. Meissner G. Molecular regulation of cardiac ryanodine receptor ion channel. *Cell calcium.* 2004;35(6):621-8.
103. Reeves JP, Hale CC. The stoichiometry of the cardiac sodium-calcium exchange system. *Journal of Biological Chemistry.* 1984;259(12):7733-9.
104. Reuter H, Pott C, Goldhaber JI, Henderson SA, Philipson KD, Schwinger RH. Na<sup>+</sup>-Ca<sup>2+</sup> exchange in the regulation of cardiac excitation-contraction coupling. *Cardiovascular Research.* 2005;67(2):198-207.
105. Cheng H, Lederer W, Cannell MB. Calcium sparks: elementary events underlying excitation-contraction coupling in heart muscle. *Science.* 1993;262(5134):740-4.
106. Frank J, Mottino G, Reid D, Molday R, Philipson K. Distribution of the Na<sup>+</sup>-Ca<sup>2+</sup> exchange protein in mammalian cardiac myocytes: an immunofluorescence and immunocolloidal gold-labeling study. *The Journal of Cell Biology.* 1992;117(2):337-45.
107. Schuessler RB. Abnormal sinus node function in clinical arrhythmias. *Journal of cardiovascular electrophysiology.* 2003;14(2):215-7.
108. Bleeker W, Mackaay A, Masson-Pévet M, Bouman LN, Becker AE. Functional and morphological organization of the rabbit sinus node. *Circ Res.* 1980;46(1):11-22.

109. Fedorov VV, Glukhov AV, Chang R, KostECKI G, Aferol H, Hucker WJ, et al. Optical mapping of the isolated coronary-perfused human sinus node. *Journal of the American College of Cardiology*. 2010;56(17):1386-94.
110. Fedorov VV, Schuessler RB, Hemphill M, Ambrosi CM, Chang R, Voloshina AS, et al. Structural and functional evidence for discrete exit pathways that connect the canine sinoatrial node and atria. *Circ Res*. 2009;104(7):915-23.
111. Matsuyama T-a, Inoue S, Kobayashi Y, Sakai T, Saito T, Katagiri T, et al. Anatomical diversity and age-related histological changes in the human right atrial posterolateral wall. *Europace*. 2004;6(4):307-15.
112. Sanchez-Quintana D, Cabrera J, Farre J, Climent V, Anderson R, Ho S. Sinus node revisited in the era of electroanatomical mapping and catheter ablation. *Heart*. 2005;91(2):189-94.
113. Csepe TA, Zhao J, Hansen BJ, Li N, Sul LV, Lim P, et al. Human sinoatrial node structure: 3D microanatomy of sinoatrial conduction pathways. *Progress in biophysics and molecular biology*. 2015.
114. Tellez JO, Dobrzynski H, Greener ID, Graham GM, Laing E, Honjo H, et al. Differential expression of ion channel transcripts in atrial muscle and sinoatrial node in rabbit. *Circ Res*. 2006;99(12):1384-93.
115. Park DS, Fishman GI. The cardiac conduction system. *Circulation*. 2011;123(8):904-15.
116. Boyett MR, Honjo H, Kodama I. The sinoatrial node, a heterogeneous pacemaker structure. *Cardiovascular research*. 2000;47(4):658-87.
117. Verheijck EE, Wessels A, van Ginneken AC, Bourier J, Markman MW, Vermeulen JL, et al. Distribution of Atrial and Nodal Cells Within the Rabbit Sinoatrial Node Models of Sinoatrial Transition. *Circulation*. 1998;97(16):1623-31.
118. Kodama I, Nikmaram M, Boyett M, Suzuki R, Honjo H, Owen J. Regional differences in the role of the Ca<sup>2+</sup> and Na<sup>+</sup> currents in pacemaker activity in the sinoatrial node. *Am J Physiol-Heart C*. 1997;272(6):H2793-H806.
119. Rook M, Jongasma H, Van Ginneken A. Properties of single gap junctional channels between isolated neonatal rat heart cells. *Am J Physiol-Heart C*. 1988;255(4):H770-H82.
120. Unwin P, Zampighi G. Structure of the junction between communicating cells. *Nature*. 1980;283(5747):545-9.
121. Boyett M, Inada S, Yoo S, Li J, Liu J, Tellez J, et al. Connexins in the sinoatrial and atrioventricular nodes. 2006.
122. Gaudesius G, Miragoli M, Thomas SP, Rohr S. Coupling of cardiac electrical activity over extended distances by fibroblasts of cardiac origin. *Circ Res*. 2003;93(5):421-8.
123. Mond HG, Proclemer A. The 11th World Survey of Cardiac Pacing and Implantable Cardioverter-Defibrillators: Calendar Year 2009—A World Society of Arrhythmia's Project. *Pacing and Clinical Electrophysiology*. 2011;34(8):1013-27.
124. Dobrzynski H, Boyett MR, Anderson RH. New insights into pacemaker activity promoting understanding of sick sinus syndrome. *Circulation*. 2007;115(14):1921-32.
125. Elvan A, Wylie K, Zipes DP. Pacing-induced chronic atrial fibrillation impairs sinus node function in dogs electrophysiological remodeling. *Circulation*. 1996;94(11):2953-60.
126. Sparks PB, Jayaprakash S, Vohra JK, Kalman JM. Electrical remodeling of the atria associated with paroxysmal and chronic atrial flutter. *Circulation*. 2000;102(15):1807-13.

127. Boink GJ, Verkerk AO, van Amersfoort S, Tasseron SJ, van der Rijt R, Bakker D, et al. Engineering physiologically controlled pacemaker cells with lentiviral HCN4 gene transfer. *The journal of gene medicine*. 2008;10(5):487-97.
128. Michaëlsson M, Jonzon A, Riesenfeld T. Isolated congenital complete atrioventricular block in adult life A prospective study. *Circulation*. 1995;92(3):442-9.
129. Rosen MR, Brink PR, Cohen IS, Robinson RB. Genes, stem cells and biological pacemakers. *Cardiovascular research*. 2004;64(1):12-23.
130. Brooks CM, Lu H-H. *The sinoatrial pacemaker of the heart*: Charles C. Thomas Publisher; 1972.
131. Kusumoto FM, Goldschlager N. Cardiac Pacing. *New England Journal of Medicine*. 1996;334(2):89-99.
132. Ferrari AD, Borges AP, Albuquerque LC, Pelzer Sussenbach C, Rosa PR, Pianta RM, et al. Cardiomyopathy induced by artificial cardiac pacing: myth or reality sustained by evidence? *Rev Bras Cir Cardiovasc*. 2014;29(3):402-13.
133. Kurtz SM, Ochoa JA, Lau E, Shkolnikov Y, Pavri BB, Frisch D, et al. Implantation trends and patient profiles for pacemakers and implantable cardioverter defibrillators in the United States: 1993–2006. *Pacing and Clinical Electrophysiology*. 2010;33(6):705-11.
134. Boink GJ, Christoffels VM, Robinson RB, Tan HL. The past, present, and future of pacemaker therapies. *Trends in cardiovascular medicine*. 2015.
135. Lyon A, Sato M, Hajjar R, Samulski R, Harding S. Gene therapy: targeting the myocardium. *Heart*. 2008;94(1):89-99.
136. Vinge LE, Raake PW, Koch WJ. Gene therapy in heart failure. *Circ Res*. 2008;102(12):1458-70.
137. Mason D, Chen Y-Z, Krishnan HV, Sant S. Cardiac gene therapy: Recent advances and future directions. *Journal of Controlled Release*. 2015;215:101-11.
138. Cai J, Yi F-F, Li Y-H, Yang X-C, Song J, Jiang X-J, et al. Adenoviral gene transfer of HCN4 creates a genetic pacemaker in pigs with complete atrioventricular block. *Life sciences*. 2007;80(19):1746-53.
139. Bucchi A, Plotnikov AN, Shlapakova I, Danilo P, Kryukova Y, Qu J, et al. Wild-type and mutant HCN channels in a tandem biological-electronic cardiac pacemaker. *Circulation*. 2006;114(10):992-9.
140. Kass-Eisler A, Falck-Pedersen E, Alvira M, Rivera J, Buttrick PM, Wittenberg BA, et al. Quantitative determination of adenovirus-mediated gene delivery to rat cardiac myocytes in vitro and in vivo. *Proceedings of the National Academy of Sciences*. 1993;90(24):11498-502.
141. Zhao J, Pettigrew GJ, Thomas J, Vandenberg JI, Delriviere L, Bolton EM, et al. Lentiviral vectors for delivery of genes into neonatal and adult ventricular cardiac myocytes in vitro and in vivo. *Basic research in cardiology*. 2002;97(5):348-58.
142. Zhao J, Pettigrew G, Bolton E, Murfitt C, Carmichael A, Bradley J, et al. Lentivirus-mediated gene transfer of viral interleukin-10 delays but does not prevent cardiac allograft rejection. *Gene therapy*. 2005;12(20):1509-16.
143. Seppen J, Barry SC, Harder B, Osborne WR. Lentivirus administration to rat muscle provides efficient sustained expression of erythropoietin. *Blood*. 2001;98(3):594-6.
144. Edelberg J, Huang D, Josephson M, Rosenberg R. Molecular enhancement of porcine cardiac chronotropy. *Heart*. 2001;86(5):559-62.
145. Miake J, Marbán E, Nuss HB. Gene therapy: biological pacemaker created by gene transfer. *Nature*. 2002;419(6903):132-3.

146. Qu J, Plotnikov AN, Danilo P, Shlapakova I, Cohen IS, Robinson RB, et al. Expression and function of a biological pacemaker in canine heart. *Circulation*. 2003;107(8):1106-9.
147. Rosen MR, Brink PR, Cohen IS, Robinson RB. Cardiac Pacing From Biological to Electronic... to Biological? *Circulation: arrhythmia and electrophysiology*. 2008;1(1):54-61.
148. Kehat I, Khimovich L, Caspi O, Gepstein A, Shofti R, Arbel G, et al. Electromechanical integration of cardiomyocytes derived from human embryonic stem cells. *Nature biotechnology*. 2004;22(10):1282-9.
149. Potapova I, Plotnikov A, Lu Z, Danilo P, Valiunas V, Qu J, et al. Human mesenchymal stem cells as a gene delivery system to create cardiac pacemakers. *Circ Res*. 2004;94(7):952-9.
150. Plotnikov AN, Shlapakova I, Szabolcs MJ, Danilo P, Lorell BH, Potapova IA, et al. Xenografted adult human mesenchymal stem cells provide a platform for sustained biological pacemaker function in canine heart. *Circulation*. 2007;116(7):706-13.
151. Valiunas V, Doronin S, Valiuniene L, Potapova I, Zuckerman J, Walcott B, et al. Human mesenchymal stem cells make cardiac connexins and form functional gap junctions. *The Journal of physiology*. 2004;555(3):617-26.
152. Soonpaa MH, Field LJ. Survey of studies examining mammalian cardiomyocyte DNA synthesis. *Circ Res*. 1998;83(1):15-26.
153. Chien KR, Olson EN. Converging pathways and principles in heart development and disease: CV@ CSH. *Cell*. 2002;110(2):153-62.
154. Claycomb WC. Control of cardiac muscle cell division. *Trends in cardiovascular medicine*. 1992;2(6):231-6.
155. Beltrami AP, Barlucchi L, Torella D, Baker M, Limana F, Chimenti S, et al. Adult cardiac stem cells are multipotent and support myocardial regeneration. *Cell*. 2003;114(6):763-76.
156. Oh H, Bradfute SB, Gallardo TD, Nakamura T, Gaussin V, Mishina Y, et al. Cardiac progenitor cells from adult myocardium: homing, differentiation, and fusion after infarction. *Proceedings of the National Academy of Sciences*. 2003;100(21):12313-8.
157. Martin CM, Meeson AP, Robertson SM, Hawke TJ, Richardson JA, Bates S, et al. Persistent expression of the ATP-binding cassette transporter, *Abcg2*, identifies cardiac SP cells in the developing and adult heart. *Developmental biology*. 2004;265(1):262-75.
158. Matsuura K, Nagai T, Nishigaki N, Oyama T, Nishi J, Wada H, et al. Adult cardiac Sca-1-positive cells differentiate into beating cardiomyocytes. *Journal of Biological Chemistry*. 2004;279(12):11384-91.
159. Messina E, De Angelis L, Frati G, Morrone S, Chimenti S, Fiordaliso F, et al. Isolation and expansion of adult cardiac stem cells from human and murine heart. *Circ Res*. 2004;95(9):911-21.
160. Orlic D, Kajstura J, Chimenti S, Jakoniuk I, Anderson SM, Li B, et al. Bone marrow cells regenerate infarcted myocardium. *Nature*. 2001;410(6829):701-5.
161. Kajstura J, Rota M, Whang B, Cascapera S, Hosoda T, Bearzi C, et al. Bone marrow cells differentiate in cardiac cell lineages after infarction independently of cell fusion. *Circ Res*. 2005;96(1):127-37.
162. Laugwitz K-L, Moretti A, Lam J, Gruber P, Chen Y, Woodard S, et al. Postnatal isl1+ cardioblasts enter fully differentiated cardiomyocyte lineages. *Nature*. 2007;446:934.
163. Anversa P, Sussman MA, Bolli R. Molecular genetic advances in cardiovascular medicine focus on the myocyte. *Circulation*. 2004;109(23):2832-8.

164. Dimmeler S, Zeiher AM, Schneider MD. Unchain my heart: the scientific foundations of cardiac repair. *Journal of Clinical Investigation*. 2005;115(3):572.
165. Torella D, Ellison GM, Nadal-Ginard B, Indolfi C. Cardiac stem and progenitor cell biology for regenerative medicine. *Trends in cardiovascular medicine*. 2005;15(6):229-36.
166. Hoogaars WM, Tessari A, Moorman AF, de Boer PA, Hagoort J, Soufan AT, et al. The transcriptional repressor Tbx3 delineates the developing central conduction system of the heart. *Cardiovascular research*. 2004;62(3):489-99.
167. Bakker ML, Boukens BJ, Mommersteeg MT, Brons JF, Wakker V, Moorman AF, et al. Transcription factor Tbx3 is required for the specification of the atrioventricular conduction system. *Circ Res*. 2008;102(11):1340-9.
168. Frank DU, Carter KL, Thomas KR, Burr RM, Bakker ML, Coetzee WA, et al. Lethal arrhythmias in Tbx3-deficient mice reveal extreme dosage sensitivity of cardiac conduction system function and homeostasis. *Proceedings of the National Academy of Sciences*. 2012;109(3):E154-E63.
169. Walsh S, Pontén A, Fleischmann BK, Jovinge S. Cardiomyocyte cell cycle control and growth estimation in vivo—an analysis based on cardiomyocyte nuclei. *Cardiovascular research*. 2010;86(3):365-73.
170. Noorman M, van der Heyden MA, van Veen TA, Cox MG, Hauer RN, de Bakker JM, et al. Cardiac cell–cell junctions in health and disease: electrical versus mechanical coupling. *J Mol Cell Cardiol*. 2009;47(1):23-31.
171. Sheikh F, Ross RS, Chen J. Cell-cell connection to cardiac disease. *Trends in cardiovascular medicine*. 2009;19(6):182-90.
172. Janmey PA, Miller RT. Mechanisms of mechanical signaling in development and disease. *Journal of cell science*. 2011;124(1):9-18.
173. Swift J, Ivanovska IL, Buxboim A, Harada T, Dingal PDP, Pinter J, et al. Nuclear lamin-A scales with tissue stiffness and enhances matrix-directed differentiation. *Science*. 2013;341(6149):1240104.
174. Majkut S, Dingal PDP, Discher DE. Stress sensitivity and mechanotransduction during heart development. *Current Biology*. 2014;24(10):R495-R501.
175. Li F, Wang X, Capasso JM, Gerdes AM. Rapid transition of cardiac myocytes from hyperplasia to hypertrophy during postnatal development. *J Mol Cell Cardiol*. 1996;28(8):1737-46.
176. Soonpaa MH, Kim KK, Pajak L, Franklin M, Field LJ. Cardiomyocyte DNA synthesis and binucleation during murine development. *Am J Physiol-Heart C*. 1996;271(5):H2183-H9.
177. Porrello ER, Mahmoud AI, Simpson E, Hill JA, Richardson JA, Olson EN, et al. Transient regenerative potential of the neonatal mouse heart. *Science*. 2011;331(6020):1078-80.
178. Harary I, Farley B. In vitro studies on single beating rat heart cells: II. Intercellular communication. *Experimental cell research*. 1963;29(3):466-74.
179. Harary I, Farley B. In vitro studies on single beating rat heart cells: I. Growth and organization. *Experimental cell research*. 1963;29(3):451-65.
180. Tung L, Bursac N, Aguel F. Rotors and spiral waves in two dimensions. *Cardiac Electrophysiology: From Cell to Bedside Philadelphia: WB Saunders*. 2004:336-44.
181. Mowla S, Pinnock R, Leaner V, Goding C, Prince S. PMA-induced up-regulation of TBX3 is mediated by AP-1 and contributes to breast cancer cell migration. *Biochem J*. 2011;433:145-53.

182. Goel G, Makkar HP, Francis G, Becker K. Phorbol esters: structure, biological activity, and toxicity in animals. *International journal of toxicology*. 2007;26(4):279-88.
183. Liu W, Heckman C. The sevenfold way of PKC regulation. *Cellular signalling*. 1998;10(8):529-42.
184. Nishizuka Y. Studies and perspectives of protein kinase C. *Science*. 1986;233(4761):305-12.
185. Burns DJ, Bell R. Protein kinase C contains two phorbol ester binding domains. *Journal of Biological Chemistry*. 1991;266(27):18330-8.
186. Lamph WW, Wamsley P, Sassone-Corsi P, Verma IM. Induction of proto-oncogene JUN/AP-1 by serum and TPA. 1988.
187. Li J, Ma C, Huang Y, Luo J, Huang C. Differential requirement of EGF receptor and its tyrosine kinase for AP-1 transactivation induced by EGF and TPA. *Oncogene*. 2003;22(2):211-9.
188. Wagner EF. AP-1--Introductory remarks. *Oncogene*. 2001;20(19):2334-5.
189. Karin M. The regulation of AP-1 activity by mitogen-activated protein kinases. *Journal of Biological Chemistry*. 1995;270(28):16483-6.
190. Kieser A, Seitz T, Adler HS, Coffey P, Kremmer E, Crespo P, et al. Protein kinase C-zeta reverts v-raf transformation of NIH-3T3 cells. *Genes & development*. 1996;10(12):1455-66.
191. LeHoux J-G, Lefebvre A. Novel protein kinase C-epsilon inhibits human CYP11B2 gene expression through ERK1/2 signalling pathway and JunB. *Journal of molecular endocrinology*. 2006;36(1):51-64.
192. Clément SA, Tan CC, Guo J, Kitta K, Suzuki YJ. Roles of protein kinase C and  $\alpha$ -tocopherol in regulation of signal transduction for GATA-4 phosphorylation in HL-1 cardiac muscle cells. *Free Radical Biology and Medicine*. 2002;32(4):341-9.
193. Lindemann R, Braig M, Hauser C, Nordheim A, Dittmer J. Ets2 and protein kinase Cepsilon are important regulators of parathyroid hormone-related protein expression in MCF-7 breast cancer cells. *Biochem J*. 2003;372:787-97.
194. Song H, Hwang HJ, Chang W, Song B-W, Cha M-J, Kim I-K, et al. Cardiomyocytes from phorbol myristate acetate-activated mesenchymal stem cells restore electromechanical function in infarcted rat hearts. *Proceedings of the National Academy of Sciences*. 2011;108(1):296-301.
195. Slaga TJ. *Mechanisms of tumor promotion*: CRC Press; 1984.
196. Mond JJ, Feuerstein N, June CH, Balapure AK, Glazer RI, Witherspoon K, et al. Bimodal effect of phorbol ester on B cell activation. Implication for the role of protein kinase C. *Journal of Biological Chemistry*. 1991;266(7):4458-63.
197. Tangye SG, Weston KM, Raison RL. Phorbol ester activates CD5+ leukaemic B cells via a T cell-independent mechanism. *Immunology and cell biology*. 1995;73:44-.
198. Katiyar SK, Agarwal R, Mukhtar H. Inhibition of tumor promotion in SENCAR mouse skin by ethanol extract of Zingiber officinale rhizome. *Cancer research*. 1996;56(5):1023-30.
199. Baird AC, Lloyd F, Lawrance IC. Prostaglandin E2 and Polyenylphosphatidylcholine Protect Against Intestinal Fibrosis and Regulate Myofibroblast Function. *Digestive diseases and sciences*. 2015:1-14.
200. Patil RH, Babu R, Kumar MN, Kumar KK, Hegde SM, Ramesh GT, et al. Apigenin inhibits PMA-induced expression of pro-inflammatory cytokines and AP-1 factors in A549 cells. *Molecular and cellular biochemistry*. 2015;403(1-2):95-106.

201. Baruscotti M, Barbuti A, Bucchi A. The cardiac pacemaker current. *J Mol Cell Cardiol.* 2010;48(1):55-64.
202. Bucchi A, Tognati A, Milanese R, Baruscotti M, DiFrancesco D. Properties of ivabradine-induced block of HCN1 and HCN4 pacemaker channels. *The Journal of physiology.* 2006;572(2):335-46.
203. Bucchi A, Baruscotti M, DiFrancesco D. Current-dependent block of rabbit sino-atrial node If channels by ivabradine. *The Journal of general physiology.* 2002;120(1):1-13.
204. Ishii TM, Takano M, Xie L-H, Noma A, Ohmori H. Molecular characterization of the hyperpolarization-activated cation channel in rabbit heart sinoatrial node. *Journal of Biological Chemistry.* 1999;274(18):12835-9.
205. Shi W, Wymore R, Yu H, Wu J, Wymore RT, Pan Z, et al. Distribution and prevalence of hyperpolarization-activated cation channel (HCN) mRNA expression in cardiac tissues. *Circ Res.* 1999;85(1):e1-e6.
206. Liu J, Dobrzynski H, Yanni J, Boyett MR, Lei M. Organisation of the mouse sinoatrial node: structure and expression of HCN channels. *Cardiovascular research.* 2007;73(4):729-38.
207. Morris GM, Boyett MR. Perspectives -- biological pacing, a clinical reality? *Ther Adv Cardiovasc Dis.* 2009;3(6):479-83.
208. Clay JR, DeHaan RL. Fluctuations in interbeat interval in rhythmic heart-cell clusters. Role of membrane voltage noise. *Biophys J.* 1979;28(3):377-89.
209. Boudreau-Beland J, Duverger JE, Petitjean E, Maguy A, Ledoux J, Comtois P. Spatiotemporal stability of neonatal rat cardiomyocyte monolayers spontaneous activity is dependent on the culture substrate. *PLoS One.* 2015;10(6):e0127977.
210. Duverger JE, Boudreau-Béland J, Le MD, Comtois P. Multicellular automaticity of cardiac cell monolayers: effects of density and spatial distribution of pacemaker cells. *New Journal of Physics.* 2014;16(11):113046.
211. Ponard JG, Kondratyev AA, Kucera JP. Mechanisms of intrinsic beating variability in cardiac cell cultures and model pacemaker networks. *Biophys J.* 2007;92(10):3734-52.
212. Comtois P, Vinet A. Curvature effects on activation speed and repolarization in an ionic model of cardiac myocytes. *Phys Rev E.* 1999;60(4 Pt B):4619-28.
213. Xie Y, Sato D, Garfinkel A, Qu Z, Weiss JN. So little source, so much sink: requirements for afterdepolarizations to propagate in tissue. *Biophys J.* 2010;99(5):1408-15.
214. Weiss JN, Qu Z, Chen P-S, Lin S-F, Karagueuzian HS, Hayashi H, et al. The dynamics of cardiac fibrillation. *Circulation.* 2005;112(8):1232-40.
215. Lo C-F. A modified stochastic Gompertz model for tumour cell growth. *Computational and Mathematical Methods in Medicine.* 2010;11(1):3-11.
216. Puglisi JL, Yuan W, Timofeyev V, Myers RE, Chiamvimonvat N, Samarel AM, et al. Phorbol ester and endothelin-1 alter functional expression of Na<sup>+</sup>/Ca<sup>2+</sup> exchange, K<sup>+</sup>, and Ca<sup>2+</sup> currents in cultured neonatal rat myocytes. *Am J Physiol Heart Circ Physiol.* 2011;300(2):H617-26.
217. Joyner RW, Van Capelle F. Propagation through electrically coupled cells. How a small SA node drives a large atrium. *Biophysical Journal.* 1986;50(6):1157.
218. Puglisi JL, Yuan W, Timofeyev V, Myers RE, Chiamvimonvat N, Samarel AM, et al. Phorbol ester and endothelin-1 alter functional expression of Na<sup>+</sup>/Ca<sup>2+</sup> exchange, K<sup>+</sup>, and Ca<sup>2+</sup> currents in cultured neonatal rat myocytes. *Am J Physiol-Heart C.* 2011;300(2):H617-H26.

219. Morikawa K, Bahrudin U, Miake J, Igawa O, Kurata Y, Nakayama Y, et al. Identification, isolation and characterization of HCN4-positive pacemaking cells derived from murine embryonic stem cells during cardiac differentiation. *Pacing Clin Electrophysiol.* 2010;33(3):290-303.